12-16-2016

Sorption and Metabolism of Explosives in Sediment of Coastal Marine Ecosystems

Thivanka S. Ariyarathna
University of Connecticut, thivankaariyarathna@gmail.com

Sorption and Metabolism of Explosives in Sediment of Coastal Marine Ecosystems

Thivanka Ariyarathna, Ph.D.

University of Connecticut, 2016

Abstract

The lack of knowledge on fate and transport of explosive compounds, 2,4,6-trinitrotoluene (TNT) and hexahydro-1,3,5-trinitro-1,3,5-triazine (RDX) in marine ecosystems limits the ability to predict toxicological impacts and natural attenuation of these suspected carcinogens in contaminated coastal sites. This study focuses on improving our understanding of the sorption and transformation of TNT and RDX in coastal ecosystems by using stable nitrogen isotopes.

Abiotic and biotic bench-top experiments using sediment slurries evaluated sorption kinetics and anaerobic biotransformation. Marine silt showed higher compound-uptake rates (> ~100) than freshwater silt for both compounds though equilibrium partition constants (Kp's) were on the same order of magnitude. Kp's of TNT and RDX varied linearly with total organic carbon (TOC) in sediment and were inversely correlated to temperature. TNT was transformed from the slurry water at a faster rate than RDX and accumulation in sediment was higher in the TNT microcosms than for RDX. TNT was mineralized to NO_X (NO_2^- and NO_3^-) and NH_4^+ via denitration, and deamination, possibly facilitated by iron and sulfate reducing bacteria. RDX was mineralized anaerobically to NO_X, NH_4^+ and N_2 gas via denitration, ring breakdown and denitrification.

Studies were extended to mesocosm scales representing subtidal non-vegetated, subtidal vegetated and intertidal marsh to evaluate the fate and transport of RDX in multi-component, coastal settings at steady state conditions. Time series of dissolved RDX, derivatives and mineralization products (NH_4^+, NO_X, N_2 and N_2O) in surface water, porewater, and solids were

analyzed. Transformation of RDX was enhanced by microbial assemblages and lower redox potentials. Nitroso-derivatives were further converted to N_2O (primarily) and N_2 (secondarily). Subtidal vegetated and intertidal marsh (TOC-rich, fine grained sediments and sulfate reducers) showed higher mineralization of RDX. Subtidal non-vegetated mesocosm (TOC-poor, sandy sediment and iron reducers) yielded the highest persistence of RDX in the system. Sediment sorption decreased from intertidal marsh > subtidal vegetated >subtidal non-vegetated and was correlated to the available TOC (positively) and grain size (negatively) of the sediment though partitioning of RDX and derivatives onto sediment was a negligible sink for RDX. The greatest predictor of RDX fate was prevailing sediment redox conditions in the ecosystem.

Sorption and Metabolism of Explosives in Sediment of Coastal Marine Ecosystems

Thivanka Ariyarathna

B.S., University of Peradeniya, 2010

A Dissertation

Submitted in Partial Fulfillment of the

Requirements for the Degree of

Doctor of Philosophy

at the

University of Connecticut

2016

APPROVAL PAGE

Doctor of Philosophy Dissertation

Sorption and Metabolism of Explosives in Sediment of Coastal Marine Ecosystems

Presented by

Thivanka Ariyarathna, B.S.

Major Advisor _____
Penny Vlahos

Associate Advisor _____
Craig Tobias

Associate Advisor _____
Robert Mason

University of Connecticut
2016

Acknowledgments

I would like to express my special appreciation and thanks to my advisor Professor Dr. Penny Vlahos, you have been a tremendous mentor for me. I would like to thank you for encouraging my research and for allowing me to grow as a research scientist. Your advice on both research as well as on my career have been priceless. I would also like to thank prof. Craig Tobias and prof. Robert Mason for serving as my committee members even at hardship. I also want to thank you for letting my defense be an enjoyable moment, and for your brilliant comments and suggestions, thanks to you. I would like to thank Dr. Richard Smith and Mark Ballantine for your support

A special thanks to my family. Words cannot express how grateful I am to my parents, Owala udage Swarnalatha and Cyril Ariyarathna for all of the sacrifices that you've made on my behalf. Your prayer for me was what sustained me thus far. I would also like to thank all of my friends who supported me in writing, and incented me to strive towards my goal. At the end I would like express my heartiest appreciation to my beloved husband, Sampath Rathnayaka who spent sleepless nights with and was always my support in the moments when there was no one to answer my queries.

Table of Contents

1.0 Introduction

1.1 Exposure and toxicity of TNT and RDX in the environment

The explosive compounds, 2,4,6-trinitrotoluene (TNT) and Hexahtdro-1,3,5-trinitro-1,3,5-triazine (RDX) are common contaminants of military munitions worldwide including areas off the US coasts and Hawaii, Gulf of Mexico, North Sea, Baltic Sea, Mediterranean Sea and off the coasts of Europe and Russia [1]. Though the disposal of explosives into the ocean has been prohibited in the united states since the "ocean dumping act" in 1972 [1], intact, breached or buried munitions from past disposal activities slowly release explosive chemicals into the adjacent marine settings through corrosion and leaking [2]. Ongoing Military training and weapon testing activities of the department of defense (DoD), is also a continuous source of explosives in coastal environments where marine aquatic life is exposed, as are humans through direct exposure and/or the food chain [3]. TNT has been linked to liver damage and anemia in humans and both TNT and derivatives have shown toxicity and mutagenic potential in aquatic species [3]. RDX is considered a known neurotoxin for humans [3] and both TNT and RDX are classified as possible human carcinogens under group 3 in the International Agency for Research on Cancer carcinogenic categorization and Group C by the United States Environmental Protection Agency (USEPA) [4]. Since the estimated cost of complete cleanup at active military installations, closed bases, and other former military properties is in the tens of billions of US dollars [1], it is extremely important to have a better understanding of natural attenuation of explosives including sorption, biodegradation and mineralization in coastal marine habitats.

1.2 The fate of TNT and RDX in the environment

The fate of TNT and RDX in the environment is determined by physico-chemical properties of the compounds (solubility, octanol-water partition constant, vapour pressure, Henry's law

constant) (Table 1) and environmental conditions (sediment properties, ionic strength, pH, redox conditions and biological factors) [4]. Geochemical differences in sediments including grain size, clay content and type, and quantity of organic carbon are critical variables in rate and extent of adsorption of explosive compounds onto sediment [4]. Marine systems are significantly different from freshwater environments in terms of pH, ionic strength and sulfate concentration which can result in different sorption kinetics for these compounds.

It is well established that TNT and RDX biodegrade forming various reduced by-products although significant uncertainties are observed in breakdown pathways [5-7]. Under both aerobic and anaerobic conditions, TNT is transformed to derivatives such as hydroxylamine nitro-toluenes, mono-amino-dinitro-toluenes (2-ADNT, 4-ADNT) and di-amino-nitro-toluenes (2,4-DANT, 2,6-DANT) those are more toxic than TNT. Under strict anaerobic conditions, triaminonitrotoluene (TAT) is produced, when all three nitro groups are substituted by NH_2 (Figure 1). And TAT can irreversibly bind onto the sediment so that it can serve as an effective remediation technique. That supports the idea that TNT is readily biodegradable, but, has poor mineralization and higher sorption affinity [8] But, some sulfate reducing bacteria, *Clostridium* and *Desulfovibrio* have the enzyme, reductive deaminase, which is responsible for converting triaminotoluene to toluene through deamination and complete mineralization of toluene to CO_2 has also been demonstrated under sulfate reducing conditions[9]. It has been recently found that mineralization rates were significantly lower than bacterial biomass incorporation rates for TNT by marine bacterial assemblages [10]. As nitrogen containing compounds, TNT and especially RDX with high N/C ratios are quite susceptible to microbial breakdown in nitrogen-limited marine ecosystems [11]. Higher organic content in marine environments facilitates the transformation of RDX compared to the organic poor groundwaters where RDX seems quite

persistent.

Table 1: Physical-chemical properties reported at STP. NA= Not available. Table was obtained from SERDP project proposal 11 ER01-008 (Funded project ER-2122).

Compound	Formula	Structure	MWt (g/mol)	Cw (mol/l)	Log v.p. (Pa)	Log Kow	Kaw (l atm/mol)
2,4,6-trinitrotoluene (TNT)	$C_7H_5N_3O_6$	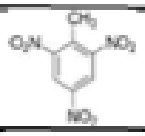	227.13	5.75×10^{-4}	8.51×10^{-4}	1.98	6.0×10^{-7}
2,6-dinitrotoluene (2,6-DNT)	$C_7H_6N_2O_4$	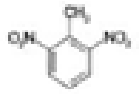	182.14	1.00×10^{-3}	7.59×10^{-2}	2.03	3.1×10^{-5}
2,4-dinitrotoluene (2,4-DNT)	$C_7H_6N_2O_4$		182.14	1.38×10^{-3}	2.88×10^{-2}	2.00	5.6×10^{-6}
2-methylnitrobenzene (2-MNB)	$C_7H_7NO_2$		137.14	4.47×10^{-3}	26.9	2.30	2.5×10^{-3}
4-methylnitrobenzene (4-MNB)	$C_7H_7NO_2$		137.14	3.73×10^{-3}	15.8	2.38	1.7×10^{-3}
hexahydro-1,3,5- trinitro-1,3,5-triazine (RDX)	$C_3H_6N_6O_6$		222.12	2.69×10^{-5}	3.27×10^{-2}	0.87	1.2×10^{-2}
hexahydro-1-nitroso-3, 5-nitro-1,3,5-triazine (MNX)	$C_3H_6N_4O_3$		206.12	-	-	0.92*	NA
hexahydro-1,3-dinitroso-5-nitro-1,3,5-triazine (DNX)	$C_3H_6N_4O_4$		190.12	-	-	0.97*	NA
hexahydro-1,3,5-trinitroso-1,3,5-triazine (TNX)	$C_3H_6N_6O_3$	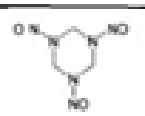	178.12	-	-	1.2*	NA
4 nitro 2,4 diaza butanal (NDAB) (aerobic)	$C_3H_5N_3O_3$		119.06	-	-	-2.93*	NA

Figure 1: TNT biodegradation pathways under anaerobic conditions (Obtained from Khan et al., 2012) [12].

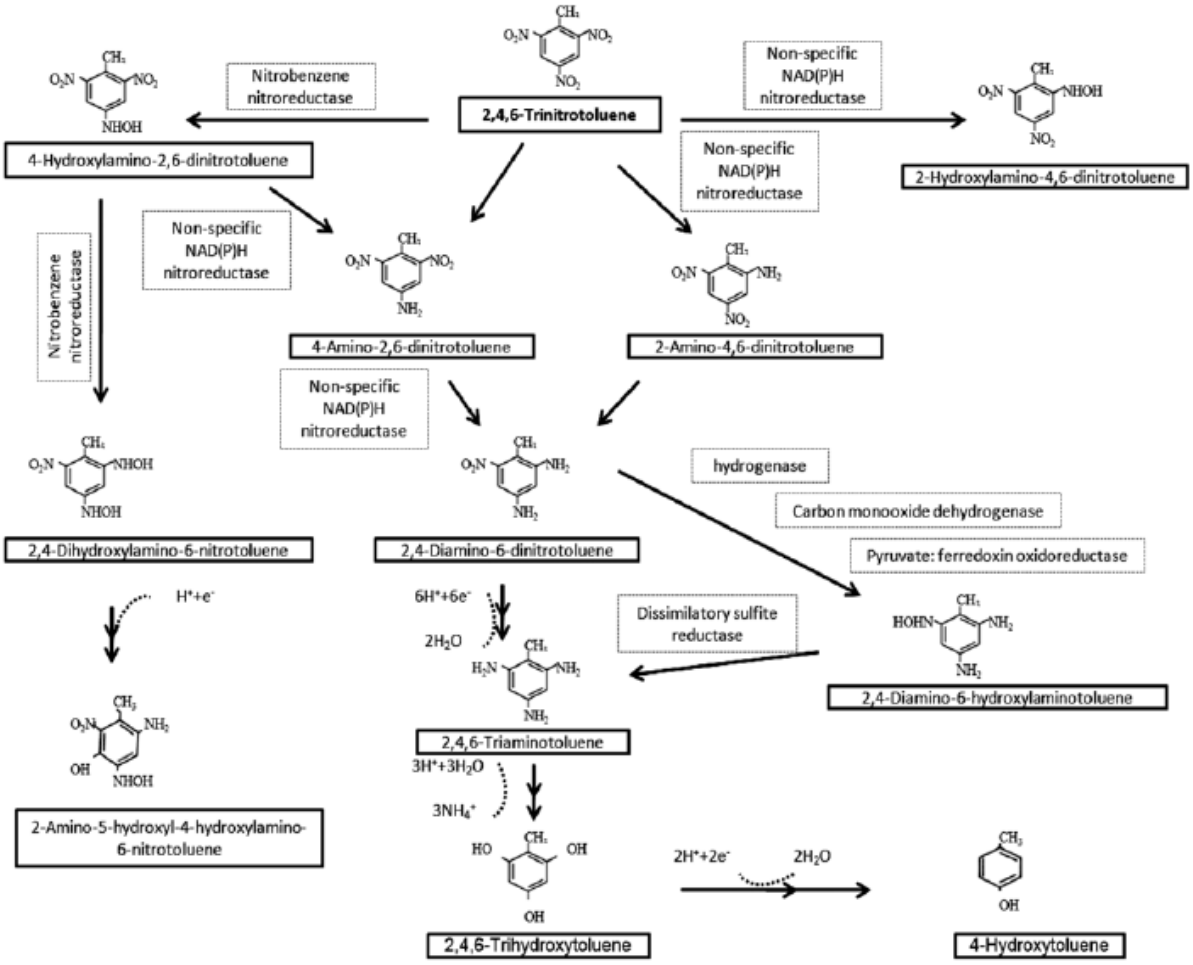

Based on the physico-chemical properties of RDX, it is less soluble in water [13] and more persistent in surface water bodies where aerobic conditions prevail [14]. But, still biotransformation of RDX forming 4-nitro-2,4-diaza butanal (NDAB) was reported under aerobic conditions [7] (Figure 2). Anoxic/hypoxic sediment is a favorable biodegradation zone of RDX in natural coastal habitats and the extent of biodegradation relies on sediment properties [6]. Several benchtop studies have proven the microbial potential of biodegradation of RDX under anaerobic and/or hypoxic conditions coupled with microbial populations from soil,

sediment and sewage sludge [6]. It has been identified that nitro groups in RDX are reduced forming nitroso-triazines (MNX, DNX and TNX) [7] and characterization of N –containing derivatives is vital in N-limited coastal systems. Denitration, denitrification and ring breakdown involve in further mineralization of RDX [6,7,15], Resulted nitrites, nitrates and ammonium can be used as nitrogen sources by microorganisms [11,16]. N_2O and N_2 are formed as ultimate mineralization products, mainly in low oxygen conditions [6,17,18].

Figure 2: RDX transformation pathways under aerobic conditions. (Obtained from Halasz and Hawari, 2011) [7].

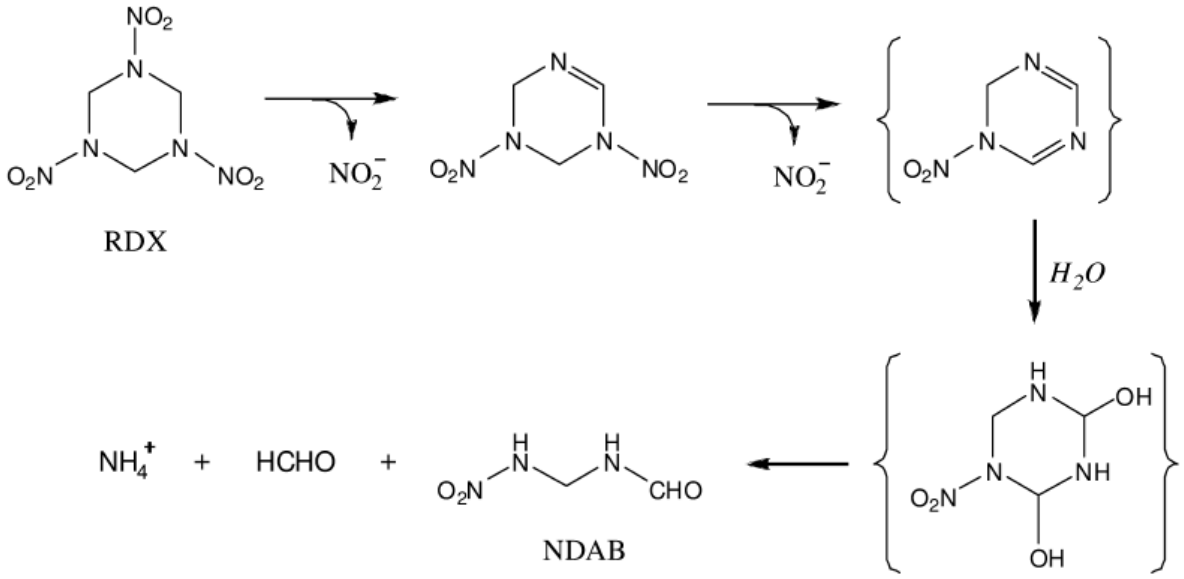

Figure 3: RDX transformation pathways under anaerobic conditions. (Obtained from Hawari et al., 2000) [7].

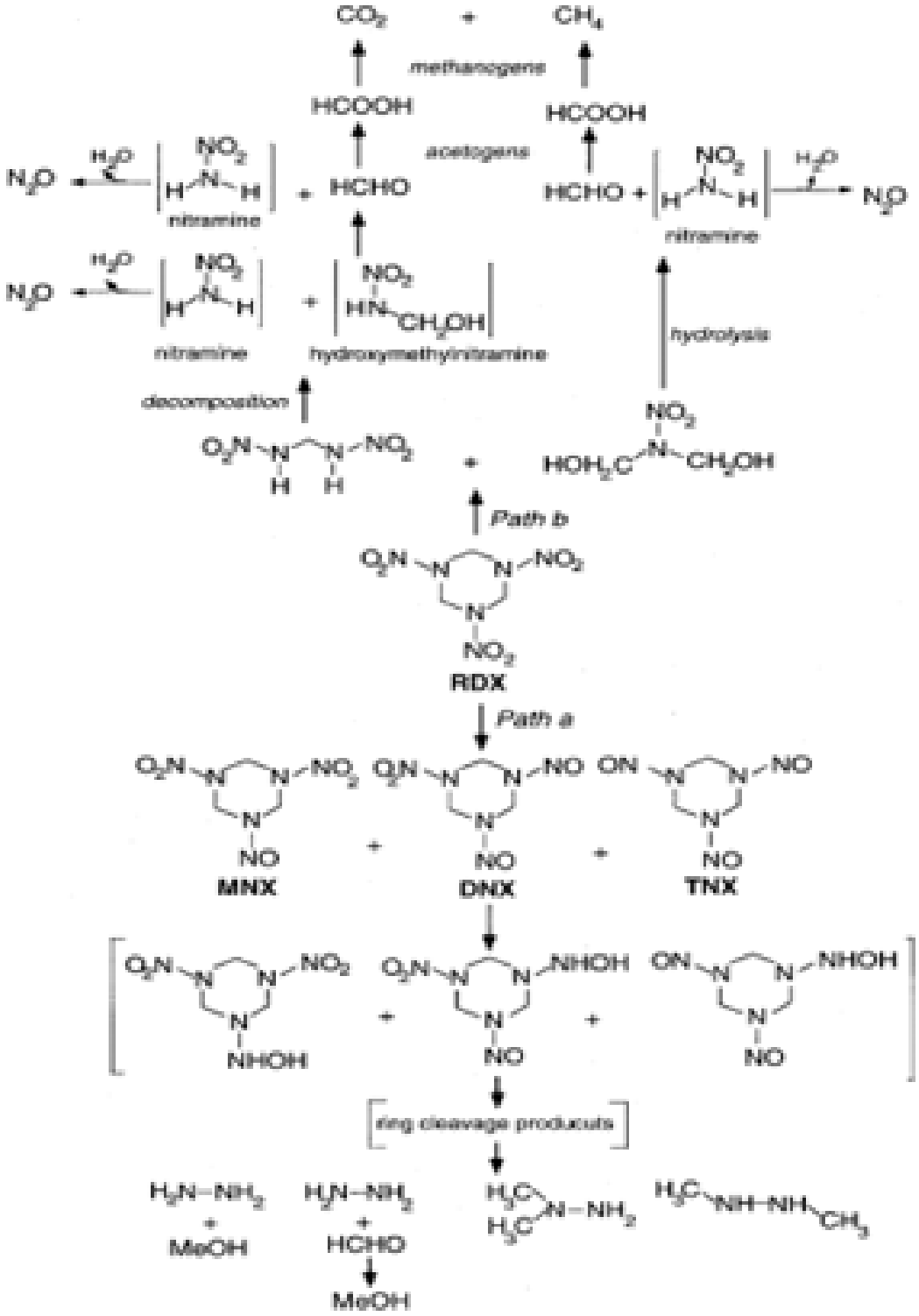

1.3 Aims, Goals and experimental approach

Currently available literature on fate of TNT and RDX address freshwater and groundwater systems extensively [3] and a limited number of studies have been focused on marine environment in terms of identifying sorption kinetics and influence of environmental variables on fate of explosives, characterizing metabolites and mass balancing in the systems [5,10,11]. Characterizing the dependence of temperature and ionic strength on sorption kinetics of these explosives is valuable for environmental process descriptors that have not been studied extensively in marine systems and for which available data is inconsistent [4]. A comparative study of sorption kinetics of munitions in fresh and marine environments has yet to be done in order to reveal the importance of sorption as a sink for explosives from the aqueous environment. Microbial involvement of transformation of TNT and RDX should be evaluated as a comparative study to abiotic experiments to compare removal kinetics and biotransformation pathways. Most studies have been conducted using specific microbial cultures in controlled laboratory conditions [6,16,17,19] and the relative importance of fate and transport of TNT and RDX in natural systems, particularly marine settings, is unknown. It is vital to examine the biodegradation extent and pathways in different micro-environments with different redox conditions including surface water, porewater and sediment in the ecosystem [6] (Figure 4). Further, different geochemical parameters prevail in systems may yield considerable differences in the transformation of RDX in terms of breakdown products (quality and quantity), compound removal rates, biodegradation and mineralization efficiencies etc.

Figure 4: Possible pathways of RDX that enters the surface water in a coastal marine mesocosm.

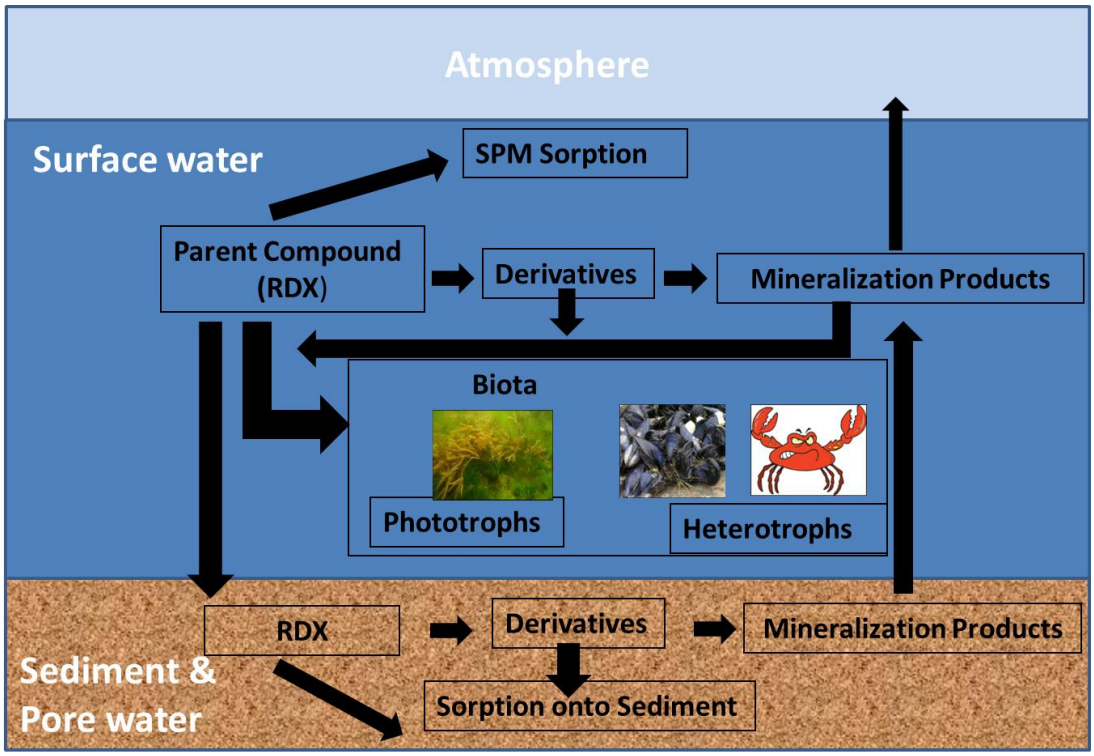

Here, we evaluated sorption kinetics of TNT and RDX and formation of degradation products under abiotic conditions using two sediment types (fine and coarse grained) in freshwater and marine systems at different temperatures for long term preservation of these compounds. Comparative bench-top sediment slurry experiments using fine grained, organic rich marine sediment were also conducted using ^{15}N isotopically labelled TNT and RDX in order to characterize anaerobic biodegradation and mineralization in addition to sorption of these compounds onto sediment. The use of ^{15}N labeled compounds in tracing the breakdown pathways of TNT and RDX entering inorganic nitrogen pools such as ammonium (NH_4^+), nitrates (NO_3^-), nitrites (NO_2^-) and nitrogen gas (N_2) provides the nitrogen based mass balance of the systems that will help to reveal anaerobic transformation pathways and kinetics [5].

We have extended our laboratory studies on fate of RDX to mesocosms that replicate multiple ecosystem components including typical sed-water interface, and flora and fauna in order to minimize the data gap in sorption, biodegradation and mineralization of RDX in coastal marine ecosystems containing natural microbial assemblages. Using isotopically labelled RDX helps to trace the pathways of RDX in an ecosystem and enables a full nitrogen based, mass balance of the system. We conducted large, aquarium-scale and mesocosm-scale laboratory-simulated coastal marine habitats over 15 days and mesocosm-scale ecosystems represent different coastal environmental settings including subtidal non-vegetated, subtidal vegetated and intertidal marsh with different sediment characteristics, redox potentials and habituated microbial populations. RDX and its transformation products including reduced nitroso-derivatives and mineralization products in terms of dissolved inorganic nitrogen (DIN) in dissolved (surface water and porewater) and solid phases (suspended particulate matter, sediment and biota) of the ecosystem were monitored during the experiments. ^{15}N enrichments of bulk sediment ($^{15}N_{sed}$), suspended particulate matter ($^{15}N_{SPM}$) and biota ($^{15}N_{\ biota}$) were also measured in order to acquire a ^{15}N mass balance of the system. Mechanistic differences in RDX transformation in different pools of the ecosystem including well aerated surface water and hypoxic/anoxic sediment were examined comprehensively in order to compare the ultimate fate of RDX in different nitrogen limited coastal marine habitats that has not been performed to date. Moreover, we use multi-variant analysis to evaluate the covariance of geochemical and physical conditions with RDX metabolism.

Resulting outcomes from above mentioned comprehensive analysis of fate and metabolism of RDX help to evaluate the efficacy of natural attenuation of TNT and RDX in coastal marine habitats. This study also benefits the future studies related to the investigations and

characterization of munition contaminated coastal sites since it identifies variations in removal rates and pathways of TNT and RDX based on environmental characteristics.

1.4 References

[1] *U.S. Disposal of Chemical Weapons in the Ocean: Background and Issues for Congress.* 2007.

[2] Craig HD, Taylor S. 2011. Framework for evaluating the fate, transport, and risks from conventional munitions compounds in underwater environments. *Mar Technol Soc J* 45:35-46.

[3] Pichtel J. 2012. Distribution and fate of military explosives and propellants in soil: A review. *Applied and Environmental Soil Science* 2012.

[4] Ariyarathna T, Vlahos P, Tobias C, Smith R. 2015. Sorption kinetics of TNT and RDX in anaerobic freshwater and marine sediments: Batch studies. *Environ Toxicol Chem* 35(1):47-55.

[5] Smith RW, Vlahos P, Böhlke JK, Ariyarathna T, Ballentine M, Cooper C, Fallis S, Groshens TJ, Tobias C. 2015. Tracing the Cycling and Fate of the Explosive 2,4,6-Trinitrotoluene in Coastal Marine Systems with a Stable Isotopic Tracer, 15N-[TNT]. *Environ Sci Technol* 49:12223-12231.

[6] Smith RW, Tobias C, Vlahos P, Cooper C, Ballentine M, Ariyarathna T, Fallis S, Groshens TJ. 2015. Mineralization of RDX-derived nitrogen to N2 via denitrification in coastal marine sediments. *Environ Sci Technol* 49:2180-2187.

[7] Halasz A, Hawari J. 2011. Degradation routes of RDX in various redox systems. *ACS Symp Ser* 1071:441-462.

[8] Hawari J, Halasz A, Sheremata T, Beaudet S, Groom C, Paquet L, Rhofir C, Ampleman G, Thiboutot S. 2000. Characterization of metabolites during biodegradation of hexahydro- 1,3,5-trinitro-1,3,5-triazine (RDX) with municipal anaerobic sludge. *Appl Environ Microbiol* 66:2652-2657.

[9] Boopathy R, Kulpa CF, Manning J. 1998. Anaerobic biodegradation of explosives and related compounds by sulfate-reducing and methanogenic bacteria: A review. *Bioresour Technol* 63:81-89.

[10] Montgomery MT, Coffin RB, Boyd TJ, Smith JP, Walker SE, Osburn CL. 2011. 2,4,6-Trinitrotoluene mineralization and bacterial production rates of natural microbial assemblages from coastal sediments. *Environ Pollut* 159:3673-3680.

[11] Montgomery MT, Coffin RB, Boyd TJ, Osburn CL. 2013. Incorporation and mineralization of TNT and other anthropogenic organics by natural microbial assemblages from a small, tropical estuary. *Environ Pollut* 174:257-264.

[12] Khan MI, Lee J, Park J. 2013. A toxicological review on potential microbial degradation intermediates of 2,4,6-trinitrotoluene, and its implications in bioremediation. *KSCE J Civ Eng* 17:1223-1231.

[13] Kalderis D, Juhasz AL, Boopathy R, Comfort S. 2011. Soils contaminated with explosives: Environmental fate and evaluation of state-of the-art remediation processes (IUPAC technical report). *Pure and Applied Chemistry* 83:1407-1484.

[14] Felt D.R., Bednar A., Arnett C., Kirgan R. 2009. Bio-Geochemical factors that affect RDX degradation. *Proceedings of the Annual International Conference on Soils, Sediments, Water and Energy* 14:article 17.

[15] Hawari J, Halasz A, Sheremata T, Beaudet S, Groom C, Paquet L, Rhofir C, Ampleman G, Thiboutot S. 2000. Characterization of metabolites during biodegradation of hexahydro- 1,3,5-trinitro-1,3,5-triazine (RDX) with municipal anaerobic sludge. *Appl Environ Microbiol* 66:2652-2657.

[16] Beller HR. 2002. Anaerobic biotransformation of RDX (hexahydro-1,3,5-trinitro-1,3,5-triazine) by aquifer bacteria using hydrogen as the sole electron donor. *Water Res* 36:2533-2540.

[17] Sheremata TW, Halasz A, Paquet L, Thiboutot S, Ampleman G, Hawari J. 2001. The fate of the cyclic nitramine explosive RDX in natural soil. *Environmental Science and Technology* 35:1037-1040.

[18] Hawari J, Beaudet S, Halasz A, Thiboutot S, Ampleman G. 2000. Microbial degradation of explosives: Biotransformation versus mineralization. *Appl Microbiol Biotechnol* 54:605-618.

[19] Sheremata TW, Hawari J. 2000. Mineralization of RDX by the white rot fungus Phanerochaete chrysosporium to carbon dioxide and nitrous oxide. *Environ Sci Technol* 34:3384-3388.

2.0 Sorption kinetics of TNT and RDX in anaerobic freshwater and marine sediments: Batch studies

SORPTION KINETICS OF TNT AND RDX IN ANAEROBIC FRESHWATER AND MARINE SEDIMENTS: BATCH STUDIES

THIVANKA ARIYARATHNA,† PENNY VLAHOS,*† CRAIG TOBIAS,† and RICHARD SMITH†‡
†Department of Marine Sciences, University of Connecticut, Groton, Connecticut, USA
‡Global Aquatic Research, Sodus, New York, USA

(Submitted 6 May 2015; Returned for Revision 10 June 2015; Accepted 3 July 2015)

Abstract: Examination of the partitioning of explosives onto sediment in marine environments is critical to predict the toxicological impacts of worldwide explosive-contaminated sites adjacent to estuaries, wetlands, and the coastal ocean. Marine sediments have been identified as sites of enhanced munitions removal, yet most studies addressing these interactions focus on soils and freshwater sediments. The present study measured the kinetics of 2,4,6-trinitrotoluene (TNT) and hexahydro-1,3,5-trinitro-1,3,5-triazine (RDX) sorption onto 2 marine sediments of varying grain sizes (silt vs sand) and organic carbon (OC) content. Abiotic sediment sorption tests were performed at 23 °C, 15 °C, and 4 °C by spiking TNT and RDX solutions directly into anaerobic sediment slurries. Marine sediments showed significantly higher compound uptake rates (0.30–0.80 h^{-1}) than freshwater silt (0.0046–0.0065 h^{-1}) for both compounds, probably because of lower compound solubilities and a higher pH in marine systems. Equilibrium partition constants are on the same order of magnitude for marine silt (1.1–2.0 L kg^{-1} sediment) and freshwater silt (1.4–3.1 L kg^{-1} sediment) but lower for marine sand (0.72–0.92 L kg^{-1} sediment). Total organic carbon content in marine sediments varied linearly with equilibrium partition constants for TNT and was moderately linear for RDX. Uptake rates and equilibrium constants of explosives are inversely correlated to temperature regardless of sediment type because of kinetic barriers associated with low temperatures. *Environ Toxicol Chem* 2016;35:47–55. © 2015 SETAC

Keywords: Sediment sorption TNT RDX Equilibrium partition coefficient Temperature dependence

INTRODUCTION

The explosive compounds 2,4,6-trinitrotoluene (TNT) and hexahydro-1,3,5-trinitro-1,3,5-triazine (RDX) are common components of military munitions worldwide [1,2]. Contamination of soil, surface water, groundwater, wetlands, and coastal ecosystems with TNT and RDX has become a global environmental issue [3,4]. For example, TNT has been identified in at least 20 of the 1397 hazardous waste sites on the US Environmental Protection Agency (USEPA) National Priorities List [5], and RDX has been identified at 31 of the 1699 hazardous waste sites that have been proposed for inclusion on the USEPA National Priorities List [5,6]. These compounds enter the environment mainly through low-order detonations, manufacturing, improper handling, and disposal of unexploded ordnances [7]. These sources lead to levels of contamination that can be toxic to ecological receptors at impacted sites and nearby areas subjected to offsite migration of TNT and RDX [7]. Concentrations of RDX in sediment samples from army depots and composts prepared from contaminated sediments have been identified ranging from <0.1 mg/kg to 3574 mg/kg and from >2.9 mg/kg to 896 mg/kg, respectively. Groundwater contamination levels of RDX in munition plants in the United States (<1–14 100 μg/L) and Germany (21–3800 μg/L) have been documented [6]. These concentrations are above the accepted drinking water values for both TNT and RDX (2 μg/L) established by the USEPA [8,9]. A link to liver damage and anemia in humans has been demonstrated for TNT, and both TNT and RDX are classified as possible human carcinogens (Group C) by the USEPA [8,9] and under Group 3 in the International Agency for Research on Cancer carcinogenic categorization [10].

The fate of contaminants in the environment is determined by the physicochemical properties of the compounds and environmental conditions [7]. Sorption to sediments and particles in aquatic systems can significantly attenuate freely dissolved concentrations and alter bioavailability in both sediments and overlying water. Existing studies of TNT and RDX sorption have focused primarily on terrestrial soils and freshwater sediments in which equilibrium partition coefficients for TNT are 1 order of magnitude higher than RDX [11–15]. Similar studies in marine systems are comparatively less available [13,16], and no marine studies are available on RDX, although it is believed to be more persistent in the environment than TNT [17]. Both TNT and RDX can be sorbed onto minerals, amorphous grain coatings of metal oxide, humic materials, and organic/inorganic colloids present in sediment [18]. The rate and extent of sorption can be influenced by the hydrophobicity of compounds, temperature, ionic strength of the water, surface area, and nature of the sorbent and energy input. For example, the salting-out effect in saline systems decreases the solubility of explosives and increases the fugacity in water [19–21].

Geochemical differences in sediments are critical variables in adsorption of explosive compounds onto sediment. Grain size, clay content and type [11,16], and quantity of organic carbon [11] affect the equilibrium partition constants of TNT and RDX. Seasonal temperature changes in the environment may cause differences in sorption and release of TNT and RDX into the aqueous phase and transport processes. For example, organic contaminants such as atrazine, simazine, and naphthalene have shown a 50% decrease in equilibrium partition coefficients by increasing temperatures from 0 °C to 50 °C [22]. Characterizing the temperature dependence on sorption kinetics of these explosives is valuable for environmental process descriptors that have not been studied

This article includes online-only Supplemental Data.
* Address correspondence to thivanka.ariyarathna@uconn.edu
Published online 14 July 2015 in Wiley Online Library (wileyonlinelibrary.com).
DOI: 10.1002/etc.3149

extensively and for which available data are inconsistent [13,14]. Marine systems are significantly different from freshwater environments in terms of pH, ionic strength, and sulfate concentration, which can result in different sorption kinetics for these compounds. Although anion exchange is probably not a dominant mechanism in sorption, the principal component analysis done by Chappell et al. [13] supports the fact that higher elemental sulfur content in sediment correlates with higher sorption rates for some sediments. A comparative study of sorption kinetics of munitions in fresh and marine environments has yet to be done to reveal the importance of sorption as a sink for explosives from the aqueous environment.

In the present study, the sorption kinetics of TNT and RDX and the formation of degradation products were evaluated for 2 sediment types (fine and coarse grained) in freshwater and marine systems to compare differences in kinetics and the potential for long-term preservation of these compounds. The objective was to fill the data gap in the literature on sorption characteristics of TNT and RDX, including the determination of uptake and equilibrium partition coefficients, examination of abiotic compound breakdown using a mass balance approach, and an evaluation of sorption kinetics.

MATERIALS AND METHODS

To examine sorption kinetics of TNT and RDX, we conducted a series of abiotic slurry experiments using a single freshwater and 2 marine sediment types. Fine-grained freshwater sediment samples were collected from a pond in eastern Connecticut (41°19′13.93″N, 72°04′01.80″W). Fine-grained (silt), and coarse-grained (sand) marine sediments were collected from 41°18′03.42″N, 72°07′14.09″W and 41°19′04.50″N, 72°04′00.52″W in the intertidal zones of Waterford and Groton, Connecticut (USA), respectively. Freshwater and seawater were also collected from the same sampling locations of sediments, respectively. All experiments were performed at 3 temperatures for the purpose of yielding sorption kinetics. The data were used to calculate sorption rates and sediment–water equilibrium partition coefficients for TNT and RDX.

Sediment characterization

All sediments were characterized for total organic carbon (TOC), total nitrogen (TN), and sulfur (S) using a PerkinElmer elemental analyzer (NA 1500). Sediment texture was determined using a mechanical sieve analyzer with a set of sieves from 0.063 mm to 2.0 mm. Clay compositions in the sediment were determined by an X-ray diffractometer (XRD; Rigaku Ultima IV/Cu Kα [$\lambda = 0.15406$ nm] radiation; beam voltage 40 kV; beam current 44 mA). The redox potentials of sediment systems were measured using a platinum electrode (Paleo Terra) relative to an Ag/AgCl reference electrode (Fisher Scientific) over the course of the experiment.

Incubation experiments

Two types of marine sediments were each mixed with filtered (polyethersulfone, 0.2 μm) seawater (30‰) at a mass ratio of 1:4 [23] with 100 g of sediment, in 500-mL glass bottles. Freshwater sediment slurries were prepared the same way using filtered (polyethersulfone, 0.2 μm) freshwater. Biological activity in sediment slurries was inhibited by adding mercuric chloride, and bottles were covered with aluminum foil to inhibit photodegradation. Sediment slurries were mixed with continuous stirring on magnetic stirrer plates in temperature-controlled chambers of 4 °C, 15 °C, and 23 °C over the course of the experiment and selected as representative seasonal environmental temperature ranges.

The target compounds, TNT and RDX (>99 purity), were purchased from the US Naval Munitions Command. Sediment slurries were allowed to equilibrate for 24 h prior to spiking. After 24 h, slurries were spiked with target compounds dissolved in (1 mL) acetonitrile to achieve concentrations of 4 mg L^{-1} and 2.5 mg L^{-1} for TNT and RDX, respectively. The acetonitrile slug was less than 0.25% of the total volume such that the final concentration was 0.04 M acetonitrile and was substantially diluted to avoid any cosolvent interferences. These target concentrations of TNT and RDX adequately represent the underwater point source concentrations from military-related activities and disposal of unexploded ordnance before substantial dilution in the environment [24]. All treatments were done in duplicate and included 2 controls: sediment slurries with no compound introduction and a compound-spiked control with no sediment to correct for matrix effects and any compound loss in the absence of sediment. Samples to quantify aqueous munitions concentrations were collected at preset intervals (7 total) over the 2-wk duration of the experiment. The 1-mL samples were filtered through 0.2-μm polyethersulfone filters and mixed with 1 mL of acetonitrile.

A modified salting-out method [25] was adapted for smaller sample sizes wherein 0.65 g of sodium chloride was added to each sample, sonicated for 15 min, and vortexed for 5 min to extract the munition compounds from sediment slurries. The extraction was repeated twice, and extracts were combined. An average recovery of 99.1 ± 0.5% was obtained for known amounts of 1,2-dinitrobenzene (1,2-DNB) in water extractions. Sediment-bound munitions were measured at the end of the experiment. Sediment samples were extracted (by a method adapted from USEPA 8330 [26]) using 10 mL of acetonitrile and 2 g of freeze-dried sediments. After 1 h of sonication and 5 min of vortexing, samples were centrifuged for 10 min to separate the supernatant from the sediment. Filtrate was blown to dryness with N_2 followed by an addition of 2 mL of acetonitrile. Average recoveries of munitions from sediment samples were 82 ± 7% based on 1,2-DNB added to the replicate sediment samples. Both water and sediment extractions were analyzed using gas chromatography (GC)/electron-capture detection (ECD) following the methods described by Pan et al. [27], USEPA [28], and Zhang et al. [29,30]. Then 3,4-dinitrotoluene was added to each extract prior to injection to monitor detection efficiency.

Explosive analysis was performed with an Agilent GC/ECD instrument [27] equipped with an HP-DB5 column (30 m × 320 μm, 0.25 μm; Agilent). One microliter of sample was injected onto a splitless liner in pulsed injection mode. Helium was used as a carrier gas at a flow rate of 11.9 mL min^{-1}. The oven temperature was maintained at 90 °C with 2 ramps: ramp 1 was 10.9 min to 200 °C and held for 1.5 min, and ramp 2 was 14.2 min to 250 °C and held for 1.9 min. Quantification was based on an external calibration curve of available standard munitions: TNT, 2-amino-4,6-dinitrotoluene (2-ADNT), 4-amino-2,6-dinitrotoluene (4-ADNT), RDX, hexahydro-1-nitroso-3,5-dinitro-1,3,5-triazine (MNX), hexahydro-1,3-dinitroso-5-nitro-1,3,5-triazine (DNX), and hexahydro-1,3,5-trinitroso-1,3,5-nitro-1,3,5-triazine (TNX) (AccuStandard). The average reporting limit for all compounds was 7.8 ng mL^{-1} (see Supplemental Data, Table S3 for compound-specific reporting limits). Sample chromatograms of GC/ECD for parent compounds and derivatives are shown in the Supplemental Data, Figure S1.

Data analysis

Sorption uptake model. The measured time series concentrations of TNT and RDX in water [C_i], for each sediment type were used to calculate sorption rate constants according to Equation 1

$$\ln [C_i] = -kt + \ln [C_i]_{t=0} \quad (1)$$

where t is time (h) and k is the first order sorption rate constant in h^{-1}.

Equilibrium partitioning model and sorption energetics. Equilibrium partition constants (K_d) of target compounds were calculated using measured concentrations of compounds in sediment (C_{is}) and in water (C_{iw}) when equilibrium was reached at the end of the experiment as follows

$$K_d = (C_{is})/(C_{iw}) \quad (2)$$

Aqueous concentrations were further analyzed for partitioning of TNT and RDX onto dissolved colloidal organic matter using Equation 3

$$C_{iw} = C_{iaq} + C_{iaq} [K_{OC} \times DOC] \quad (3)$$

where C_{iw} is the total compound concentration in water, C_{iaq} is the truly dissolved aqueous compound concentration, K_{OC} is the experimental partition coefficient to organic carbon calculated using K_d and the organic carbon fraction of sediment (f_{OC}), and DOC is the dissolved organic carbon concentration in water. The second term on the right-hand side of Equation 3 is the functionally soluble portion of the total dissolved concentration that is associated with DOC. The f_{OC} is determined using acid fumigation and elemental analyzer (EA) analysis after Hedges and Stern [31], and DOC in the aqueous phase was analyzed using 40-mL samples acidified to a pH value of 2 followed by TOC analysis on a Shimadzu TNM-1 instrument.

Experimental values of K_{OC} for TNT and RDX were calculated using modeled K_{OC} and the organic carbon fraction of sediment ($K_d = K_{OC}/f_{OC}$) and compared with those derived from Di Toro's equation [32]

$$\log K_{OC} = 0.00028 + (0.983 + \log K_{OW}) \quad (4)$$

where K_{OW} is the octanol–water partition coefficient for the compounds.

The Di Toro's relationship was used because it has been shown to be consistent with observations of a large set of absorption–desorption data of nonionizing hydrophobic organic compounds.

Mass balancing model

At the end of the experiment, the total amount of target compounds and their identifiable degradation products in both water and sediment phases were quantified to obtain a mass balance for each system and to identify losses that were not accounted for

$$\begin{aligned} M_{TNT\ spiked} = {} & M_{TNT,dissolved} + M_{TNT,particles} \\ & + M_{2A\text{-}DNT,dissolved} + M_{4A\text{-}DNT,particles} \\ & + M_{2A\text{-}DNT,dissolved} + M_{4A\text{-}DNT,particles} \\ & + \text{unknown} \end{aligned} \quad (5)$$

$$\begin{aligned} M_{RDX\ spiked} = {} & M_{RDX,dissolved} + M_{RDX,particles} \\ & + M_{MNX,dissolved} + M_{MNX,particles} \\ & + M_{DNX,dissolved} + M_{DNX,particles} \\ & + M_{TNX,dissolved} + M_{TNX,particles} \\ & + \text{unknown} \end{aligned} \quad (6)$$

In Equations 5 and 6, $M_{X,spiked}$, $M_{X,dissolved}$ and $M_{X,particles}$ represent the mass of compound X spiked to the system, the mass of compound X in the aqueous phase at equilibrium (truly dissolved and sorbed to DOC), and the mass of compound X partitioned onto sediment at equilibrium, respectively.

RESULTS

Sediment characterization

Sediments used in incubation experiments were chemically and texturally different from each other, as shown in Table 1. Sediments were classified as freshwater silt, marine silt, and marine sand based on grain size. Grain size increased in the order of marine silt, freshwater silt, and marine sand considering their graphic mean (0.16 mm < 0.37 mm < 0.41 mm) and median (0.11 mm < 0.31 mm < 0.36 mm). Fine-grained freshwater sediment was rich in organic carbon (9.32 mg g^{-1} sediment) and considerably poor in elemental sulfur (0.40 mg g^{-1} sediment) compared with both marine sediments. Fine-grained marine silt had a higher organic carbon (4.10 mg g^{-1} sediment) and elemental sulfur level (3.70 mg g^{-1} sediment) than medium to coarse-grained marine sand (organic carbon and sulfur contents of 0.038 mg g^{-1} sediment and 1.00 mg g^{-1} sediment, respectively). Marine sand had a negligible clay content (0.8%), whereas marine silty sediment and freshwater sediment contained 56% and 34% of silt and clay content, respectively. The XRD spectra showed that both marine silt and freshwater silt had smectite group clays and feldspar [33] (Supplemental Data, Figure S2).

Behavior of explosives in freshwater systems

Both TNT and RDX were rapidly removed from the aqueous phase in freshwater slurries at all 3 temperatures, followed by a slow removal that approached equilibrium (Figure 1 and Supplemental Data, Figure S3). Table 2 summarizes the kinetic parameters of uptake of the target explosives (TNT and RDX) onto freshwater sediment at the 3 temperatures. Uptake rate constants of both TNT and RDX increase with decreasing temperature for freshwater sediments. In the present study,

Table 1. Chemical and textural properties of sediments and slurry-water used in the present study ($n = 2$)

Property	Freshwater silt	Marine silt	Marine sand
Particle size distribution data			
Sand (%)	66	44	99.2
Silt & clay (%)	34	56	0.8
Statistical parameters			
Graphic mean (mm)	0.37	0.16	0.41
Median (mm)	0.31	0.11	0.36
IGSD (mm)	0.63	0.16	0.25
Physical properties			
Bulk density (g cm^{-3})	1.3	1.4	1.7
Porosity (%)	48.3	45.6	31.0
pH	7.0	7.9	7.9
Salinity (‰)	0.1	30.0	30.0
Chemical properties			
DOC (μM)	1350 ± 11	550 ± 27	250 ± 14
TOC (mg g^{-1} sediment)	9.320 ± 0.070	4.101 ± 0.694	0.038 ± 0.007
TN (mg g^{-1} sediment)	0.559 ± 0.001	0.615 ± 0.252	0.060 ± 0.002
S (mg g^{-1} sediment)	0.4 ± 0.1	3.7 ± 0.3	1.0 ± 0.5

IGSD = inclusive graphic standard deviation; DOC = dissolved organic carbon; TOC = total organic carbon; TN = total nitrogen; S = elemental sulfur.

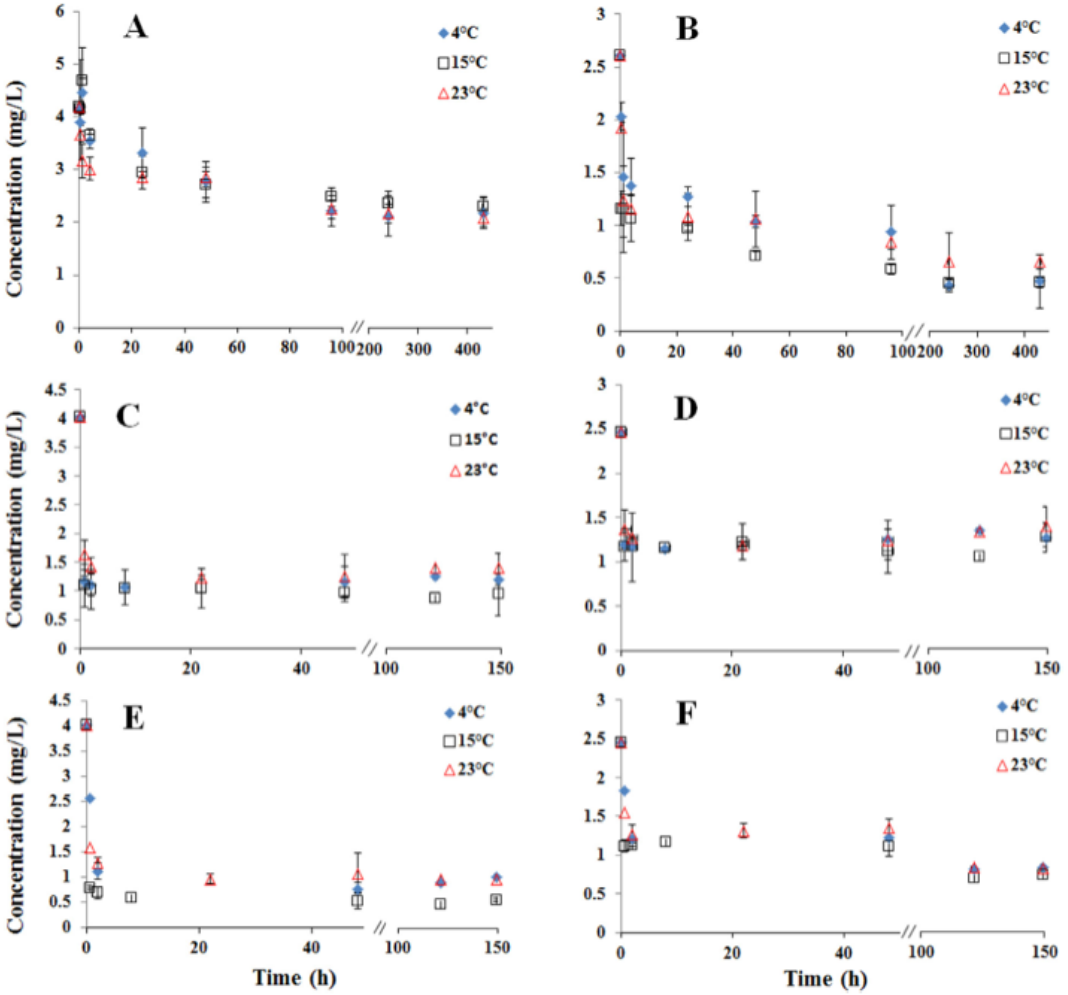

Figure 1. Time series aqueous concentrations of (**A**) 2,4,6-trinitrotoluene (TNT) in the freshwater silt system, (**B**) hexahydro-1,3,5-trinitro-1,3,5-triazine (RDX) in the freshwater silt system, (**C**) TNT in the marine sand system, (**D**) RDX in the marine sand system, (**E**) TNT in the marine silt system, and (**F**) RDX in the marine silt system at 3 different temperatures: 4 °C, 15 °C, and 23 °C. Error bars represent standard deviations of measurements ($n = 2$).

Table 2. Sorption kinetic parameters of explosives onto marine and freshwater sediments at 3 different temperatures[a]

		TNT				RDX			
Temp. (°C)	Sediment Type	k (h^{-1})	$t_{1/2}$ (h)	K_p ($L\,kg^{-1}$ sed)	ΔG ($kJ\,mol^{-1}$)	k (h^{-1})	$t_{1/2}$ (h)	K_p ($L\,kg^{-1}$ sed)	ΔG ($kJ\,mol^{-1}$)
4	Freshwater	0.0065 ($R^2 = 0.92$)	110	3.1	–2.6	0.0060 ($R^2 = 0.83$)	120	3.0	–2.5
	Marine silt	0.64 ($R^2 = 0.99$)	1.1	2.0	–1.6	0.36 ($R^2 = 0.99$)	2.0	1.3	–0.65
	Marine sand	0.58 ($R^2 = 0.64$)	1.2	1.3	–0.63	0.33 ($R^2 = 0.64$)	2.2	0.87	0.33
15	Freshwater	0.0053 ($R^2 = 0.81$)	130	2.3	–2.0	0.0052 ($R^2 = 0.69$)	130	2.5	–2.0
	Marine silt	0.80 ($R^2 = 0.68$)	0.9	1.4	–0.80	0.35 ($R^2 = 0.60$)	2.0	1.2	–0.37
	Marine sand	0.62 ($R^2 = 0.66$)	1.1	0.92	0.20	0.34 ($R^2 = 0.62$)	2.1	0.82	0.48
23	Freshwater	0.0046 ($R^2 = 0.71$)	150	1.9	–1.6	0.0048 ($R^2 = 0.79$)	140	1.4	–0.78
	Marine silt	0.53 ($R^2 = 0.78$)	1.3	1.3	–0.58	0.31 ($R^2 = 0.87$)	2.2	1.1	–0.18
	Marine sand	0.48($R^2 = 0.72$)	1.5	0.82	0.50	0.30($R^2 = 0.71$)	2.3	0.72	0.82

[a]Experimental data were fit to the 1st-order kinetic equation, $\ln [C_i] = -kt + \ln [C_i]_{t=0}$. Half-lives ($t_{1/2}$) of compounds in water were calculated using $t_{1/2} = \ln 2/k$. Gibbs free energy (ΔG) is calculated using the expression $\Delta G = -R\,T \ln(K_p)$ where R is the universal gas constant ($8.314\,J\,K^{-1}\,mol^{-1}$) and T is the temperature in K.

TNT = 2,4,6-trinitrotoluene; RDX = hexahydro-1,3,5-trinitro-1,3,5-triazine; k = first order sorption rate constant in h^{-1}; K_p = equilibrium partition coefficient.

uptake rate constants ranged between 0.0046 h^{-1} and 0.0065 h^{-1} and 0.0048 h^{-1} to 0.0060 h^{-1} for TNT and RDX, respectively, in anaerobic freshwater sediment slurries at 3 different temperatures. The corresponding half-lives of TNT and RDX (110–150 h) consistently increased with increasing temperature.

Equilibrium partition constants measure the distribution of explosives in water and sediment phases at equilibrium. Values of K_d of both TNT and RDX for freshwater silt ranged from 1.4 L kg^{-1} sediment to 3.1 L kg^{-1} sediment (Table 2) and decreased with increasing temperatures (Figure 2). The amount of TNT and RDX partitioned onto dissolved organic matter in the freshwater sediment slurry represented 0.5% and 0.4%, respectively, of the total aqueous phase concentrations for both compounds.

Mass balances of TNT in the freshwater systems showed that 55% of the TNT was in the dissolved phase whereas 38% was in the particle phase at these mixing ratios and that the balance was reasonably close, with only 2% to 7% unknown. After the 14-d period, 34% to 35% of the spiked RDX was unidentifiable, and 29% and 11% remained in water and sediment phases, respectively, without degradation (Table 3). Of the spiked RDX, 25% was accounted for as the derivatives MNX, DNX, and TNX in freshwater systems at all 3 temperatures (Supplemental Data, Table S2).

Behavior of explosives in marine systems

Similar to the freshwater silt incubations, both compounds were rapidly removed from the slurry water in marine sand and silt, as shown in Figure 1 and Supplemental Data, Figure S3.

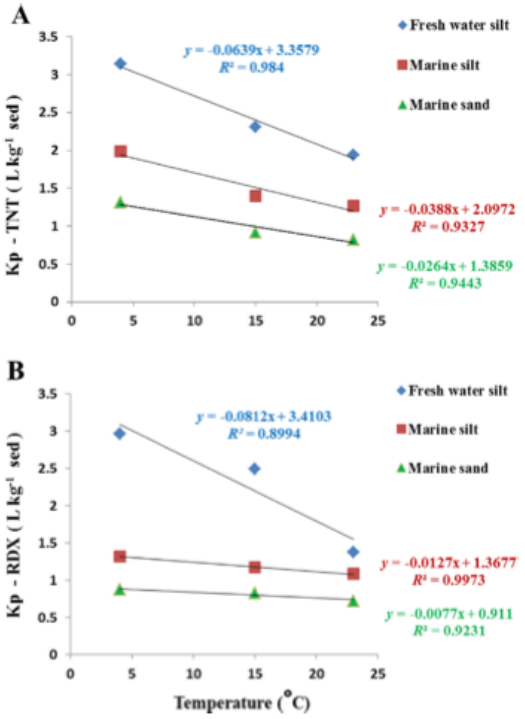

Figure 2. Correlation between temperature and equilibrium partition coefficient (K_p) of (**A**) 2,4,6-trinitrotoluene (TNT) and (**B**) hexahydro-1,3,5-trinitro-1,3,5-triazine (RDX) for freshwater silt, marine silt, and marine sand.

Uptake rate constants in marine sediments (Table 2) were approximately 100 times higher than those in freshwater silt. Observed sorption rates were in the ranges of 0.48 h^{-1} to 0.80 h^{-1} and 0.30 h^{-1} to 0.36 h^{-1} for TNT and RDX, respectively. Marine silt had slightly higher uptake rate constants for TNT (0.53–0.80 h^{-1}) and RDX (0.31–0.36 h^{-1}) than did marine sand (0.48–0.62 h^{-1} and 0.30–0.34 h^{-1}), respectively, at all temperatures, at 95% confidence ($p \leq 0.05$) based on a paired t test. Uptake rate constants of TNT for both marine silt (0.53 h^{-1}) and sand (0.48 h^{-1}) at 23 °C were lower than those at 4 °C (0.64 h^{-1} and 0.58 h^{-1}, respectively). In marine silt, RDX showed a consistent decrease in uptake rates from 0.36 h^{-1} to 0.31 h^{-1} with increasing temperature from 4 °C to 23 °C.

The K_d values for marine sediments (Table 2) decreased with increasing temperature (Figure 2). Equilibrium partitioning of TNT (0.82–2.0 L kg^{-1} sediment) onto marine sediments was higher than that of RDX (0.72–1.3 L kg^{-1} sediment) in anaerobic sediment slurries. The K_d values of explosives were on the same order of magnitude for both freshwater silt (1.4–3.1 L kg^{-1} sediment) and marine silt (1.1–2.0 L kg^{-1} sediment), although marine silt exhibited rapid sorption with uptake rates 100 times greater than freshwater silt. Marine sand had lower K_d values (0.72–0.92 L kg^{-1} sediment) than marine silt (1.1–2.0 L kg^{-1} sediment) and freshwater silt (1.4–3.1 L kg^{-1} sediment) for both compounds at all treatments except for 1 K_d value observed for TNT at 4 °C (1.3 L kg^{-1} sediment). Partitioning of TNT and RDX onto dissolved organic matter in marine silt slurry water was 0.25% and 0.19% of the aqueous phase concentrations for both compounds. Similarly, for marine sand, TNT and RDX partitioned onto dissolved organic matter represented 0.17% and 0.13% of the total aqueous phase concentrations for both compounds.

After 14 d, 22% to 43% of TNT remained in the systems (Table 3). Approximately 3% of the spiked TNT abiotically degraded into identifiable compounds, forming mostly 4-aminodinitrotoluene, leaving a considerable portion (64%) of unknowns at all 3 temperatures in both marine systems. Nearly 58% of the spiked RDX remained unchanged in the marine systems, whereas 24% was abiotically transformed to identifiable compounds in 14 d (Table 3 and Supplemental Data, Table S2). The unaccounted portion of RDX (18%) is comparatively less than for TNT in all the marine treatments. These results differ from the freshwater systems.

DISCUSSION

Removal of dissolved TNT and RDX at a rapid rate in our incubations regardless of the sediment type indicates the importance of uptake of energetic compounds onto sediments. Redox potentials of the sediment systems were in the range of 100 mV to 150 mV, maintaining anaerobic conditions [34] throughout the experiment. Both compound removals were consistent with first-order kinetics and attained equilibrium with sediment in all treatments of marine systems within 2 h after spiking, which was consistent with previous studies [13,21], as opposed to 96 h to 240 h in freshwater incubations. The uptake rate constants onto marine sediments were nearly 100 times higher than for freshwater sediment. The lower solubility of compounds in seawater (salinity of 30‰ in these experiments) may drive rapid uptake onto marine sediments through hydrophobic bonding, chemisorption, and electrostatic interactions, as they are polarizable organic compounds [22]. Hydrophobic sorption should have an

Table 3. Mass balance of target compounds in freshwater and marine systems at 3 different temperatures

SedimentType	Treatment	Physicalphase	Compoundname	Compound % 4 °C	15 °C	23 °C
Freshwater silt	TNT	Aqueous	TNT	48.8	57.9	56.9
			To. Tr. Pro.	1.4	1.4	1.1
		Particle	TNT	41.6	36.7	35.7
			To. Tr. Pro.	1.2	1.7	1.9
		Unknown		7.1	2.3	4.4
	RDX	Aqueous	RDX	26.9	29.0	30.4
			To. Tr. Pro.[a]	16.1	15.2	15.6
		Particle	RDX	12.8	10.9	8.7
			To. Tr. Pro.[b,c]	8.5	10.4	10.9
		Unknown		35.6	34.5	34.4
Marine silt	TNT	Aqueous	TNT	23.6	15.6	21.8
			To. Tr. Pro.[d]	2.22	2.0	2.0
		Particle	TNT	7.6	7.2	9.0
			To. Tr. Pro.[d]	0.1	0.2	—
		Unknown		66.6	75.0	67.1
	RDX	Aqueous	RDX	52.0	48.4	52.2
			To. Tr. Pro.[a,c]	29.1	16.0	0.4
		Particle	RDX	8.7	13.4	14.3
			To. Tr. Pro.[a,b]	3.6	4.6	4.61
		Unknown		6.7	17.6	28.6
Marine sand	TNT	Aqueous	TNT	34.1	25.9	32.4
			To. Tr. Pro.[d,e]	5.2	2.8	2.4
		Particle	TNT	8.8	3.2	8.4
			To. Tr. Pro.[d]	0.1	—	0.1
		Unknown		51.8	68.1	56.7
	RDX	Aqueous	RDX	53.3	45.0	48.6
			To. Tr. Pro.[a,c]	20.0	17.2	42.9
		Particle	RDX	0.1	7.4	5.3
			To. Tr. Pro.[a]	—	2.2	1.1
		Unknown		26.5	28.2	2.0

[a]Hexahydro-1-nitroso-3,5-dinitro-1,3,5-triazine (MNX).
[b]Hexahydro-1,3-dinitroso-5-nitro-1,3,5-triazine (DNX).
[c]Hexahydro-1,3,5-trinitroso-1,3,5-nitro-1,3,5-triazine (TNX).
[d]4-Amino-2,6-dinitrotoluene (4A-DNT).
[e]2-amino-4,6-dinitrotoluene (2A-DNT).
To. Tr. pro. = total transformation products.

important role for these compounds because they exhibit some hydrophobicity. This is also true for several of the degradation products, such as triaminotoluene (an anaerobic degradation product of TNT), which is also known to partition to sediments [35]. Electrostatic interactions may also occur between variable charged surfaces, such as soil organic matter, mineral oxides, and the edge sites of layered silicate minerals (feldspar and smectite group clays) and these explosive compounds. The charges on these surfaces arise most commonly through protonation and deprotonation reactions and are highly pH dependent [35].

Freshwater systems have lower pH values (7.0) than marine systems (7.9), and more protonation may lead to competition between the munition compounds studied (TNT, RDX) and H^+, which can be reversibly sorbed onto the sites of exchangeable cations and OH^- of clay surfaces in sediment [22]. Marine sediments with higher pH values may experience less site-specific competition and higher uptake of TNT and RDX ($0.30–0.80\,h^{-1}$) than that in freshwater sediments ($0.0046–0.0065\,h^{-1}$).

As for many other organic compounds, sorption is also influenced by the organic matter and clay content in the sediment, as has been observed for both marine and freshwater sediments [3,11,13,22,36]. Considering the mineralogy of the sediments used in the present study, marine sand contained a negligible amount of clay compared with both marine and freshwater silts. Finer grains, higher clay content, and high TOC and TN levels in marine silt compared with marine sand may facilitate sorption, resulting in higher uptake rates and K_d values. Although higher clay content may increase sorption of compounds, the presence of similar clay types in both silts suggests that clay mineralogy has a secondary role on sorption of munitions onto silts. However, it appears that the difference in K_d values for all slurries is sufficiently described linearly by the TOC content of the sediment for TNT (Figure 3A). The linearity of TOC content in sediment and K_d of TNT ($R^2 = 0.99$) was further confirmed from the Pearson correlation coefficient values, which were in the range of 0.95 to 0.98. For RDX, the K_d and TOC content in sediment showed a moderately linear relationship ($R^2 = 0.94–0.98$, Pearson correlation coefficient = 0.51–0.85), which suggests RDX sorption may undergo secondary sorption that may be significant at low TOC concentrations (Figure 3B). Although the uptake rates were much higher in marine sediments ($0.30–0.80\,h^{-1}$) relative to freshwater silt ($0.0046–0.0065\,h^{-1}$), equilibrium partition constants were in the same order of magnitude for both freshwater silt ($1.4–3.1\,L\,kg^{-1}$ sediment) and marine silt ($1.1–2.0\,L\,kg^{-1}$ sediment). Equilibrium partition constants for both freshwater and marine systems are consistent with reported literature values [8,11,12,26,28]. Marine sand had the lowest equilibrium partition constants, in a range of $0.72\,L\,kg^{-1}$ sediment to $0.92\,L\,kg^{-1}$ sediment. These results suggest fast sorption of TNT and RDX through electrostatic forces to marine sand (which may be reversible) followed by a small fraction of

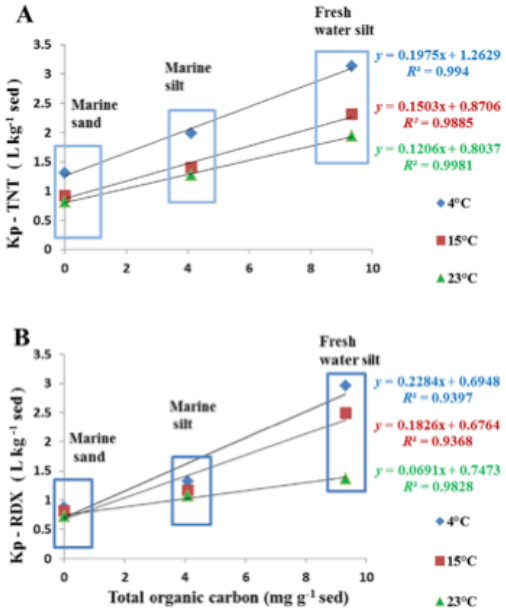

Figure 3. Correlation between total organic carbon of sediment and equilibrium partition coefficient (K_p) of (**A**) 2,4,6-trinitrotoluene (TNT) and (**B**) hexahydro-1,3,5-trinitro-1,3,5-triazine (RDX) at 4 °C, 15 °C, and 23 °C.

less reversible organic carbon sorption. Both marine silt and freshwater silt partitioning may be dominated by relatively high hydrophobic sorption of compounds, because both sediments contain considerable amounts of organic carbon (Table 1) and negative free energies of sorption (Table 2). Strong linear correlations between organic carbon and equilibrium partition constants of TNT (Figure 3A) further confirmed the importance of hydrophobic sorption of TNT onto the sediments.

Partitioning of TNT and RDX onto DOC was not significant in the slurries studied. Percentages of total aqueous munitions sorbed onto DOC are on the order of 0.13% to 0.49% among all sediment types. This is attributable to the dilution of the sediments into seawater; it is expected that porewaters of intact sediments would have DOC concentrations that are at least 10 times higher [37], and therefore the fraction of munitions on DOC in intact sediment porewaters would be on the order of 1% to 5%. The experimental partition coefficients derived in these experiments (K_{OC}) for TNT (320± 57 L/kg) and RDX (260± 25 L/kg) were on the same order of magnitude as values reported in the literature [8,9,38,39]. Predicted K_{OC} values using Equation 4 from Di Toro [32] for TNT were higher (920 L/kg) than those obtained experimentally for TNT and significantly lower for RDX (71 L/kg). Differences between predicted values based on hydrophobic parameters and those obtained experimentally may help to identify important secondary sorption processes. Quantitative structure–activity relationships based on Hammett substituent constants were consistent with derived K_{OC} values and reaction constants of 0.22 and 0.80 for TNT and RDX, respectively [40]. It is possible that the experimental K_d values for RDX contain both hydrophobic partitioning, as would be predicted in the 71 L/kg, and secondary sorption mechanism that accounts for the additional sorption. Further research is required to address these differences.

Higher sorption rates of TNT (0.48–0.80 h^{-1}) were observed than for RDX (0.30–0.35 h^{-1}) on both marine sediments. These results are consistent with published data that include sorption rates for TNT and RDX of 0.1 h^{-1} to 0.2 $h^{-1}$and 0.0005 h^{-1} to 0.0067 h^{-1}, respectively [41]. A higher K_{OW} of TNT supports hydrophobic sorption of TNT onto the organic matter in the sediment [42]. The K_d values of TNT and RDX clearly decreased as temperature increased for both freshwater and marine sediments (Figure 2), and the same trend was observed for the uptake rate constant except for the 15 °C treatment of marine sediments, which has the least data precision. Low temperatures are kinetically unfavorable for dissolution [19,20], resulting in more sorption onto sediments (Figure 2). Negative Gibbs free energies of sorption indicate that sorption of TNT and RDX onto freshwater and marine silt is spontaneous, whereas it is nonspontaneous for all the marine sand treatments, except at 4 °C for TNT. This factor further reveals that marine sand cannot act as a sink for these compounds as it does for both marine and freshwater silts. Spontaneity of the sorption reaction increased with decreasing temperature for both marine silt and freshwater silt (Table 2).

Marine systems show faster abiotic degradation than freshwater systems for TNT, as alkaline hydrolysis of TNT is facilitated by higher alkalinity in marine systems [3]. For TNT, the transformation product triaminotoluene, which is not identified in the present study, may be covalently bound onto the sediment [43] and comprise a significant portion of unknowns of the TNT pool. Gregory et al. [44] have identified ring-cleaved intermediate transformation products of RDX including NH_4^+, N_2O, and formaldehyde end products as a result of sequential reduction of RDX. In the present study, we did not analyze ring-cleaved intermediate transformation

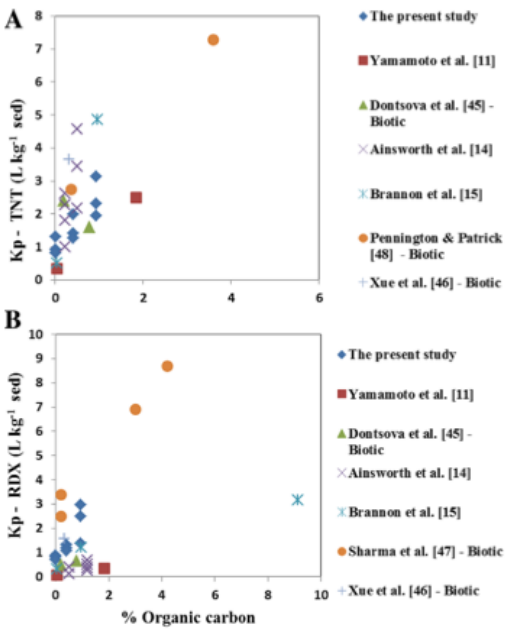

Figure 4. Relationship between percent organic carbon and equilibrium partition coefficient (K_p) of (**A**) 2,4,6-trinitrotoluene (TNT) and (**B**) hexahydro-1,3,5-trinitro-1,3,5-triazine (RDX) for sediments in freshwater and marine systems under different conditions published in the literature, including the present study.

products of RDX that could be key components to close the mass balance.

A comprehensive analysis of available data in the literature to date [11–15,41,45–48] shows agreement with our K_d values for TNT in all published data. Organic carbon is a reliable predictor for K_d of both compounds, and equilibrium partition constant values are in reasonable agreement between freshwater and marine systems (Figure 4). There are not enough uptake data at high salinities (the present study is the only one for RDX) to complete a comprehensive comparison.

However, among the 3 abiotic studies shown in Supplemental Data, Table S1, there was an exponential increase in uptake rates with salinity. A modest to negligible increase occurred between sorption rates from salinities between 0‰ and 20‰; between 20‰ and 30‰, however, the increase appears to be very significant (>50 times). There does not appear to be a relationship between uptake rate and percentage of organic carbon in the present study, although only 3 sediment types were tested. The present study provides the lower rate limit of transport and fate of these environmentally significant compounds. These constraints permit more robust modeling of total compound fate (biotic and abiotic) in marine settings.

Supplemental Data—Supplemental Data are available on the Wiley Online Library at DOI: 10.1002/etc.3149.

Acknowledgement—The present work was funded by US Department of Defense SERDP under project ID ER-2122. The authors thank C. Cooper for sediment collecting and D. Cady for laboratory support.

Data availability—All the data used can be accessed on request to the first author (thivanka.ariyarathna@uconn.edu).

REFERENCES

1. Jenkins TF, Pennington JC, Ampleman G. 2007. Characterization and fate of gun and rocket propellant residues on testing and training ranges: Interim report 1. ERDC TR-07-01. US Army Corps of Engineers Engineer Research and Development Center, Vicksburg, MS.
2. Pennington JC, Jenkins TF, Ampleman G. 2006. Distribution and fate of energetics on DOD test and training ranges: Final report. ERDC TR-06-13. US Army Corps of Engineers Engineer Research and Development Center, Vicksburg, MS.
3. Pichtel J. 2012. Distribution and fate of military explosives and propellants in soil: A review. *Appl Environ Soil Sci* 2012:617236.
4. Mittal AK. 2003. Military munitions: DOD needs to develop a comprehensive approach for cleaning up contaminated sites: Report to the Honorable John D. Dingell, Ranking Minority Member, Committee on Energy and Commerce, House of Representatives. GAO-04-147. US General Accounting Office, Washington, DC.
5. Agency for Toxic Substances and Disease Registry. 1995. Toxicological profile for 2,4,6-trinitrotoluene. US Department of Health and Human Services, Atlanta, GA. [cited 2015 February 10]. Available from: http://www.atsdr.cdc.gov/toxprofiles/tp81.pdf
6. Agency for Toxic Substances and Disease Registry. 2012. Toxicological profile for RDX. US Department of Health and Human Services, Atlanta, GA. [cited 2015 February 12]. Available from: http://www.atsdr.cdc.gov/toxprofiles/tp78.pdf
7. Kalderis D, Juhasz AL, Boopathy R, Comfort S. 2011. Soils contaminated with explosives: Environmental fate and evaluation of state-of the-art remediation processes (IUPAC technical report). *Pure Appl Chem* 83:1407–1484.
8. US Environmental Protection Agency. 2014. Technical fact sheet—2,4,6-Trinitrotoluene (TNT). EPA 505/F-14/009. Washington, DC. [cited 2015 February 15]. Available from: http://www2.epa.gov/sites/production/files/2014-03/documents/ffrrofactsheet_contaminant_tnt_january2014_final.pdf
9. US Environmental Protection Agency. 2014. Technical fact sheet—Hexahydro-1,3,5-trinitro- 1,3,5-triazine (RDX). EPA 505/F-14/008. Washington, DC. [cited 2015 February 15]. Available from: http://www2.epa.gov/sites/production/files/2014-03/documents/ffrrofactsheet_contaminant_rdx_january2014_final.pdf
10. International Agency for Research on Cancer. 1996. IARC Monographs on the Evaluation of Carcinogenic Risks to Humans, Vol. 65. [cited 2015 February 22]. Available from: http://monographs.iarc.fr/ENG/Classification/ClassificationsAlphaOrder.pdf
11. Yamamoto H, Morley MC, Speitel GE Jr., Clausen J. 2004. Fate and transport of high explosives in a sandy soil: Adsorption and desorption. *Soil Sed Contam* 13:459–477.
12. Sheremata TW, Halasz A, Paquet L, Thiboutot S, Ampleman G, Hawari J. 2001. The fate of the cyclic nitramine explosive RDX in natural soil. *Environ Sci Technol* 35:1037–1040.
13. Chappell MA, Porter BE, Price CL, Pettway BA, George RD. 2011. Differential kinetics and temperature dependence of abiotic and biotic processes controlling the environmental fate of TNT in simulated marine systems. *Mar Pollut Bull* 62:1736–1743.
14. Ainsworth CC, Harvey SD, Szecsody JE, Simmons MA, Cullinan VI, Resch CT, Mong GH. 1993. Relationship between the leachability characteristics of unique energetics compounds and soil properties. Project 91PP1800. US Army Biomedical Research and Development Laboratory, Fort Detrick, MD.
15. Brannon JM, Adrian GG, Pennington JC, Hayes C, Myers TE. 1992. Slow release of PCB, TNT and RDX from soils and sediments. Technical report EL-92-38. US Army Corps of Engineers, Waterways Experiment Station, Vicksburg, MS.
16. Harrison I, Vane CH. 2010. Attenuation of TNT in seawater microcosms. *Water Sci Technol* 61:2531–2538.
17. Spalding RF, Fulton JW. 1988. Groundwater munition residues and nitrate near Grand Island, Nebraska, U.S.A. *J Contam Hydrol* 2:139–153.
18. Juhasz AL, Naidu R. 2007. Explosives: Fate, dynamics, and ecological impact in terrestrial and marine environments. *Rev Environ Contam Toxicol* 191:163–215.
19. Brannon JM PJ. 2002. Environmental fate and transport process descriptors for explosives. ERDC/EL TR-02-10. US Army Engineer Research and Development Center, Vicksburg, MS.
20. Lynch JC, Brannon JM, Delfino JJ. 2002. Dissolution rates of 3 high explosive compounds: TNT, RDX, and HMX. *Chemosphere* 47:725–734.
21. Zhao XK, Yang GP, Gao XC. 2003. Studies on the sorption behaviors of nitrobenzene on marine sediments. *Chemosphere* 52:917–925.
22. Site AD. 2001. Factors affecting sorption of organic compounds in natural sorbent/water systems and sorption coefficients for selected pollutants. A review. *J Phys Chem* 30:187–439.
23. Pennington JC, Myers T, Davis WM, Olin TJ, McDonald TA, Hayes CA, Townsend DM. 1995. Impacts of sorption on in situ bioremediation of explosives-contaminated soils. TR-IRRP-95-1. US Army Engineer Waterways Experiment Station, Washington, DC.
24. Craig HD, Taylor S. 2011. Framework for evaluating the fate, transport, and risks from conventional munitions compounds in underwater environments. *Mar Technol Soc J* 45:35–46.
25. Miyares PH JT. 1990. Salting-out solvent extraction for determining low levels of nitroaromatics and nitramines in water. Special Report 90-30. US Army Corps of Engineers, Cold Regions Research and Engineering Laboratory, Hanover, NH.
26. US Environmental Protection Agency. 1994. Method 8330: Nitroaromatics and nitramines by high performance liquid chromatography (HPLC). SW846. Office of Solid Waste and Emergency Response, Washington, DC.
27. Pan X, Zhang B, Cobb GP. 2005. Extraction and analysis of trace amounts of cyclonite (RDX) and its nitroso-metabolites in animal liver tissue using gas chromatography with electron capture detection (GC-ECD). *Talanta* 67:816–823.
28. US Environmental Protection Agency. 2007. Method 8095: Explosives by gas chromatography. Office of Solid Waste and Emergency Response, Washington, DC.
29. Zhang B, Pan X, Smith JN, Anderson TA, Cobb GP. 2007. Extraction and determination of trace amounts of energetic compounds in blood by gas chromatography with electron capture detection (GC/ECD). *Talanta* 72:612–619.
30. Zhang B, Pan X, Cobb GP, Anderson TA. 2005. Use of pressurized liquid extraction (PLE)/gas chromatography-electron capture detection (GC-ECD) for the determination of biodegradation intermediates of hexahydro-1,3,5-trinitro-1,3,5-triazine (RDX) in soils. *J Chromatogr B* 824:277–282.
31. Hedges JI, Stern JH. 1984. Carbon and nitrogen determinations of carbonate-containing solids. *Limnol Oceanogr* 29:657–663.

32. Di Toro DM. 1985. A particle interaction model of reversible organic chemical sorption. *Chemosphere* 14:1503–1538.
33. Menking KM, Musler HM, Fitts JP, Bischoff JL, Anderson RS. 1993. Clay mineralogical analyses of the Owens Lake Core. 93-683. Open-File Report. US Geological Survey, Reston, VA.
34. Delaune RD RK. 2005. Redox potential. In Hillel D, ed, *Encyclopedia of Soils in the Environment*. Academic Press, New York, NY, USA, pp 366–371.
35. Weber WJ Jr, Voice TC, Pirbazari M, Hunt GE, Ulanoff DM. 1983. Sorption of hydrophobic compounds by sediments, soils and suspended solids—II. Sorbent evaluation studies. *Water Res* 17:1443–1452.
36. Weissmahr KW, Sedlak DL. 2000. Effect of metal complexation on the degradation of dithiocarbamate fungicides. *Environ Toxicol Chem* 19:820–826.
37. Moore TR. 2003. Dissolved organic carbon in a northern boreal landscape. *Global Biogeochem Cycles* 17:20–21.
38. Rosenblatt DH, Burrows EP, Mitchell WR, Parmer DL. 1991. Organic explosives and related compounds. In *The Handbook of Environmental Chemistry*, Vol 3, Part G. Spring-Verlag, Berlin, Germany.
39. Spanggord R, Mill T, Chou T, Mabey W, Smith J. 1980. Environmental fate studies on certain munition wastewater constituents. Phase III, laboratory studies, final report. 197, AD-A099256. SRI International, Menlo Park, CA, USA.
40. Hammett LP. 1937. The effect of structure upon the reactions of organic compounds. Benzene derivatives. *J Am Chem Soc* 59:96–103.
41. Brannon JM, Price CB, Yost SL, Hayes C, Porter B. 2005. Comparison of environmental fate and transport process descriptors of explosives in saline and freshwater systems. *Mar Pollut Bull* 50:247–251.
42. Haderlein SB, Weissmahr KW, Schwarzenbach RP. 1996. Specific adsorption of nitroaromatic explosives and pesticides to clay minerals. *Environ Sci Technol* 30:612–622.
43. Hawari J, Beaudet S, Halasz A, Thiboutot S, Ampleman G. 2000. Microbial degradation of explosives: Biotransformation versus mineralization. *Appl Microbiol Biotechnol* 54:605–618.
44. Gregory KB, Larese-Casanova P, Parkin GF, Scherer MM. 2004. Abiotic transformation of hexahydro-1,3,5-trinito-1,3,5-triazine by Fe II bound to magnetite. *Environ Sci Technol* 38:1408–1414.
45. Dontsova KM, Yost SL, Šimunek J, Pennington JC, Williford CW. 2006. Dissolution and transport of TNT, RDX, and composition B in saturated soil columns. *J Environ Qual* 35:2043–2054.
46. Xue SK, Iskandar IK, Selim HM. 1995. Adsorption-desorption of 2,4,6-trinitrotoluene and hexahydro-1,3,5-trinitro-1,3,5-triazine in soils. *Soil Sci* 160:317–327.
47. Sharma P, Mayes MA, Tang G. 2013. Role of soil organic carbon and colloids in sorption and transport of TNT, RDX and HMX in training range soils. *Chemosphere* 92:993–1000.
48. Pennington JC, Patrick WH Jr. 1990. Adsorption and desorption of 2,4,6-trinitrotoluene by soils. *J Environ Qual* 19:559–567.

2.7 Supplementary Material

Table: S-1: Published sorption parameters of TNT and RDX under abiotic and biotic conditions.

Study	Water type/Location	Sediment Type	Sediment Characteristics			System Characteristics		Kinetic parameters			
								TNT		RDX	
			% OC	Clay%	CEC ($cmolkg^{-1}$)	Temp (^0C)	pH	k (hr^{-1})	K_p ($Lkg^{-1}sed$)	k (hr^{-1})	K_p ($Lkg^{-1}sed$)
This Study	Marine/Long Island Sound (30 ppt)	Upper tidal sand	0.0038	0.80	-	4	7.9	0.5821	1.31	0.3163	0.87
						15		0.6180	0.92	0.3356	0.82
						23		0.4752	0.82	0.3013	0.72
		Intertidal silt	0.4101	56	-	4	7.9	0.6411	1.99	0.3554	1.32
						15		0.8001	1.40	0.3348	1.17
						23		0.5332	1.27	0.3120	1.08
	Fresh/Avery Point, CT (0.1ppt)	Fresh water silt	0.9320	34	-	4	7.0	0.0065	3.14	0.0060	2.96
						15		0.0053	2.31	0.0052	2.49
						23		0.0046	1.94	0.0048	1.37
Chappel et al., (2011)	Marine (Artificial, 20ppt)	Coarse, Low OC	0.12	2.4	22	8	8.0	0.0115	-	-	-
						15		0.0040	-	-	-
						25		0.0016	-	-	-
		Medium, Low OC	0.84	10.0	53	8	8.2	0.0040	-	-	-
						15		0.0045	-	-	-
						25		0.0084	-	-	-
		Fine, High OC	2.27	40.0	188	8	7.9	0.0113	-	-	-
						15		0.0110	-	-	-
						25		0.0141	-	-	-
Yamamoto et al., (2010)	Ground water/MMR, MA	Surface soil	1.84	7.9	9.20	22	4.73	0.00295*	2.5	0.00126*	0.36
		Deep soil	0.04	2.7	1.17		6.12	0.00144*	0.34	0.0031*	0.072
Sheremata et al., (2001)	Deionized water (Fresh)	Agricultural top soil /	8.4	4	14.6	25	5.6	-	-	0.0043*	0.83
Brannon et al., (2005) - **Biotic**	Marine/Artificial (20ppt)	Medium, high OC	7.41	14	47	20	5.4	0.105	-	0.00048	-
		Medium, low OC	0.83	11	13		6.8	0.198	-	0.00108	-
		fine, high OC	1.92	39	40		6.6	0.0985	-	0.00671	-
	Deionized water (Fresh, 0 ppt)	University Lake	7.41	14	47	20	5.4	0.102	-	0.00037	-
		Browns Lake	0.83	11	13		6.8	0.244	-	0.0009	-
		Texas Lake	1.92	39	40		6.6	0.158	-	0	-
Dontsova et	Fresh water	Plymouth loamy sand/	0.78	5.0	7.05	-	5.1	-	1.6	-	0.65

al., (2006) - **Biotic**		Alder silt loam	0.20	4.5	7.83	-	8.2	-	2.4	-	0.48
Ainsworth et al., (1993)	Fresh water	Soil,Horizon C	0.23	13	55.00	10	7.1	-	2.625*	-	-
						20	-	-	1.804*	-	-
						23	-	0.012*	2.267*	-	-
						50	-	-	0.999*	-	-
		Soil,Horizon BC	0.50	44	162.00	10	6.7	-	4.569*	-	0.400*
						20	-	-	3.435*	-	0.132*
						50	-	-	2.159*	-	-
		Soil,Horizon AP	1.19	11	2.49	10	5.3	-	-	-	0.514*
						20	-	-	-	-	0.370*
						23	-	-	-	0.0036*	0.690*
						50	-	-	-	-	0.274*
Brannon et al., (1992)	Fresh water	Massonry sand	0.036	2.5	1.73	-	-	-	0.517	-	0.305
		Tunica silt	0.960	6.3	73.00	-	-	-	4.850	-	1.220
		Muck soil	9.130	-	168.00	-	-	-	-	-	3.170
Pennington & Patrick, (1990) - **Biotic**	Fresh water	High OC	3.592	23.8	102.0	-	6.77	0.7156*	7.2725	-	-
		Low OC	0.367	10.6	16.3	-	4.40	0.5637*	2.7377	-	-
Xue et al., (1995) - **Biotic**	Fresh water	Norwood soil	0.32	18.0	4.10	-	7.4	-	3.64	-	1.57
		Kolin soil	-	10.6	16.3	-	4.4	-	2.66	-	1.59
Sharma et al., (2013) - **Biotic**	Fresh water	Low OC	0.2	6.9	1.8	25	4.6	-	-	-	3.4
		Low OC, Soil horizon B	0.2	9.7	1.8	25	4.3	-	-	-	2.5
		High OC, Soil horizon E	3.0	1.5	3.9	25	3.8	-	-	-	6.9
		High OC	4.2	<1	7.1	25	5.2	-	-	-	8.7

* Calculated from original data

Table: S-2: Mass balance of target compounds in fresh water and marine systems at three different temperatures.

Sediment type	Treatment	Physical phase	Compound Name	Compound %		
				4 ^{0}C	15 ^{0}C	23 ^{0}C
Fresh Water silt	TNT	Aqueous	TNT	48.8	57.9	56.9
			4A-DNT	1.4	1.4	1.1
		Particle	TNT	41.6	36.7	35.7
			4A-DNT	1.2	1.7	1.9
		Unknown		7.1	2.3	4.4
	RDX	Aqueous	RDX	26.9	29.0	30.4
			MNX	16.1	15.2	15.6
		Particle	RDX	12.8	10.9	8.7
			DNX	2.6	2.8	2.7
			TNX	5.9	7.6	8.2
		Unknown		35.6	34.5	34.4
Marine Silt	TNT	Aqueous	TNT	23.6	15.6	21.8
			4A-DNT	2.2	2.0	2.1
		Particle	TNT	7.6	7.2	9.0
			4A-DNT	0.1	0.2	-
		Unknown		66.6	75.0	67.1
	RDX	Aqueous	RDX	52.0	48.4	52.2
			MNX	1.5	-	-
			TNX	27.6	15.9	0.4
		Particle	RDX	8.7	13.4	14.3
			MNX	1.2	2.2	2.2
			DNX	2.4	2.4	2.4
		Unknown		6.7	17.6	28.6
Marine Sand	TNT	Aqueous	TNT	34.1	25.9	32.4
			4A-DNT	4.7	2.8	2.4
			2A-DNT	0.6	-	-
		Particle	TNT	8.8	3.2	8.4
			4A-DNT	0.1	-	0.1
		Unknown		51.8	68.1	56.7
	RDX	Aqueous	RDX	53.3	45.0	48.6
			MNX	6.5	7.8	18.7
			TNX	13.5	9.4	24.2
		Particle	RDX	0.1	7.4	5.3
			MNX	-	2.2	1.1
		Unknown		26.5	28.2	2.0

Table S3: Compound specific recoveries and detection limits for parent and transformation products.

Compound	Detection limit (ng/mL)
TNT	7.8
2A-DNT	7.5
4A-DNT	7.5
RDX	7.2
MNX	7.4
DNX	7.3
TNX	7.4

Figure S-1: GC-ECD chromatograms of munition compounds of A) standards B) water extraction from marine sand system C) sediment extraction from marine sand system

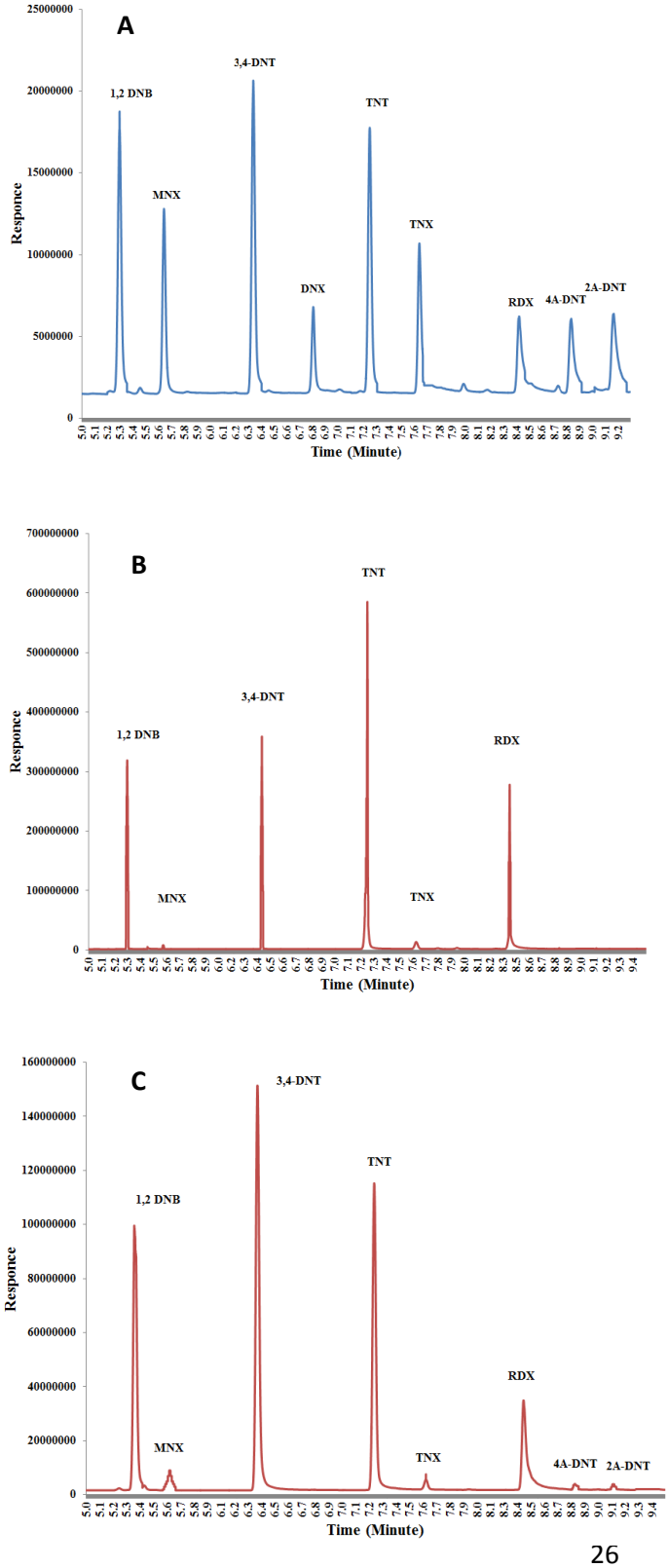

Figure S-2: X-ray diffractometer (XRD) spectrums of clay compositions of A) freshwater silt B) Marine silt ; Peaks corresponds to plagioclase (Na-feldspar), k-feldspar and smectite group clays are shown at series of 2Θ angles of (3.18, 27.9) , (3.24, 27.5) and (5.2, 17) respectively.

(Reference: Open-File Report, US geological Survey)

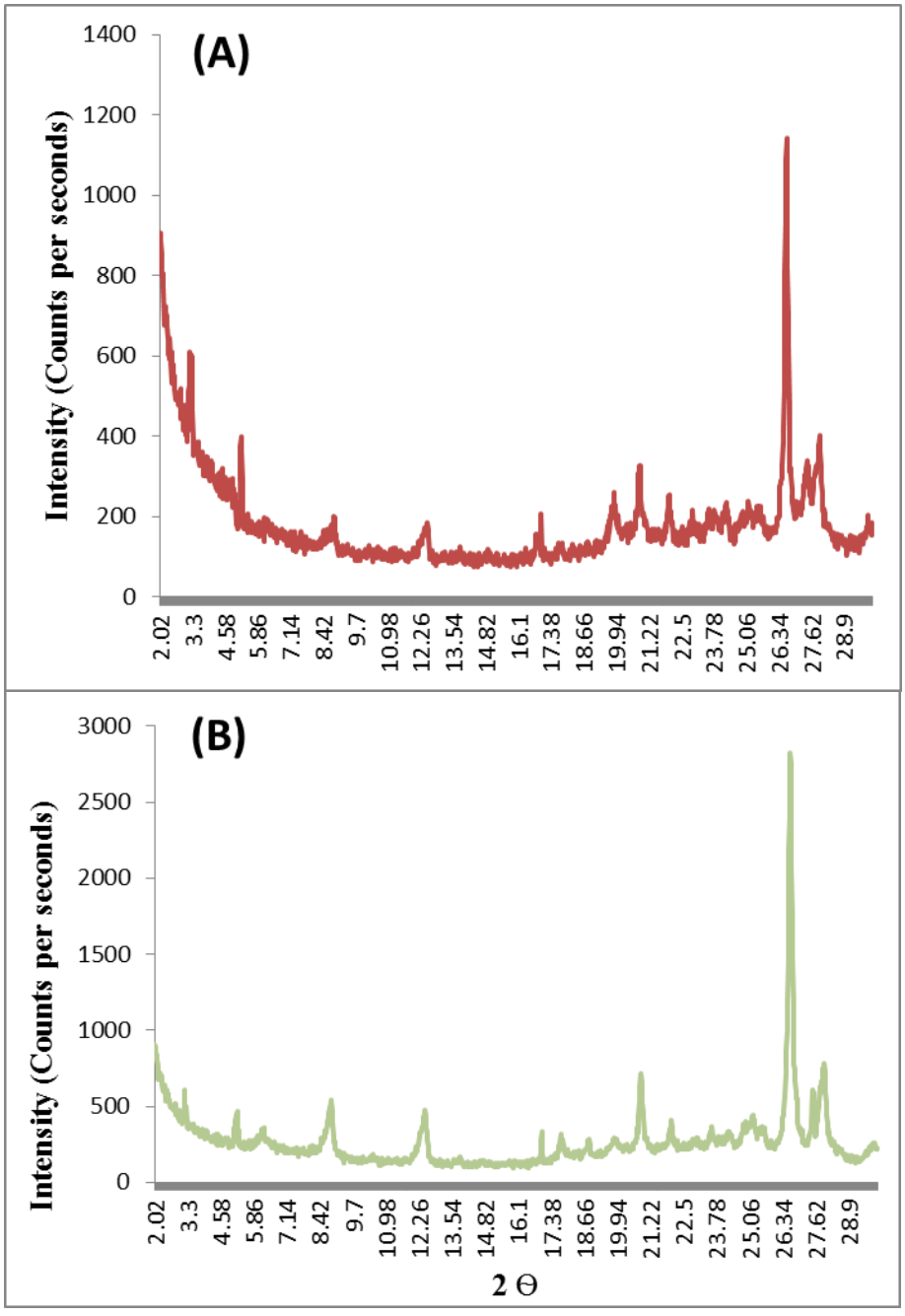

Figure S-3: Time series ln values of aqueous concentrations of A) TNT in the marine sand system B) RDX in the marine sand system C) TNT in the marine silt system D) RDX in the marine silt system E) TNT in the freshwater silt system F) RDX in the freshwater silt system at three different temperatures, 4^0C, 15^0C, 23^0C.

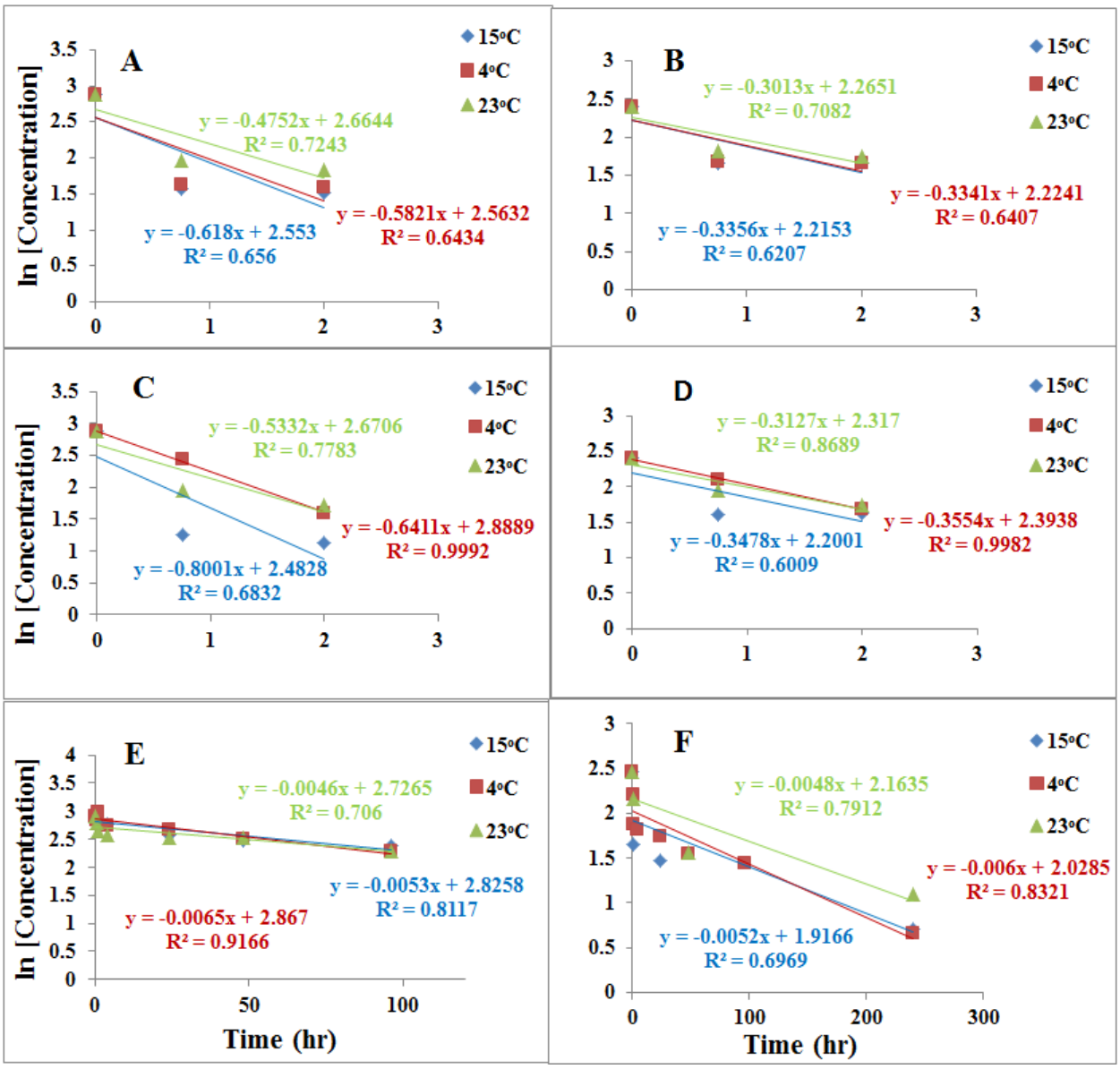

3.0 Biodegradation and mineralization of isotopically labeled TNT and RDX in anaerobic marine sediments

3.1 Abstract

The lack of knowledge on fate of explosive compounds, 2,4,6-trinitrotoluene (TNT) and hexahydro-1,3,5-trinitro-1,3,5-triazine (RDX) particularly in marine ecosystems constrains the application of bioremediation techniques in explosive-contaminated coastal sites. Here, we present a comparative study on anaerobic biodegradation and mineralization of ^{15}N-nitro group isotopically labeled TNT and RDX in organic-carbon-rich, fine-grained marine sediment with native microbial assemblages. Separate sediment slurry experiments were carried out for TNT and RDX at 23°C for 16 days. Dissolved and sediment-sorbed fractions of parent and transformation products, isotopic compositions of sediment and mineralization products of the dissolved inorganic nitrogen (DIN) pool ($^{15}NH_4^+$,$^{15}NO_3^-$,$^{15}NO_2^-$ and $^{15}N_2$) were measured. TNT was removed from the aqueous phase at a faster rate (0.75 hr^{-1}) than RDX (0.37 hr^{-1}) and ^{15}N accumulation in sediment was higher in the TNT microcosms (13%) than RDX (2%). Mono-amino-dinitrotoluenes were identified as intermediate biodegradation products of TNT. TNT-N (2% of the total spiked) is mineralized to DIN through two different pathways: denitration, and deamination and formation of NH_4^+, facilitated by iron and sulfate reducing bacteria in the sediments. Majority of the spiked TNT-N (85%) is in unidentified pools by day 16. RDX (10%) biodegrades to nitroso-derivatives, while 13% of RDX-N in nitro groups is mineralized to DIN anaerobically by the end of the experiment. NH_4^+ is the primary identified mineralization end-product of RDX (40%) generated through either deamination or mono-denitration followed by ring breakdown. A reasonable production of N_2 gas (13%) was seen in the RDX system but not

in the TNT system. RDX-N (68% of the total spiked) is in an unidentified pool by day16 and may include unquantified mineralization products dissolved in water.

Keywords

TNT, RDX, Anaerobic biodegradation, Marine sediment, ^{15}N isotopically labeled

3.2 Introduction

Though the disposal of explosives into the ocean has been prohibited in the United States since the "ocean dumping act" in 1972 [1], intact, breached or buried munitions from past disposal activities slowly release explosive chemicals into the adjacent marine settings through corrosion and leaking resulting in potential risks to human health and the marine resources [2]. Ongoing Military training and weapon testing activities of the department of defense (DoD), which owns more than 10% of the 1,240 sites currently on the National Priorities List [3], is a continuous source of explosives in coastal environments where marine aquatic life is exposed, as are humans through direct exposure and/or the food chain [4]. Energetic compounds are not expected to persist over timescales of several years in coastal environments, but, explosive dumping sites and areas proximal to military training sites have shown persistent concentrations of energetic compounds [1,5].

TNT has been linked to altered liver function and anemia in humans [3] and both TNT and derivatives including 1,3,5-trinitrobenzene, 2,4,6-trinitrobenzaldehyde , 4,6-dinitroanthranil, 2,4,6-trinitrobenzonitril and N-hydroxylamines have shown toxicity and mutagenic potential in salmonella Typhimurium Strains, mammals and aquatic species (fathead minnow, rainbow trout, channel catfish, worms, oyster larvae) [4]. RDX is considered a known neurotoxin for humans [4] and both TNT and RDX are classified as possible human carcinogens under group 3 in the International Agency for Research on Cancer carcinogenic categorization and Group C by the

United States Environmental Protection Agency (USEPA) [6].

Munitions contamination from explosives is widespread globally, including areas off the US coasts and Hawaii, Gulf of Mexico, North Sea, Baltic Sea, Mediterranean Sea and off the coasts of Europe and Russia [1]. Since the estimated cost of complete cleanup at active military installations, closed bases, and other former military properties is in the tens of billions of US dollars [1], it is extremely important to have a better understanding of natural biodegradation, mineralization pathways and rates to plan cost effective bioremediation techniques. Currently available literature on biodegradation of TNT and RDX address freshwater and groundwater systems extensively [4,7] and a limited number of studies have been focused on marine environment in terms of characterizing metabolites and mass balancing in the systems [8-10]. As nitrogen containing compounds, TNT and especially RDX with high N/C ratios are quite susceptible to microbial breakdown in nitrogen-limited marine ecosystems [9].

The breakdown of TNT and RDX is determined by both the environment and the physical-chemical properties of the compounds which include solubility, octanol-water partition constants, vapor pressure, Henry's Law constants and bond energies [6]. It is well established that TNT and especially RDX anaerobically biodegrade forming various reduced by-products although significant uncertainties are observed in breakdown pathways [10-12]. Anoxic sediment is a favorable biodegradation zone of TNT and RDX in natural coastal habitats [10,11] and the extent of biodegradation relies on sediment properties including organic carbon content, surface charge and oxidation state, sediment texture and mineralogy, diversity and quantity of microbial populations and redox conditions [6,7]. It has been documented that nitro groups of TNT are reduced to amino groups forming mono, di and tri-aminotoluenes under anaerobic conditions [4,13,14]. Mineralization of TNT also has been reported in nitrate reducing [15] and sulfate

reducing conditions [14,15], but the extent and pathways of mineralization remain controversial [8,9,11]. RDX is known to anaerobically biodegrade through sequential reduction to form more toxic nitroso-derivatives [16]. Though it has been identified that denitration, denitrification, deamination and ring breakdown are involved in further mineralization of RDX [11,12,17], the relative importance of these mechanisms in natural systems, particularly marine settings, is unknown.

Most of the existing studies evaluating the breakdown of TNT and RDX in sediments incubate pure microbial strains in nutrient rich media under laboratory controlled conditions [16,18]. A few studies have used natural coastal microbial assemblages to study TNT and RDX breakdown using isotopically ^{14}C labeled [8,9] and ^{15}N labeled compounds [10,11] suggesting the necessity of more experiments to characterize the metabolites and kinetic pathways of these compounds in marine sediments.

In this study, bench-top sediment slurry experiments using fine grained, organic rich marine sediment were conducted using ^{15}N isotopically labelled TNT and RDX. Separate experiments were conducted for the two compounds over 16 days and time series data was obtained for a subset of degradation and mineralization products of target compounds over the course of the experiment. The data were combined to calculate transformation rates, trace the degradation pathways and develop mass balance models for TNT and RDX. Further, this study allows for comparison of the removal of TNT and RDX from aqueous phases via both sorption and degradation under biotic conditions with that of a previous study performed under abiotic conditions [6] which had been conducted using a similar experimental set-up and sediment from the same field location, offering a novel and incremental comparison and this type of study has not been done related to the explosives in the past. The use of ^{15}N labeled compounds in tracing

the breakdown pathways of TNT and RDX entering inorganic nitrogen pools such as ammonium (NH_4^+), nitrates (NO_3^-), nitrites (NO_2^-) and nitrogen gas (N_2) provides the nitrogen based mass balance of the systems that will help to reveal pathways [10]. Identification and quantification of prominent pathways/ultimate pools of TNT and RDX facilitate determining the most suitable bioremediation techniques applied to marine sediments in coastal environments. Moreover, this approach may provide insight to favorable conditions for bioremediation including sediment properties and environmental parameters such as pH, redox, reduced sulfur and iron species.

3.3 Materials and methods

TNT and RDX (>99 purity) with and without isotopically labeled nitro groups were synthesized at the Naval Munitions Command, China Lake, CA, USA. All standards were purchased from Accustandard, New Haven, CT and solvents were high purity from Fisher Scientific. Sediment and sea water were collected from 41°18′03.42″N / 72°07′14.09″W and 41°19′04.50″N / 72°04′00.52″W in the intertidal zones of Waterford and Groton, Connecticut, USA respectively.

3.3.1 Incubation experiments

Fine grained, organic rich marine sediment (100g) was mixed with filtered (polyethersulfone-0.2μm) sea water (30 ‰) at a mass ratio of 1:4 [19] in 500mL glass bottles covered with aluminum foil to inhibit photo-degradation. Sediment slurries were continuously mixed on magnetic stirrer plates at 23^0C over the course of the experiment. After a 24 hr equilibration time, slurries were separately spiked with 36 μL of nitro group labeled ^{15}N-TNT (15 atom % ^{15}N total) or 41 μL ^{15}N-RDX (7.5 atom% ^{15}N total) dissolved in acetone to achieve concentrations of 4 mg L^{-1} and 2.5 mg L^{-1} for TNT and RDX respectively. The final concentration of acetone was less than 0.01% by volume. Two separate experiments for TNT and RDX were conducted including three controls for each. Samples were collected in triplicates at preset intervals (5 total)

over the 2 week duration of the experiment and each slurry was sacrificed at the time of sampling. Aqueous samples were collected for quantifying target and breakdown products including a subset of transformation and mineralization products while sediment samples were analyzed for target and breakdown products and sediment bulk ^{15}N.

3.3.2 System characterization

Physical parameters of the systems including pH, temperature and salinity were measured using a YSI probe (YSI 556 MPS). Redox potentials of sediment systems were measured using a platinum electrode (Paleo Terra, Amsterdam) relative to an Ag/AgCl reference electrode (Fisher Scientific) over the course of the experiment. Water samples were filtered through polyethersulfone - 0.2µm (0.2 µM PES) syringe tip filters and analyzed for nutrients including NH_4^+ and total NO_3^- and NO_2^- using a Smartchem nutrient analyzer (Westco-W12623) following cadmium azo-dye and phenol hypochlorite methods [7], respectively. A 40 ml water sample was filtered (0.2 µM PES) and acidified with hydrochloric acid to a pH of 2 for dissolved organic carbon (DOC) analysis using a total organic carbon (TOC) analyzer (Shimadzu TNM-1). 3 ml of water were filtered (0.2 µM PES) and analyzed using a ferrozine method [20] and methylene blue method [21] for dissolved ferrous and hydrogen sulfide respectively in aqueous phase by UV/Vis spectrophotometer (Hitachi-U-30110).Sediment was characterized for TOC, total nitrogen (TN) and total elemental sulfur (S) using a Perkin Elmer elemental analyzer (NA 1500). Sediment texture was determined using a mechanical sieve analyzer with a set of sieves from 0.063 mm to 2.0 mm. Clay compositions in the sediment were determined by X-ray diffractometer (XRD) (Rigaku Ultima IV / Cu Kα (λ = 0.15406 nm) radiation; beam voltage 40 kV; beam current 44 mA).

3.3.3 Explosives analysis

Reduced degradation products, including TNT-derived 2-amino-4,6-dinitrotoluene (2-ADNT) and 4-amino-2,6-dinitrotoluene (4-ADNT), and RDX-derived Hexahyro-1-nitroso-3,5-dinitro-1,3,5-triazine (MNX), Hexahyro-1,3-dinitroso-5-nitro-1,3,5-triazine (DNX), and Hexahyro-1,3,5-trinitroso-1,3,5-nitro-1,3,5-triazine (TNX), were analyzed in aqueous and sediment samples. A modified salting-out method [22] adapted for smaller sample sizes was used for extraction of munition compounds from aqueous samples following methods described in Ariyarathna et al. [6]. An average recovery of 99.1 ± 0.5% was obtained for known amounts of 1, 2-dinitrobenzene (1,2-DNB) in water extractions. Sediment bound munitions were extracted using 2g of freeze dried sediments [6] and average recoveries of munitions from sediment samples were 82 ± 7 % based on 1,2-DNB added to the triplicate sediment samples. Both water and sediment extractions were analyzed using gas chromatography (GC)/electron-capture detection (ECD) following the methods described by Ariyarathna et al. [6]. 3, 4-dinitrotoluene (3,4-DNT) was added to each extract prior to injection to monitor detection efficiency. Explosive analysis was performed with an Agilent GC/ECD [6] equipped with an HP-DB5 column (30 m x 320 µm, 0.25-µm; Agilent). Quantification was based on an external calibration curve of available standard munitions TNT, 2-ADNT, 4-ADNT, RDX, MNX, DNX and TNX. (AccuStandard, New Haven, CT). The average reporting limit for all compounds was 7.8 ng mL^{-1}.

3.3.4 Bulk ^{15}N analysis in sediment

Freeze dried sediment samples were analyzed using a continuous flow elemental analyzer – isotope ratio mass spectrometry (EA-IRMS: Delta V, Thermofisher) at the University of Connecticut for ^{15}N enrichments. Nitrogen isotope ratios are reported in δ notation as follows:

$$\delta^{15}N = [(R_{sample} - R_{STD})/R_{STD}] \quad (1)$$

where R_{STD} is the $^{15}N/^{14}N$ ratio of atmospheric nitrogen and R_{sample} is the $^{15}N/^{14}N$ ratio of the sample. $\delta^{15}N$ values are reported in parts per mil (‰) and external calibration was done using glutamic acid standards purchased from US Geological Survey. USGS 40 and USGS 41 were used for the quantification of ^{15}N mass in sediment (Equation 2). Triplicate sediment samples replicated with coefficient of variance of 0.35.

$$^{15}N \text{ mols Excess} = N \text{ mols} * (X^{15}N_t - X^{15}N_{t0}) \quad (2)$$

where the total N mass, and mole fractions of ^{15}N at time t ($X^{15}N_t$) and time 0 ($X^{15}N_{t0}$) were obtained from an elemental analyzer – isotope ratio mass spectrometry EA-IRMS (Delta V, Thermofisher).

3.3.5 Mineralization product analysis

The mineralization products, $^{15}NH_4^+$, $^{15}N_2$ and total $^{15}NO_2^-$ and $^{15}NO_3^-$ ($^{15}NO_X$) in the aqueous phase, were quantified using IRMS techniques. Filtered (0.2 µM PES), frozen water samples were extracted for NH_4^+ following the methods from Holmes et al. [23]. NH_4^+ in aqueous samples was converted to ammonia using magnesium oxide and absorbed onto glass fiber filters trapped in a sealed filter packet. Dried glass fiber filters were analyzed for ^{15}N using a continuous flow EA-IRMS similar to the analysis of bulk ^{15}N in sediments. Microcosm samples where done in triplicates at each time point and replicated with coefficient of variance of 0.8 while extraction efficiencies were between 95-105% based on the recovery of NH_4NO_3 standards. Moles of $^{15}NH_4^+$ were calculated using NH_4^+ concentrations and mole fractions of ^{15}N ($X^{15}N_t$ and $X^{15}N_{t0}$) obtained from Smartchem nutrient analyzer and EA-IRMS respectively (equation 3).

$$^{15}NH_4^+ \text{ mols Excess} = NH_4^+ \text{ mols} * (X^{15}N_t - X^{15}N_{t0}) \quad (3)$$

$^{15}N_2$ in water samples was determined using continuous flow isotope ratio mass spectrometry on a Thermo Delta V Plus with a Gas Bench interface (GB-IRMS). Triplicate gas samples were collected at each time point by pumping unfiltered seawater into 30 ml serum bottles that had previously been sealed, pre-loaded with 750µl of 2N KOH (for preservation), and flushed with He for 12 minutes [11]. After at least 6 hours of headspace equilibration, the isotopic composition of N_2 ($\delta^{15}N_2$) was measured with coefficient of variance of 0.2. By applying Henry's law [24] , dissolved N_2 mols in aqueous phase, N_2 mols,aq was calculated by using N_2 determined based on air standards, N_2 mols,air and dimensionless Henry's law constant, K_H (equation 4).

$$N_2 \text{ mols,aq} = N_2 \text{ mols,air} / K_H \quad (4)$$

$^{15}N_2$ aq was calculated from the measured mole fraction of dissolved N_2 ($X^{15}N_2$) and aqueous N_2 concentration.

$\delta^{15}NO_X$ (total $^{15}NO_2^-$ and $^{15}NO_3^-$) values were obtained via the denitrifier method using *Pseudomonas aureofaciens* [10] at the US Geological Survey (USGS) in Reston, VA on water samples filtered through a 0.2µM PES filters and frozen. Moles of $^{15}NO_X$ were calculated using NO_X concentration and mole fractions of ^{15}N ($X^{15}N_t$ and $X^{15}N_{t0}$) obtained from Smartchem nutrient analyzer and GB-IRMS respectively (equation 5).

$$^{15}NO_X \text{ mols Excess} = NO_X \text{ mols} * (X^{15}N_t - X^{15}N_{t0}) \quad (5)$$

3.3.6 Data analysis

The measured time series concentrations of TNT and RDX in water [C_i] were used to calculate removal rate constants of compounds according to equation 6,

$$\ln [C_i] = -k_{r,i}t + \ln [C_i]_{t=0} \quad (6)$$

where t is time (hr) and $k_{r,i}$ is the first order removal rate constant of compound i in hr^{-1}.

The rate of formation of mineralization product j was used to derive the first order formation rate constant ($k_{f,j}$) wherein for n first order degradation products,

$$k_{r,i} = k_{f,1} + k_{f,2} + \ldots + k_{f,n} \quad (7)$$

The measured time series concentrations of degradation products, $C_{product\ j}$ were used to estimate the removal rate constants wherein

$$k_{f,j}[C_{parent\ i}] - k_{r,j}[C_{product\ j}] = k_{r,j}[C_{product\ j}]_{net} \quad (8)$$

where t is time (hr) and k is the first order rate constant in hr^{-1}.

Removal rate constants (Equation 6) represent the total of sorption, biotic and abiotic transformation while degradation and mineralization rate constants (Equation 7, 8) consist of biotic and abiotic transformation. Furthermore, the total biotic component was obtained by subtracting aquatic concentrations in abiotic treatments from the aquatic concentrations in biotic treatments (Total of biotic and abiotic) based on biotic removal rate constants of TNT and RDX were calculated using equation 7 and 8.

A mass balancing approach was based on ^{15}N equivalents in masses of each analyzed N-containing parent and derivative pools and illustrated in following equations (Equations 9 and 10).

$$^{15}N\text{-}TNT_{system} = {}^{15}N\text{-}TNT_{water} + {}^{15}N\text{-}TNT_{sediment} + {}^{15}N\text{-}2A\text{-}DNT_{water} + {}^{15}N\text{-}2A\text{-}DNT_{sediment} + {}^{15}N\text{-}4A\text{-}DNT_{water} + {}^{15}N\text{-}4A\text{-}DNT_{sediment} + {}^{15}N\text{-}NH_4^{+}{}_{water} + {}^{15}N\text{-}N_{2\ water} + {}^{15}N\text{-}NO_{X\ water} + \text{unidentified } {}^{15}N\text{-compounds}_{\ water\ and/or\ sediment} \quad (9)$$

where, ^{15}N-TNTsystem represents total mols of ^{15}N-TNT spiked into the system and all the other terms represent ^{15}N moles measured in different TNT-derived metabolites in water and sediment.

$$^{15}\text{N-RDX}_{\text{system}} = {}^{15}\text{N-RDX}_{\text{water}} + {}^{15}\text{N-RDX}_{\text{sediment}} + {}^{15}\text{N-MNX}_{\text{water}} + {}^{15}\text{N-MNX}_{\text{sediment}} + {}^{15}\text{N-DNX}_{\text{water}} + {}^{15}\text{N-DNX}_{\text{sediment}} + {}^{15}\text{N-TNX}_{\text{water}} + {}^{15}\text{N-TNX}_{\text{sediment}} + {}^{15}\text{N-NH}_4^{+}{}_{\text{water}} + {}^{15}\text{N-N}_{2\ \text{water}} + {}^{15}\text{N-NO}_{\text{X water}} + \text{unidentified } {}^{15}\text{N-compounds}_{\ \text{water and/or sediment}} \quad (10)$$

where, ^{15}N-RDX system represents total mols of ^{15}N-RDX spiked into the system and all the other terms represent ^{15}N measured in different RDX-derived metabolites in water and sediment. Bacterial incorporation of nitrogen from energetics are calculated using incorporation rates published in [9] (Incorporation rates for TNT and RDX are 27.3 µg C L^{-1} d^{-1} and 4 µg C L^{-1} d^{-1} respectively at salinity of 30 PSU).

Principle component analysis (PCA) was carried out to obtain a better understanding of transformation pathways and to evaluate the effect of geochemical variables on the breakdown of TNT and RDX in anaerobic marine sediment systems. PCA was performed using all measured pools of ^{15}N and geochemical variables as metrics at 16 days for both TNT and RDX microcosms separately using 'Excelstat'. Metrics used in PCA were mean normalized, and missing gaps in the data were filled using the values of the detection limit of the instruments of particular analysis.

3.4 Results

3.4.1 Removal of TNT and RDX from the aqueous phase

Incubation experiments for TNT and RDX were conducted anaerobically [25] with redox potential varying from 53mV to -133mV and from 83mV to -231mV respectively (Table 1) throughout the experiment. Table 1 summarizes the physical system over the time series.

Table 1: Time series variation of chemical and physical properties of slurry water for TNT and RDX systems in this study (n=3)

Treatment	Time point	Physical properties		Chemical properties				
		pH	Redox(mV)	DOC (µM)	NH_4^+ (µM)	Tot. NO_2^- & NO_3^- (µM)	H_2S (µM)	Fe^{+2} (µM)
TNT	T0	7.41±0.01	41.13±2.66	1685±56	36±4	3.4±1.2	ND	2.20±0.08
	T1	7.33±0.05	54.30±2.59	2437±405	70±16	7.6±3.0	ND	2.54±0.19
	T2	7.03±0.02	39.93±5.20	2419±68	78±8	0.22±0.22	ND	4.30±1.33
	T3	7.19±0.09	29.40±3.93	2066±569	86±25	2.1±0.4	ND	3.48±1.26
	T4	6.97±0.05	-26.1±19.95	909±20	24±15	3.5±1.8	ND	18.15±6.62
	T5	7.10±0.18	-133.5±4.95	918±184	21±16	ND	70.41±0.39	33.27±0.39
RDX	T0	7.50±0.08	83.37±2.00	1912±27	196±1	1.3±0.8	ND	6.94±2.34
	T1	7.53±0.16	73.97±0.91	2423±8	27±3	4.2±2.7	ND	3.95±0.63
	T2	7.38±0.05	69.57±0.90	2669±312	48±4	4.6±2.5	ND	4.10±0.36
	T3	7.17±0.01	59.33±1.53	2432±323	136±91	3.8±0.9	ND	12.62±1.53
	T4	7.03±0.12	47.03±22.3	1759±435	398±236	0.19±0.08	ND	33.92±18.32
	T5	7.14±0.09	-231±64.37	1262±263	373±61	0.17±0.09	530.94±20.32	91.54±10.26

T0, T1, T2, T3, T4 and T5 represent 0, 0.45, 2.5, 48, 244, 388 hr for TNT treatments and 0, 0.75, 2.5, 72, 244, 388 hr for RDX treatments throughout the experimental time periods; DOC = Dissolved organic carbon includes the spike of munitions; NH_4^+ = ammonium; Tot. NO_2^- & NO_3^- = Total nitrite and nitrate; H_2S = Hydrogen Sulfide; Fe^{+2} = Ferrous; ND = not detected

TNT was rapidly removed from 17.6 µM to 0.028 µM in the aqueous phase following first order kinetics with a rate constant of 0.75 ± 0.08 hr^{-1}. This was greater than that in a similar experimental set-up under abiotic conditions which contained a different batch of sediment samples from the same field location determined in Ariyarathna et al. [6] of 0.53 ± 0.08 hr^{-1} (Table 2). The total TNT removal rate constant solely from the biotic component (biodegradation and biotic mineralization) is estimated as 0.22 ± 0.11 hr^{-1} (Supplemental data, Table S1). 2-aminodinitrotoluene (2A-DNT) and 4-aminodinitrotoluene (4A-DNT) were identified as measurable derivatives of TNT in the aqueous phase (Figure 1A), rapidly forming until t = 2.5 hr at rates of 0.028 hr^{-1} (R^2 = 0.99) and 0.030 hr^{-1} (R^2 = 0.99) respectively (Table 2).

Table 2: First order rate constants of production and loss of analytes in anaerobic marine sediment slurries at 23 ^{0}C

Treatment	Medium	Analyte	Rate constant (hr^{-1})	
			Production Rate	Loss Rate
TNT/Abiotic	Aqueous	TNT	-	0.53 (R^2 = 0.78)
TNT/Biotic	Aqueous	TNT	-	0.75 (R^2=0.94)
		4A-DNT	0.030 (R^2=0.99)	0.56 (R^2=0.85)
		2A-DNT	0.028 (R^2=0.99)	0.52 (R^2=0.98)
		NH_4^+	0.047 (R^2=0.42)	Steady state at day10
		NO_X	0.47 (R^2=1)	0.0067 (R^2=0.85)
	Sediment	Bulk ^{15}N	0.017 (R^2=0.99)	Steady state at day 2
		TNT	Peaks at 0.45hr	0.0049 (R^2=0.89)
		4A-DNT	0.095 (R^2=1)*	0.046 (R^2=0.54)
		2A-DNT	0.19 (R^2=1)*	0.16 (R^2=0.59)
RDX/Abiotic	Aqueous	RDX	-	0.31 (R^2 = 0.87)
RDX/Biotic	Aqueous	RDX	-	0.37 (R^2=0.79)
		TNX	Peaks at 0.75hr	Steady state at 0.75hr
		NH_4^+ -initial	0.017 (R^2=0.83)	Approaching steady state after16 days
		NH_4^+ -final	0.0061 (R^2=0.87)	
		NO_X	0.0138 (R^2=0.99)	Not calculated
		N_2	0.041 (R^2=0.91)	Steady state at day 3
	Sediment	Bulk ^{15}N	Peaks at 0.75hr	0.0021 (R^2=0.86)
		RDX	Peaks at 0.75hr	0.0091 (R^2=0.87)
		DNX	Peaks at 0.75hr	0.0006 (R^2=0.88)
		TNX	0.0005 (R^2 =0.69)*	0.0012 (R^2=0.80)

Abiotic removal rates were obtained from Ariyarathna et al., 2015 under similar experimental conditions. Loss rate of NOx was not calculated due to the limited data availability not enough measurable data points to calculation; *Rates of DNT's and TNX in sediments are appearance rates and represent both sorption equilibrium with the dissolved phase and transformation of TNT on the sediment

Monoaminodinitrotoluenes (MADNTs) further degraded to just above detection limits in the aqueous phase by day 10. The first order removal rate constants of 2A-DNT and 4A-DNT from the aqueous phase are 0.52 hr^{-1} and 0.56 hr^{-1} respectively (Table 2). The TNT removal rate is 1.4 times higher compared to the removal rates of monoamino-derivatives from the aqueous phase. The ratio of aqueous MADNTs to TNT increased from 0.05 - 0.58 until 2.5 hr (Table 3). RDX was removed in water from 11.3 µM to 0.89 µM and the removal (0.37 ± 0.01 hr^{-1}) was greater than that of the abiotic system (0.31 ± 0.06 hr^{-1}) [15] (Table 2, Figure 1B).

Figure 1: Time series aqueous concentrations of A) TNT and amino derivatives B) RDX and nitroso derivatives

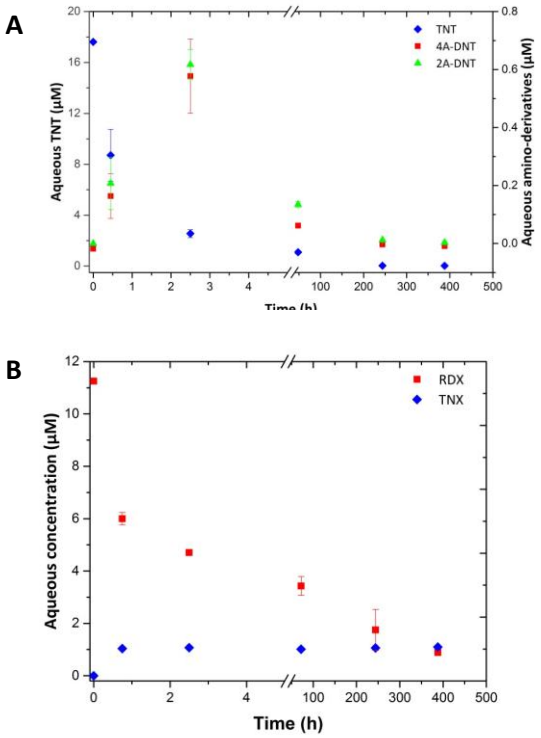

This yields a smaller RDX removal rate constant that can be attributed solely to biotic components (biodegradation and biotic mineralization) of 0.06 ± 0.06 hr^{-1} (Supplemental data, Table S1). TNX was the only identified nitroso-derivative of RDX and it appeared in the aqueous phase at 0.75 hr after spiking and remained constant throughout the experiment (14 days). The ratio of TNX to RDX increased from 0.17 to 1.29 in the aqueous phase over the experiment (Table 3). Removal rate constants of TNT and RDX in the aqueous phase increased by up to 42% and 19% respectively in the presence of marine microbial assemblages compared to abiotic conditions under the same experimental set-ups as shown in Table 2 [6]. Aqueous munition profiles of parent and daughter products comparing biotic and abiotic treatments are shown in Table S2 in supplemental section.

Table 3: Time series aqueous, sediment and total percentages of parent and transformation products in TNT and RDX microcosms

Treatment	Time (hr)	Parent compound %			Trans. products %		
		Aq	Sed	Tot	Aq	Sed	Tot
TNT	0	100.00	0	100.00	0	0	0
	0.45	49.47	0.09	49.56	2.25	0.13	2.38
	2.5	14.49	0.08	14.57	8.45	0.17	8.62
	48	6.19	0.04	6.23	1.46	0.04	1.50
	244	0.20	0.02	0.22	0.19	0.03	0.22
	388	0.16	0.01	0.17	0.09	0	0.09
RDX	0	100.00	0	100.00	0	0	0
	0.75	53.28	2.67	55.95	9.20	0.44	9.64
	2.5	41.79	1.98	43.77	9.50	0.43	9.93
	72	30.46	0.36	30.82	8.97	0.44	9.41
	244	15.54	0.11	15.65	9.46	0.33	9.79
	388	7.52	0.07	7.59	9.73	0.29	10.02

Trans. = Transformation products; Aq = Aqueous; Sed = Sediment; Tot = Total in aqueous and sediment; ND = No data

3.4.2 Partitioning of TNT, RDX and their derivatives onto sediment

Marine silty sediments with a medium grain size of 0.5 mm comprised of 56 % silt and clay with smectite group clays and feldspar as the dominant clay types were used for slurries in the experiment (chemical and textural properties of sediment are shown in Supplemental data, Table S3). The sediments had an organic carbon content of 4.10 mg g^{-1}sed (0.41 % OC) (Table S3) which raised the dissolved organic carbon content by 239-369µM in the aqueous phase of the slurries above that of normal seawater (185µM) at time 0 (Table 1). The spike added 1471-1675µM DOC due to acetone and 15-55µM DOC due to the compounds.

Bulk ^{15}N in sediment during TNT treatments increased rapidly (0.017 hr^{-1}) (Table 2) from an initial $\delta^{15}N$ value of 6‰, to 165‰ (Supplemental data, Table S4) within 2 days (Figure 2A). Only 0.1 – 5.6 % of total^{15}N in sediments during TNT treatments was identified as TNT, 4A-DNT and 2A-DNT (∑TNT) and the majority (94.4 – 99.9 %) resided in other pools (Figure 2B). The average ratio of mono-amino-derivatives to TNT found in sediment throughout the experiment was 1.2 ± 0.8 (Table 3). However, TNT, 4A-DNT and 2A-DNT concentrations started decreasing in sediment after 0.45 hr, 0.45 hr and 2.5 hr respectively. Over this time, bulk ^{15}N in sediment continued rising for 2 days where it then plateaued.

In RDX treatments, bulk ^{15}N in sediment varied from a $\delta^{15}N$ value of 9‰ to 47‰ (Table S4) and rapidly increased to a peak value of 7.7 x 10^{-4}μmol g^{-1} sed within 0.75 hr after spiking, followed by a slow decrease at a rate of 0.0021 hr^{-1} (Table 2, Figure 2A). Between 88-22% of total ^{15}N in sediment was identified as RDX, DNX and TNX (∑ RDX), and 12 – 78% resided in other pools for over the duration of the experiment (Figure 2C).

RDX disappeared from the sediment at a rate of 0.0091 hr^{-1} (Table 2), and nitroso-derivatives DNX and TNX were first observed in sediment at 0.75 hr. Sediment concentrations of DNX and TNX slowly decreased following rate constants of 0.0006 hr^{-1} and 0.0012 hr^{-1} after day 3 of spiking respectively (Table 2). The ratio of RDX to identified nitroso-derivatives in sediments decreased from 6.1 to 0.2 over the course of the experiment (Table 3). Sediment-sorbed munition profiles of parent and daughter products comparing biotic and abiotic treatments are shown in Table S2 in supplemental section.

Figure 2: Time series A) bulk ^{15}N concentrations in sediments for TNT and RDX treatments B) Contribution of total ^{15}N in sediment by munitions for TNT treatments C) Contribution of total ^{15}N in sediment by munitions for RDX treatments.

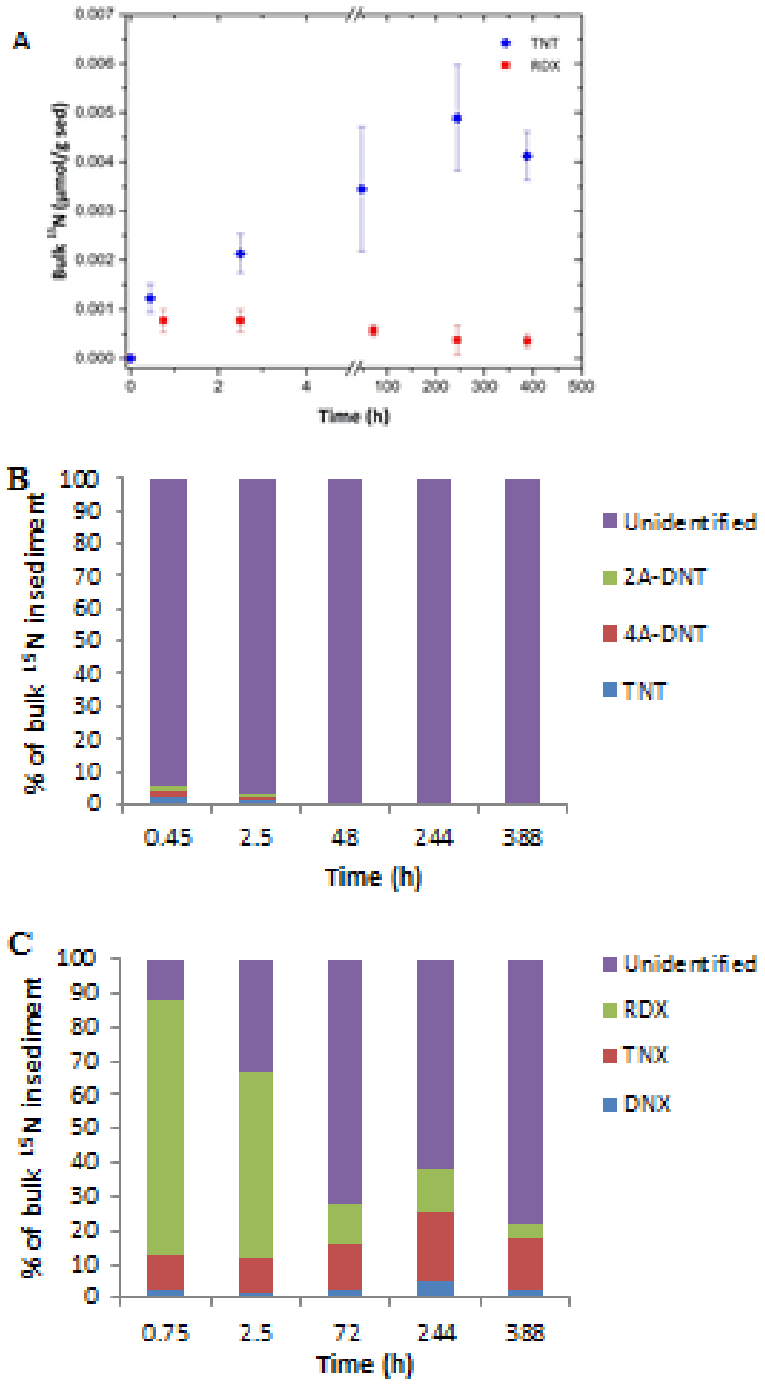

3.4.3 Mineralization of munitions to dissolved inorganic nitrogen (DIN)

Measured aqueous mineralization products including NH_4^+, NO_X and N_2 show elevated enrichments for $\delta^{15}N$ relative to the natural levels in sediment slurries (Table 4). Excess $^{15}NO_X$

concentrations in slurry water during TNT treatments rapidly increased within 0.45 hr from spiking, followed by a first order decay after 0.45hr (0.0067 hr^{-1}; $R^2 = 0.85$) and almost disappeared after the two-week time period (Table 2, 4). In RDX treatments, excess $^{15}NO_X$ concentrations in slurry water increased until day 3 with a formation rate of 0.014 hr^{-1}($R^2 = 0.99$) and were removed by day 10 (Table 2, 4). TNT derived NH_4^+ production approached steady state conditions after 10 days from spiking (Figure 3) and the formation rate constant was 0.048 hr^{-1} ($R^2 = 0.42$) (Table 2). $\delta\ ^{15}NH_4^+$ in RDX treatments continuously increased (Table 4) also approaching steady state after 10 days after a reduction in the formation rate from 0.017 hr^{-1} ($R^2 = 0.83$) to 0.0061 hr^{-1} ($R^2 = 0.87$) (Figure 3). Elevated $\delta^{15}N$ enrichments for N_2 were observed in RDX treatments, although, no N_2 production was detected in TNT treatments (Table 4). RDX-N derived N_2 was produced linearly over time at a rate of 0.041 hr^{-1} ($R^2 = 0.91$) (Figure 3) until day 3, where it reached steady state (with the exception of the last two time points, where sampling may have increased gas transfer losses).

Table 4: DIN (NH_4^+, N_2 and NO_X) production from TNT and RDX

Treatment	Time (hr)	δ $^{15}NH_4^+$	δ $^{15}NO_X$	δ $^{15}N_2$	nmol Excess $^{15}NH4^+$	nmol Excess $^{15}NO_X$	nmol Excess $^{15}N_2$	Munition derived DIN %
TNT	0	12.69	11.84	-1.77	0.83	0.300	0	0
	0.45	144.5	3203	-0.08	15.99	21.76	0	1.07
	2.5	89.01	6295	-0.70	12.48	10.89	0	0.66
	48	376.5	4654	-0.34	48.15	7.84	0	1.59
	244	2987	3424	-0.93	64.55	2.85	0	1.92
	388	1714	0	-0.67	63.85	0	0	1.81
RDX	0	10.06	0	-1.23	3.08	0	0	0
	0.75	100.9	1123	0.5	1.73	15.57	0.83	0.81
	2.5	159.9	1089	2.39	10.20	16.84	2.57	1.32
	72	311.7	9227	23.97	41.17	42.65	25.04	4.84
	244	420.5	0	14.92	223.9	0	14.81	10.61
	388	463.9	0	14.08	274.2	0	14.46	12.66

Values correspond to 0 hr indicate before spiking background levels and all the other data points are corrected for background values. Spiked ^{15}N equivalents of TNT and RDX treatments are 3520 nmol and 2250nmol respectively; ND = No data

Mineralization of RDX into all DIN pools including NH_4^+, NO_X and N_2 was 1 – 13 %, 10 times higher than the fraction observed for TNT (1% - 2%) throughout the experiment. Mineralization products in TNT sediment slurries increased until day 10 and stayed constant (1.9% relative to total TNT-N added) for the rest of the experimental time period while for RDX the percent mineralized increase from 0.8% to 13% throughout the experiment (16 days) (Table 4). NH_4^+ made up 42-86% and NO_X accounted for 58-14% of measured mineralization products for TNT sediment slurries. For RDX treatments, NH_4^+, NO_X and dissolved N_2 gas were responsible for 10-39%, 86-48% and 5-13% of total mineralization respectively.

Figure 3: Time series variation of munition derived NH_4^+ and N_2 in both TNT and RDX sediment slurries.

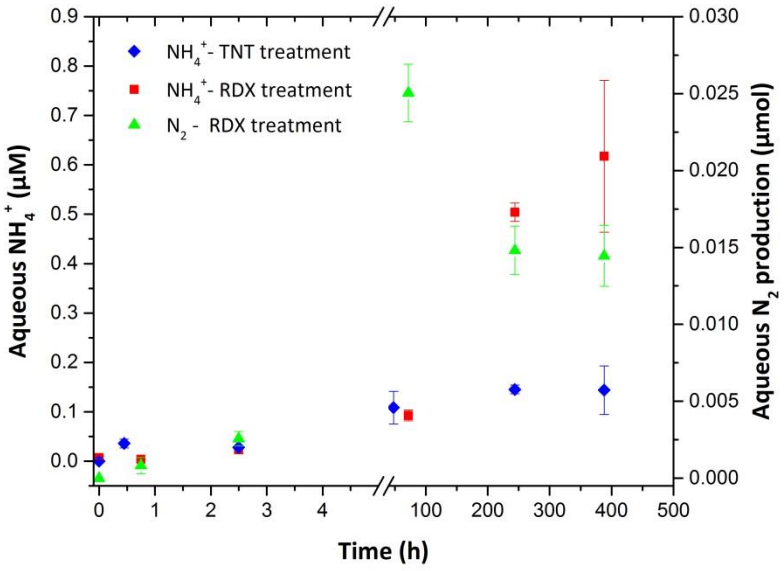

3.4.4 Mass balancing approach of TNT and RDX systems

Time series mass balances of TNT and RDX systems in terms of ^{15}N equivalents include the mineralization products (NH_4^+, NO_X and N_2), aqueous parent compound, selected derivatives, partitioning of compounds onto bulk sediment and unidentified ^{15}N incorporation onto sediments through other processes (Figure 4). Aqueous TNT dropped from 49 % to 0.2 % over the two weeks. Between 3 % -13% of spiked TNT partitioned onto sediment during the experiment. Insignificant mineralization of TNT in terms of NH_4^+ and NO_X (1% - 2%) was observed while unidentifiable ^{15}N pools increased from 45% to 85% for TNT treatments throughout the experiment. Based on uptake rates from Montgomery et al. [9], up to 0.002 – 2.0 µmol of TNT may be incorporated into the bacterial biomass over the duration of the experiment. Bacterial

incorporation could account for 0.4% of the unidentified pool at 0.45 hr but up to 100% at 10 days (Supplemental data, Table S5).

Figure 4: Time series full ^{15}N mass balance based on ^{15}N added to the system for A) TNT treatments B) RDX treatments. TNT Aq = Aqueous TNT; Tot deri-TNT Aq = Aqueous 2A-DNT and 4A-DNT; RDX Aq = Aqueous RDX; Tot deri-RDX Aq = Aqueous TNX

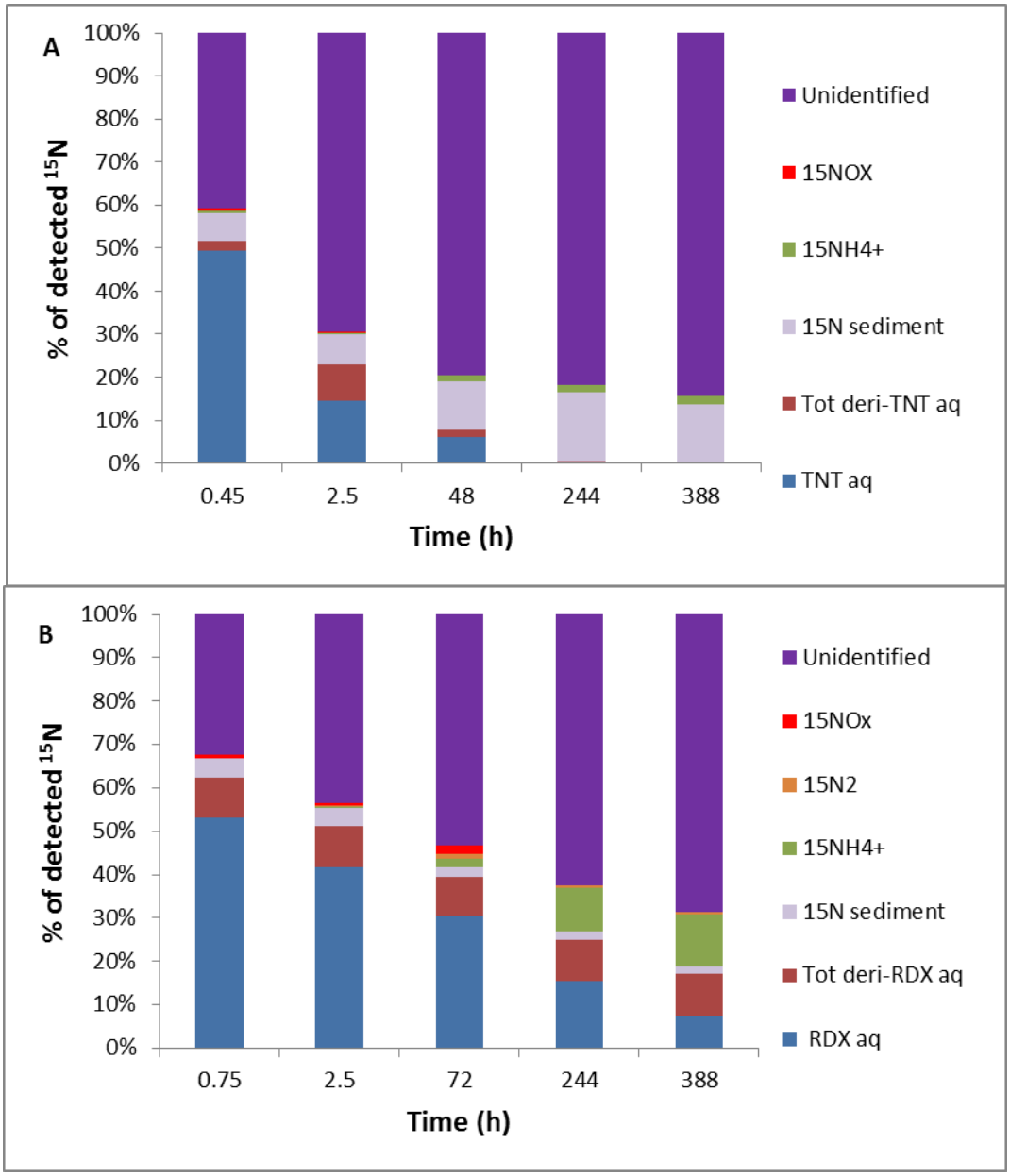

The percent of RDX remaining in the dissolved phase was higher than for TNT although it decreased from 53 % to 8 % over time. TNX remained in the water at an average constant percentage of 9.4% of total spiked RDX (Table 3). The percentage of spiked RDX that partitioned onto sediment was comparatively less than TNT and it decreased from 3.8 % to 1.8 % over the experiment. Nitrogen containing mineralization products (NH_4^+, NO_X and N_2) accounted for 1% -13% of spiked RDX throughout the experiment and unidentifiable ^{15}N pools increased for RDX treatments from 33% at the 0.75hr after spiking to 68% at the end of the experiment. For RDX, bacterial incorporation ranges from 0.0003 to 0.2 µmols and 0.1- 34% of unidentifiable pools have been identified as incorporated biomass in bacteria (Table S5).

3.5 Discussion

3.5.1 Fate of TNT in anaerobic sediments

TNT is rapidly removed from the aqueous phase following first order kinetics through initial sorption and abiotic degradation [6] and via biodegradation by microbes in anaerobic sediments [13,14,18]. TNT removal rate constants decrease from highest to lowest in the order of: biotic marine organic carbon (OC) rich silt > abiotic marine OC rich silt > abiotic marine OC poor sand > abiotic freshwater OC rich silt [6]. Increases in removal rates constants of TNT from the aqueous phase up to 42% in the presence of microbes illustrates the importance of native microbial assemblages in marine sediment towards TNT remediation. Removal rate constants of compounds in the abiotic system are composed of two parameters; sorption onto sediment and abiotic transformation. Based on the production rates of measured transformation products, abiotic transformation could account for 2% of total spiked TNT and up to 9% through sorption [6]. Therefore, sorption plays a major role in removing TNT from the aqueous in all systems and is the major removal in abiotic systems. In biotic systems, biotic transformation of TNT is up to

9% of total spiked TNT (in terms of measured transformation products confirming biotransformation) is a significant removal process. Integrated sorption and biodegradation becomes the most effective removal mechanism of TNT particularly since sediments act as a biofilm carriers by providing a surface for microbes to attach [10,26] and enhancing the dual sorption, biodegradation effects. TNT biodegrades to MADNTs (2A-DNT and 4A-DNT) along the pathway of forming further reduced transformation products [13,27] however, diaminomononitrotoluenes (DANTs) and triaminotoluene (TAT) were not quantified in this study. Formation of TAT requires a redox potential below -200mV [10,13] which was not reached in our anaerobic sediment microcosms where redox potentials ranged from 53mV to -133mV. However, the appearance and subsequent disappearance of MADNTs soon after the TNT sorption maximum suggests that 2A-DNT and 4A-DNT are intermediates of TNT break down pathways [13,27]. TNT is removed from the aqueous phase faster (1.4 times) than for MADNTs revealing other possible pathways of TNT breakdown under anaerobic conditions [13,27] than the reduction through amino derivatives. Even though rapid biodegradation of TNT is reported in this study, observed production of derivatives, 2A-DNT and 4A-DNT, is small (0.1-8.6% of spiked TNT). The persistence of MADNTs implies that the production rates and removal rates are balanced while the removal of the 2A-DNT and 4A-DNT overtakes their respective production rates as they do not persist.

Partitioning of 13% of spiked TNT onto sediment highlights the role of sediment in reducing the bioavailability of TNT and derivatives in aquatic systems [6,28] and further proposes new insights for sediment sorption related bioremediation techniques. Bulk ^{15}N values in sediment rapidly increased, followed by a plateau, strongly suggesting that TNT and then its derivatives must have been sorbed onto the sediment [10] and maintained steady state or persisted relatively

high percentages of silt and clays (56%) [29] and organic carbon (4.1 mg g^{-1} sed) [30] found in the marine sediment used in this experiment facilitate the sorption of TNT and amino derivatives through electrostatic forces and hydrophobic partitioning [6]. TNT and mono amino derivatives are responsible for a small percentage of bulk ^{15}N in sediment (2%) and also disappear soon after they reached maximum production, leaving the majority of bulk ^{15}N in sediment unaccounted for. The most likely pools for this ^{15}N include unquantified degradation products including DANTs and TAT [10] or incorporation of ^{15}N into microbial biomass [8,9].

Mineralization of dissolved TNT and derivatives by anaerobic marine microbial assemblages [8-10] to DIN, including NH_4^+ and NO_X is reported in this study, although the relatively small yields (2% of spiked TNT) agrees with previously published experiments [8,9]. Principal component analysis (PCA) of time series ^{15}N pools reveals two possible pathways of mineralization of TNT under our experimental conditions (Figure 5A). Measurements (PCA scores) found as clusters in the PCA plot are influenced by the same underlying factors. PC1 reflects the duration of the experiment, with fresh TNT in both dissolved and sorbed phases plotting in the far right quadrant, and mineralization products in the far left quadrant. PC2 represents aqueous and sediment geochemical variables, specifically, the pH and %OC content. $^{15}NH_4^+$ and $^{15}NO_X$ are negatively correlated in the PCA plot suggesting these products are involved in two different pathways of mineralization. Denitration of TNT takes place [13,31] in the early phase of the experiment when less reduced transformation products are available and redox potentials are 41 to 54 mV. The NO_X's formed are likely being removed by bacteria in the aqueous phase of the microcosms over the latter part of the experiment when redox ranges between 40mV and -26mV. The second pathway involves deamination of reduced

transformation products (2A-DNT, 4A-DNT etc.) forming NH_4^+ [10,15] towards the end of the experiment, as illustrated in the PCA plot.

Figure 5 : Principle component analysis of a) TNT microcosm – Circled box shows correlation of $^{15}NH_4^+$ production and reduced iron and sulfur species in sediment; PC1 and PC2 represent 54% and 17% variability respectively b) RDX microcosm – PC1 and PC2 have 52% and 20% variability respectively.

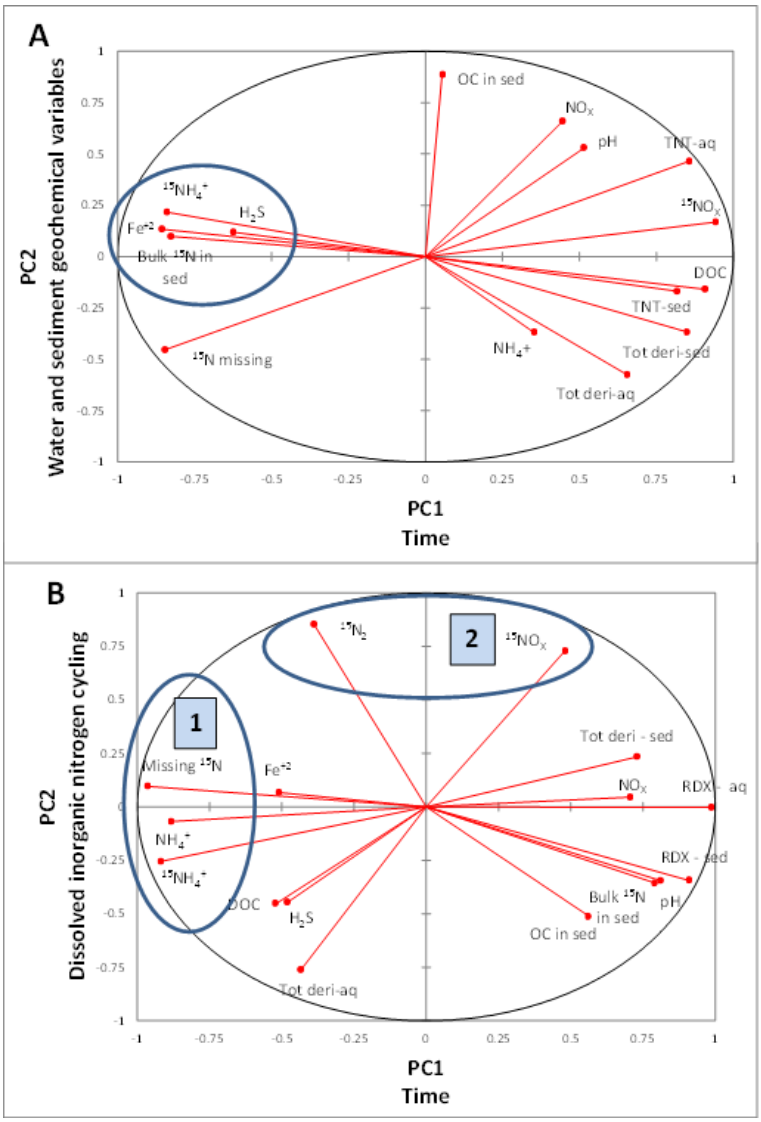

The PCA plot also suggests ammonia formation may be associated with iron and sulfate reducing bacteria [15] in sediment, as $^{15}NH_4^+$, bulk ^{15}N in sediment and reduced forms of iron and sulfur (Fe^{+2}, H_2S) are correlated in the PCA plot (Figure 5-A – circled region). Microbially mediated degradation of TNT by iron reducers has been previously documented [4]. Continuous production of Fe^{2+} from the interaction of *Shewanella putrefaciens* and iron bearing soil minerals was identified as the key factor to enhanced degradation of TNT via electron transfer [32]. This is further confirmed in our study as demonstrated by the linear relationship between dissolved $^{15}NH_4^+$ and Fe^{2+} concentrations (R^2=0.4) and continuous production of Fe^{2+} throughout the TNT experiment. Moreover, *Shewanella putrefaciens* has shown enhanced growth by elemental sulfur reduction to hydrogen sulfide (H_2S) [33] which was observed towards the end of the experiment in this study. It can also indirectly affect TNT biodegradation via Fe^{2+} production. Sulfate reducing bacteria (SRB) (*Clostridium, Desulfovibrio*) plays an important role in anaerobic marine environments in converting sulfates to H_2S by sulfate reductase. These organisms use the nitro groups present in the TNT molecule as either an electron acceptor or a nitrogen source [15]. H_2S production observed towards the end of the experiment suggests that degradation of TNT is facilitated by SRB in this study.

NH_4^+ concentrations were steady towards the end of the experiment and no further N_2 production from either NO_X or NH_4^+ was observed over 16 days. It strongly reveals that NH_4^+ serves as a terminal mineralization product of TNT in DIN pools under anaerobic conditions. However, modest production of N_2 has been reported in an aerated water column of mesocosm studies [10]. Mineralization tracking as described in this study is limited to the ring attached functional groups as the TNT ring contains no N; but it is supported with the idea of ring stability with an aromatic π system described in Hawari et al. [17]. Further, the limited number of previous studies that

describe ring breakdown of TNT to CO_2 confirms that ring carbon mineralization accounts for a lower percentage of TNT metabolic fate [8,9]. Based on recent studies, environmental factors such as matrix effects, solution chemistry, sediment texture and chemistry etc. also control, and likely enhance the decomposition of TNT [34,35]. Lower remineralization in the system supports the incorporation of nitrogen from energetics as an organic nitrogen source rather than catabolization in bacteria. Total carbon demand of the system may have affected the remineralization of microbially incorporated carbon or nitrogen from the energetics. Bacterial incorporation of carbon and nitrogen from TNT is higher than that of RDX based on the incorporation rates published in Montgomery et al. [9] and consistent with previously published data [8,9]. The unidentified TNT-N pool at the last day of the experiment (85% of spiked TNT) could be fully explained by microbial incorporation based on the calculations above.

Here, we provide evidence that TNT is likely removed from the dissolved phase primarily through partitioning onto sediment and biotransformation at relatively equal amounts rather than undergoing abiotic mineralization in anaerobic sediment systems. This is supported by the modest yield of mineralization products in terms of DIN. However, from a mass balancing point of view, there is still a significant portion of TNT which has not been traced that remains in the dissolved phase as a transformation product of TNT. Further research needs to be done to obtain full mass balances of the system by widening the analytical window to quantify additional transformation products and bulk ^{15}N in water, as well as to include measurements of additional pools such as non-particle associated microbes. Increases in the unaccounted for portion of spiked TNT (Figure 4) over the duration of the experiment suggests that unidentified (as yet unknown) or unmeasured (eg: DANTs, TAT) transformation products are accumulating with

time, as has been suggested [25]. Further research is necessary to confirm the identity of these potentially toxic products.

3.5.2 Fate of RDX in anaerobic sediments

RDX is removed from the dissolved phase following first order kinetics though removal is not as rapid as for TNT. Removal rate constants of RDX from the aqueous phase increases by up to 19% in the presence of anaerobic microbes in biotic system compared to the abiotic systems with different environmental conditions including freshwater, marine organic carbon rich and poor sediments described in Ariyarathna et al. [6]. Abiotic transformation and sorption of RDX could account for 5% and 14% of total spiked RDX respectively [6] while biotic transformation of RDX up to 9-10% in terms of measured transformation products confirming the significance of biotransformation. RDX (9.4%) biodegrades to TNX by sequential reduction through the nitroso-derivatives MNX and DNX, while keeping the nitroamine ring intact [12]. TNX is found to be relatively stable [36] in both dissolved and sorbed phases over 16 days. RDX sorbs onto the sediment reversibly through electrostatic forces [6] and is subsequently removed from sediment following first order kinetics via three possible mechanisms: abiotic transformation by mineral-bound ferrous [37], enhanced biotransformation by microbes attached to the sediment particles and organic matter [38] and desorption [39]. TNX accounts for the majority of identified degradation products in sediment due to its relative stability [36]. However, 26-70% of bulk ^{15}N in sediment was still unidentified showing an ascending trend with time similarly to TNT. This may be due to microbial assimilation and unquantified derivatives. Interestingly, unlike TNT, elevated bulk ^{15}N values of sediment in RDX treatments did not stay constant, rather, slowly decreased with a first order decay constant via either desorption of RDX, other unquantified derivatives initially sorbed onto the sediment (eg: hydrazine) [16], or mineralization to water

soluble products [12]. However, unlike TNT, the sediment was not an ultimate sink for RDX and its derivatives since the sediment contained less RDX derived ^{15}N over the experiment and decreased with time.

Both dissolved RDX [12] and nitroso-derivatives (MNX and DNX) [11] were mineralized (13%) by anaerobic microbes forming N_2 in addition to other DIN species and ultimately in the nitrogen cycle as the best case scenario of removal of RDX and derivatives from marine ecosystems. Similarly as TNT systems, PCA gives robust interpretations for identifying pathways of anaerobic mineralization of RDX (Figure 5B). PC1 reflects the duration of the experiment, with fresh RDX in both dissolved and sorbed phases plotting in the far right quadrant, and continual production of NH_4^+ approaching steady state as a mineralization product in the far left quadrant. Two distinct shaded regions, 1 and 2 in the PCA plot of RDX systems suggest two possible pathways of anaerobic mineralization of RDX including production of NH_4^+ (region 1) and N_2 (region 2) in marine sediments and the proposed mechanisms are illustrated in figure 6. NH_4^+ production approached steady state by end of the experiment confirming NH_4^+ as one of the final mineralization products of RDX that resulted from mono-denitration of RDX leading to the predominant formation of methylenedinitramine (MEDINA) which is unstable in water and decomposes to NH_4^+ and formaldehyde in anaerobic conditions [12]. Moreover, NH_4^+ production, reduced sulfur and iron species were clustered together in the PCA plot inferring the involvement of iron and sulfate reducers in the sediment on NH_4^+ production from RDX in agreement with previously published work [4,40]. The second mineralization pathway includes steady state production of N_2 via denitration of RDX and/or nitroso derivatives followed by denitrification of resulted NO_X [11], which act as intermediates in the process.

Figure 6: Proposed RDX anaerobic mineralization pathway. Modified from Smith et al, 2015 and Halasz and Hawari (2011).

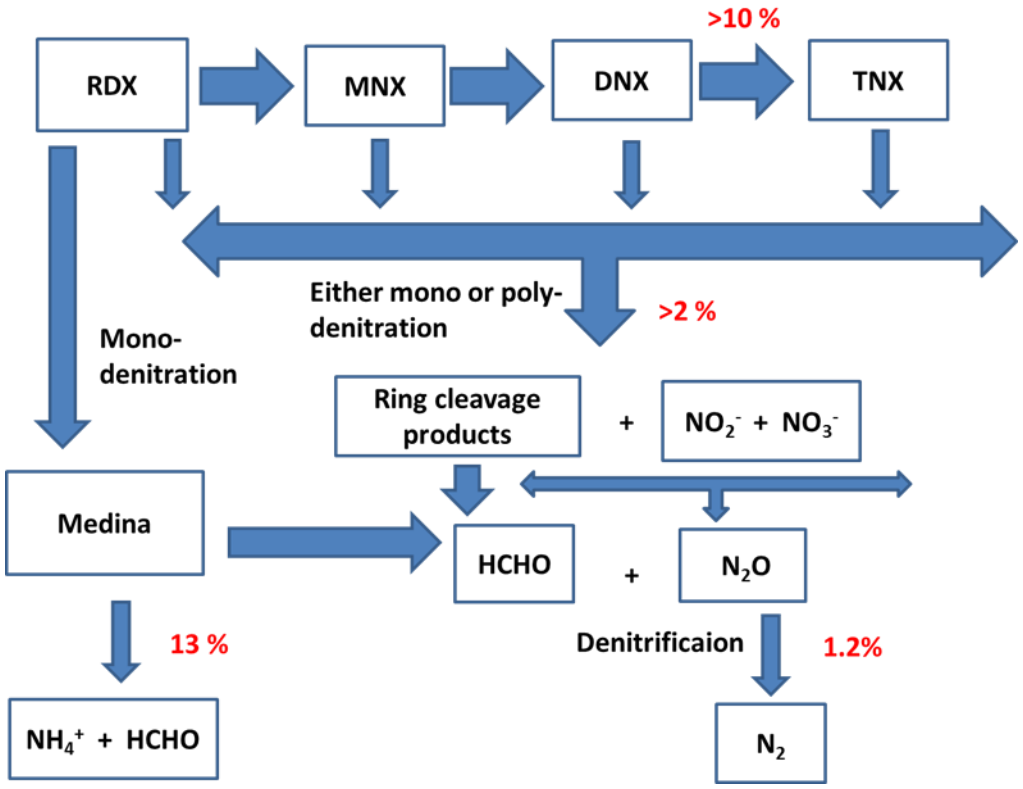

The maximum measured NO_X production is 2% in our anaerobic slurries whereas [41] has reported the nitrite production and isotopic fractionation in both anaerobic and aerobic systems, giving a nitrite yield up to around 16% in the apparent absence of coexisting nitrite reduction. NH_4^+ production out-competes N_2 formation since almost 40% of detected mineralization products were accounted by NH_4^+ at the end of the experiment in this study. Missing ^{15}N in the system also showed a strong linear correlation (R^2= 0.83) with NH_4^+ production suggesting the majority of missing ^{15}N is related to unquantified mineralization products resulting from the pathway of NH_4^+ formation, as was seen for TNT. It has been documented that nitrogen dioxide (N_2O), though not quantified in this study, can also be formed via both pathways of

mineralization discussed in this study which include breakdown of MEDINA [12] and denitrification of NO_X [11]. Therefore, further research is recommended for improved mass balancing of the system that includes tracing N_2O production.

Finally, unlike TNT, mineralization was more prominent in the RDX system because of its structural properties and the prevailing anaerobic conditions in these sediment systems. Lack of aromatic stability, weaker (<2 kcal/mol), inner C-N bonds [17], lower sorption of RDX onto sediment (which results in lower shielding of RDX from decomposition) [35] facilitate higher mineralization rates of RDX in marine sediments compared to TNT. Unidentified pools of N-RDX in nitro groups at the end of the experiment (69% of spiked RDX) may include unquantified mineralization products and bacterial incorporated nitrogen which accounts for 0.1% to 34% of the unknown pool (from 0.75hr to end of the experiment) based on the published bacterial incorporation rates in marine sediments [9].

It is clear that marine sediment plays an important role in mineralization providing favorable anaerobic conditions, iron bearing minerals and natural microbial assemblages that enhance transformation of RDX. Overall mineralization in terms of measured nitrogen containing mineralization products (NH_4^+ and N_2) dominates sorption and biodegradation of RDX as the most significant removal mechanism from marine ecosystems.

3.6 Acknowledgement

This work was funded by Department of Defense: Strategic Environmental Research and Development Program (SERDP) under project ID- ER-2122. The authors would like to thank C. Cooper for sediment collecting and D. Cady, J. K. Bohlke and V. Rollinson for laboratory support.

3.7 References

[1] Bearden DM. 2007. *U.S. disposal of chemical weapons in the ocean: background and issues for congress*. Report RL33432.

[2] Craig HD, Taylor S. 2011. Framework for evaluating the fate, transport, and risks from conventional munitions compounds in underwater environments. *Mar Technol Soc J* 45:35-46.

[3] Schmidt CW. 2004. The price of preparing for war. *Environ Health Perspect* 112:A1004-1005.

[4] Pichtel J. 2012. Distribution and fate of military explosives and propellants in soil: A review. *Applied and Environmental Soil Science* 2012.

[5] Craig HD, Taylor S. 2011. Framework for evaluating the fate, transport, and risks from conventional munitions compounds in underwater environments. *Mar Technol Soc J* 45:35-46.

[6] Ariyarathna T, Vlahos P, Tobias C, Smith R. 2015. Sorption kinetics of TNT and RDX in anaerobic freshwater and marine sediments: Batch studies. *Environ Toxicol Chem*. 35(1):47-55.

[7] Smith RW, Vlahos P, Tobias C, Ballentine M, Ariyarathna T, Cooper C. 2013. Removal rates of dissolved munitions compounds in seawater. *Chemosphere* 92:898-904.

[8] Montgomery MT, Coffin RB, Boyd TJ, Smith JP, Walker SE, Osburn CL. 2011. 2,4,6-Trinitrotoluene mineralization and bacterial production rates of natural microbial assemblages from coastal sediments. *Environ Pollut* 159:3673-3680.

[9] Montgomery MT, Coffin RB, Boyd TJ, Osburn CL. 2013. Incorporation and mineralization of TNT and other anthropogenic organics by natural microbial assemblages from a small, tropical estuary. *Environ Pollut* 174:257-264.

[10] Smith RW, Vlahos P, Böhlke JK, Ariyarathna T, Ballentine M, Cooper C, Fallis S, Groshens TJ, Tobias C. 2015. Tracing the Cycling and Fate of the Explosive 2,4,6-Trinitrotoluene in Coastal Marine Systems with a Stable Isotopic Tracer, 15N-[TNT]. *Environ Sci Technol* 49:12223-12231.

[11] Smith RW, Tobias C, Vlahos P, Cooper C, Ballentine M, Ariyarathna T, Fallis S, Groshens TJ. 2015. Mineralization of RDX-derived nitrogen to N2 via denitrification in coastal marine sediments. *Environ Sci Technol* 49:2180-2187.

[12] Halasz A, Hawari J. 2011. Degradation routes of RDX in various redox systems. *ACS Symp Ser* 1071:441-462.

[13] Esteve-Núñez A, Caballero A, Ramos JL. 2001. Biological degradation of 2,4,6-trinitrotoluene. *Microbiology and Molecular Biology Reviews* 65:335-352.

[14] Drzyzga O, Bruns-Nagel D, Gorontzy T, Blotevogel K, Gemsa D, Lo¨w E. 1998. Mass balance studies with ^{14}C-labeled 2,4,6-Trinitrotoluene (TNT) mediated by an anaerobic Desulfovibrio species and an aerobic Serratia species. *Current Microbiology* 37:380-386.

[15] Boopathy R. 2014. Biodegradation of 2,4,6-trinitrotoluene (TNT) under sulfate and nitrate reducing conditions. *Biologia* 69:1264-1270.

[16] McCormick NG, Cornell JH, Kaplan AM. 1981. *The anaerobic biotransformation of RDX, HMX and acetylated derivatives.* Natick Technical report 85-007. U.S. Army Natick Research and Development center, Natick, MA.

[17] Hawari J, Halasz A, Sheremata T, Beaudet S, Groom C, Paquet L, Rhofir C, Ampleman G, Thiboutot S. 2000. Characterization of metabolites during biodegradation of hexahydro- 1,3,5-trinitro-1,3,5-triazine (RDX) with municipal anaerobic sludge. *Appl Environ Microbiol* 66:2652-2657.

[18] Spain JC. 1995. Biodegradation of nitroaromatic compounds. *Annu Rev Microbiol* 49:523-555.

[19] Pennington JC, Myers T, Davis WM, Olin TJ, McDonald TA,Hayes CA,Townsend DM. 1995. *Impacts of sorption on in situ bioremediation of explosives-contaminated soils.* TR-IRRP-95-1. US Army Engineer Waterways Experiment Station, Washington, DC.

[20] Stookey LL. 1970. Ferrozine - A new spectrophotometric reagent for iron. *Anal Chem* 42:779-781.

[21] Cline JD. 1969. Spectrophotometric determination of hydrogen sulfide in natural waters. *Limnol Oceanogr* 14:454-455.

[22] Miyares PH, Jenkins TF. 1990. *Salting-out solvent extraction for determining low levels of nitroaromatics and nitramines in water.* Special Report 90-30. US Army Corps of Engineers, Cold Regions Research and Engineering Laboratory, Hanover, NH.

[23] Holmes R, McClelland J, Sigman D, Fry B, Peterson B. 1998. Measuring 15N-NH4+ in marine, estuarine and fresh waters: An adaptation of the ammonia diffusion method for samples with low ammonium concentrations. *Mar Chem* 60:235-243.

[24] Schwarzenbach RP, Gschwend PM, Imboden D. 2003. Air-water exchange. In *Environmental Organic Chemistry*, 2nd ed. John Wiley & Sons, Inc., Hoboken, NJ, pp 889-890.

[25] Delaune RD, Reddy KR. 2005. Redox potential. Hillel D (ed), In *Encyclopedia of Soils in the Environment*, Academic Press, pp 366-371.

[26] Chusova O, Nõlvak H, Odlare M, Truu J, Truu M, Oopkaup K, Nehrenheim E. 2015. Biotransformation of pink water TNT on the surface of a low-cost adsorbent pine bark. *Biodegradation* 26:375-386.

[27] Khan MI, Lee J, Park J. 2013. A toxicological review on potential microbial degradation intermediates of 2,4,6-trinitrotoluene, and its implications in bioremediation. *KSCE J Civ Eng* 17:1223-1231.

[28] Pennington JC, Lotufo G, Hayes CA, Porter B, George RD. 2011. TNT, RDX, and HMX Association with Organic Fractions of Marine Sediments and Bioavailability Implications. In Chappell MA, Price CL, George RD (ed), In *Environmental Chemistry of Explosives and Propellant Compounds in Soils and Marine Systems: Distributed Source Characterization and Remedial Technologies*, Vol 1069. American Chemical Society, pp 185-195.

[29] Haderlein SB, Weissmahr KW, Schwarzenbach RP. 1996. Specific adsorption of nitroaromatic explosives and pesticides to clay minerals. *Environmental Science and Technology* 30:612-622.

[30] Yamamoto H, Morley MC, Speitel Jr. GE, Clausen J. 2004. Fate and transport of high explosives in a sandy soil: Adsorption and desorption. *Soil and Sediment Contamination* 13:459-477.

[31] Qiao H, Feng H, Liu S, Wang C, Zhang Y, Gao Y, Li W, Yao J, Wang M, Shen D. 2011. The possible reduction pathways of 2,4,6-trinitrotoluene (TNT) by sulfide under simulated anaerobic conditions. *Water Sci Technol* 64:2474-2482.

[32] Cho C, Bae S, Lee W. 2012. Enhansed degradation of TNT and RDX by bio-reduced iron bearing soil minerals. *Advances in environmental research* 1(1):1-14.

[33] Moser DP, Nealson KH. 1996. Growth of facultative anaerobe Shewanella putrefaciens by elemental sulfur reduction. *Applied and Environmental Microbiology* 62(6):2100-2101-2105.

[34] Marín-Spiotta E, Gruley KE, Crawford J, Atkinson EE, Miesel JR, Greene S, Cardona-Correa C, Spencer RGM. 2014. Paradigm shifts in soil organic matter research affect interpretations of aquatic carbon cycling: Transcending disciplinary and ecosystem boundaries. *Biogeochemistry* 117:279-297.

[35] Han L, Sun K, Jin J, Xing B. 2016. Some concepts of soil organic carbon characteristics and mineral interaction from a review of literature. *Soil Biol Biochem* 94:107-121.

[36] Paquet L, Monteil-Rivera F, Hatzinger PB, Fuller ME, Hawari J. 2011. Analysis of the key intermediates of RDX (hexahydro-1,3,5-trinitro-1,3,5- triazine) in groundwater: Occurrence, stability and preservation. *J Environ Monit* 13:2304-2311.

[37] Gregory KB, Larese-Casanova P, Parkin GF, Scherer MM. 2004. Abiotic transformation of hexahydro-1,3,5-trinito-1,3,5-triazine by Fe II bound to magnetite. *Environmental Science and Technology* 38:1408-1414.

[38] Finneran KT, Kwon M, Drew SR. 2007. *Biodegradation of RDX by stimulating humic substance- and Fe(III) - reduction.* Final report:ER-1377. Strategic Environmental Research and Development Program, Arlington, VA.

[39] Selim HM and Iskandar IK. 1994. *Sorption-desorption and transport of TNT and RDX in soils.* CRREL report 94-7. U.S. Army Corps of Engineers: Cold Regions Research & Engineering Laboratory, Hanover, NH.

[40] Boopathy R, Kulpa CF, Manning J. 1998. Anaerobic biodegradation of explosives and related compounds by sulfate-reducing and methanogenic bacteria: A review. *Bioresour Technol* 63:81-89.

[41] Fuller ME, Heraty L, Condee CW, Vainberg S, Sturchio NC, Böhlke JK, Hatzinger PB. 2016. Relating carbon and nitrogen isotope effects to reaction mechanisms during aerobic or anaerobic degradation of RDX (hexahydro-1,3,5- trinitro-1,3,5-triazine) by pure bacterial cultures. *Appl Environ Microbiol* 82:3297-3309.

3.8 Supplemental data

Supplementary data associated with this article are shown in Table S1, Table S2, Figure S1.

Table S1: Concentrations of TNT and RDX removed by biotic component in microcosms.

Time (hr)	Biotically removed TNT (μM)	Biotically removed RDX (μM)
0.45	2.7	-
0.75	-	1.0
2.5	1.3	1.6
48	3.7	-
72	-	2.7
244	4.2	4.0
388	4.2	4.8

It was calculated by subtracting abiotic aquatic concentrations (Ariyarathna et al., 2015) from aquatic concentrations in biotic treatment in current study.

Table S2: Munition profile comparison of a) TNT b) RDX microcosms.

a)

Treatment	Time (hr)	Dissolved (μM)			Sediment (ng/g sed)		
		TNT	4A-DNT	2A-DNT	TNT	4A-DNT	2A-DNT
Biotic	0.45	8.7	0.25	0.23	14	10	7.9
	2.5	2.6	0.81	0.68	12	12	12
	48	2.0	0.11	0.15	5.6	1.3	3.7
	244	0.035	0.02	0.013	2.4	0.9	2.8
	388	0.028	0.01	0.0035	1.9	BD	BD
Abiotic	0.75	7.0	0.46	0.012	-	-	-
	2	5.6	0.42	0.052	-	-	-
	48	4.8	0.4	0.041	-	-	-
	122	4.3	0.39		-	-	-
	150	4.2	0.36		1067	BD	BD

b)

Treatment	Time (hr)	Dissolved (µM)				Sediment (ng/g sed)			
		RDX	MNX	DNX	TNX	RDX	MNX	DNX	TNX
Biotic	0.75	6.0	BD	BD	1.0	267	BD	6.6	29
	2.5	4.7	BD	BD	1.1	198	BD	6.2	28
	72	3.4	BD	BD	1.0	36	BD	6.1	30
	244	1.8	BD	BD	1.1	11	BD	5.3	21
	388	0.89	BD	BD	2.0	7	BD	5.3	21
Abiotic	0.75	7.0	3.4	BD	4.0	-	-	-	-
	2	5.7	3.1	3.2	3.6	-	-	-	-
	48	6.1	3.0	BD	3.6	-	-	-	-
	122	5.7	BD	BD	3.6	-	-	-	-
	150	5.6	BD	BD	3.8	794	104	101	BD

Data related to the abiotic treatment was taken from Ariyarathna et al., 2015; BD = below detection

Table S3: Chemical and textural properties of marine sediment used for both TNT and RDX systems in this study (n=3)

	Property	Value
Particle size distribution data	Sand (%)	44
	Silt & clay (%)	56
	Statistical parameters	
	1.Graphic mean (mm)	0.16
	2.Median (mm)	0.11
	3.IGSD (mm)	0.16
Physical properties	Bulk density(gcm^{-3})	1.4
	Porosity (%)	45.6
Chemical properties	TOC (mgg^{-1}sed)	4.10 ± 0.69
	TN (mgg^{-1}sed)	0.62 ± 0.25
	S (mgg^{-1}sed)	3.7 ± 0.3

IGSD = Inclusive Graphic Standard Deviation; TOC = Total Organic Carbon

TN = Total Nitrogen; S = Elemental Sulfur

Table S4: Time series bulk $\delta^{15}N$ values in sediment in TNT and RDX microcosms

Time (hr)	Bulk $\delta^{15}N$ (‰)	
	TNT microcosm	RDX microcosm
0	6	9
0.45	122	-
0.75	-	31
2.5	148	34
48	165	-
72	-	47
244	170	29
388	171	30

Table S5: Bacterial incorporation of ^{15}N from TNT and RDX in microcosms

Time (hr)	Incorporated µmols		Incorporated %	
	TNT	RDX	TNT	RDX
0.45	0.002	-	0.5	-
0.75	-	0.0003	-	0.1
2.5	0.01	0.001	2	0.3
48	0.2	-	26	-
72	-	0.03	-	8
244	1	0.1	100	23
388	2	0.2	100	34

Bacterial incorporated quantity is in µmols TNT and µmols RDX; Incorporated % represents percentage of bacterial incorporation of unidentified pool in TNT and RDX microcosms; Bacterial incorporation rates in marine sediments from Montgomery et al., 2013 was used for the calculations.

Figure S-1: Ghant diagrams for timeline of events a) TNT microcosms b) RDX microcosms

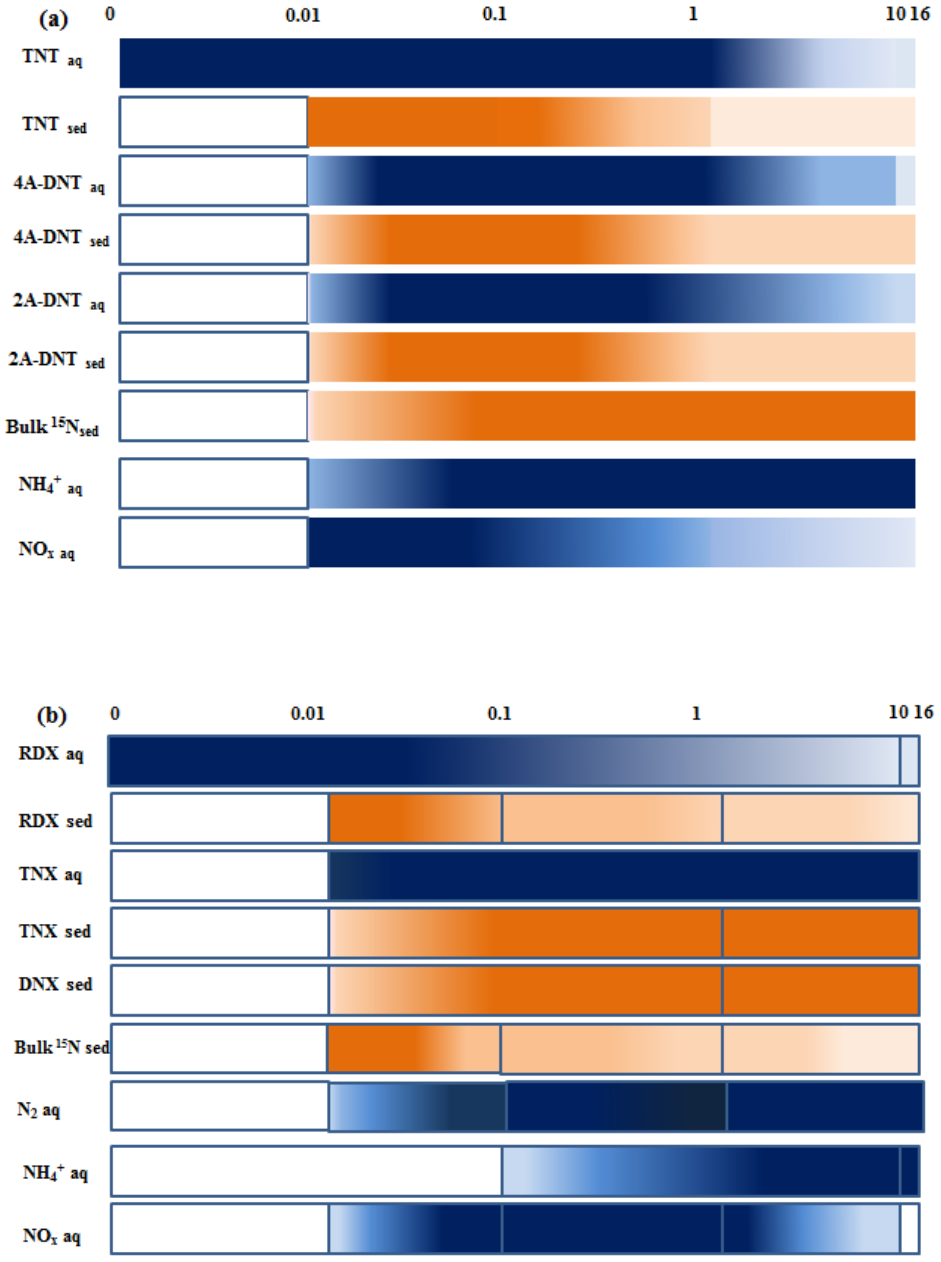

4.0 Tracing the cycling and fate of the explosive, Hexahydro-1,3,5-trinitro-1,3,5-trazine in a simulated sandy coastal marine habitat with a stable isotopic tracer, ^{15}N-[RDX]

4.1 Abstract

Coastal marine habitats are contaminated with the explosive, Hexahydro-1,3,5-trinitro-1,3,5-trazine (RDX) via military training and weapon testing and through leakage of unexploded ordnances. RDX has severe neurotoxic effects to aquatic organisms, and it is considered a human carcinogen. RDX is relatively stable in surface water and undergoes biotic uptake as a nitrogen source, possible entering into the food chains of coastal habitats. This study utilized ^{15}N labelled RDX in mesocosm to track removal pathways from surface water including sorption onto particulates, degradation and mineralization leading to dissolved inorganic nitrogen. The simulated marine mesocosm was continuously loaded with RDX to maintain a steady state concentration (0.4 mgL^{-1}) over 21 days. Time series concentrations of dissolved RDX and derivatives in surface water and porewater, RDX and derivatives sorbed onto sediment and suspended particulates, and dissolved mineralization products (ammonium, nitrates, nitrites and (N_2 +N_2O) gases) along with geochemical variables in the mesocosm were analyzed. Tri-nitroso triazine (TNX) was identified as a stable product in the water column. RDX diffused into the surface sediment where under hypoxic conditions it biodegraded forming nitroso-triazines. TNX was irreversibly, sorbed onto the surface sediment while vertical diffusion of RDX and nitroso derivatives in sediment was minimal. Total degradation of RDX in terms of measured nitroso-triazines was 6%-13%. Although, RDX derived ^{15}N rapidly partitioned onto suspended particulate matter (SPM) irreversibly, under oxygenated conditions, it was not quantitatively vital as a removal mechanism of RDX from surface water. Partitioning of RDX derived breakdown products onto surface sediment made a significant contribution (11%) to the total mass balance of the system. RDX was favorably mineralized (40%) with a continual increase in

inorganic nitrogen production in the system and gaseous mineralization products (N_2 and N_2O) accounted for the majority of it (30%). Production of inorganic nitrogen varied in terms of types of products and qualitative production in well aerated surface water and hypoxic sediment (porewater). Nitrates and nitrites (NO_X) prevailed in surface water (9%) while ammonium was formed (6%) in both surface water and sediment via different mechanisms with higher production in sediment. Thus, hypoxic sediment was the most favorable zone for the production of N_2 and N_2O. Principle component analysis revealed that iron reducing bacteria in sediment were involved may facilitate gas production. N_2 and N_2O diffused through porous sediment into the water column and then, the majority escaped to the atmosphere (28%) as the largest removal technique of RDX from the ecosystem.

4.2 Introduction

Hexahydro-1,3,5-trinitro-1,3,5-trazine (RDX) has been extensively used in munitions compounds since World War II through processes involving production, handling, loading, disposal and detonation release RDX into coastal marine habitats [1]. Although, active dumping of unexploded ordnances in the United States was prohibited by Title I of the Marine Protection, Research and Sanctuaries Act in 1972, military training and weapon testing continue to release RDX to adjacent coastal settings [2]. Studies have reported that RDX has toxic effects on aquatic organisms in marine systems [3,4] and concern has further increased due to the possible carcinogenety of RDX in humans [4].

There is considerable interest in exploring the natural remediation techniques for the removal of RDX-contaminated marine coastal habitats [5]. The fate of RDX in coastal marine ecosystems is determined by physico-chemical properties of the compound (solubility, octanol-water partition constant, vapor pressure, Henry's Law constant) [6] and environmental conditions (including

sediment properties, ionic strength, pH, redox conditions and biological factors). It has been identified that RDX has relatively low sorption affinity to sediment [7,8] and low bioconcentration potential in marine aquatic organisms [4]. The heterocyclic ring in RDX makes it unstable after the reduction of only one nitro group [9] and several benchtop studies have proven the microbial potential of biodegradation of RDX under anaerobic conditions [1,10-12]. In contrast, several studies have shown the persistency of RDX in well aerated aquatic systems [13,14] suggesting the dependence of RDX biodegradation on prevailing redox condition in the system. Therefore, it is vital to examine the biodegradation extent and pathways in different micro-environments with different redox conditions including surface water, porewater and sediment in the ecosystem [2]. Furthermore, studying the ultimate fate of RDX in coastal marine habitats by assessing the role (partitioning, biodegradation and mineralization) of different compartments (surface water, porewater, sediment, biota and suspended particulate matter) of the ecosystem is critical for the development of natural remediation techniques of RDX in coastal systems. Complete mineralization of RDX is an optimal scenario of removal of RDX from the ecosystem since dissolved inorganic mineralization products can be recycled in the system while gaseous products can escape to the atmosphere.

Studies based on RDX transformation mainly focus on ground water and fresh water systems [1,10-12] with little data for marine ecosystems [2,15]. Existing records are also limited to laboratory bench top studies leaving a considerable data gap of biodegradation and mineralization of RDX at an ecosystem scale that represent real coastal habitats containing natural microbial assemblages. Using isotopically labelled RDX helps to trace the pathways of RDX in an ecosystem and enables a full nitrogen based, mass balance of the system to track the ultimate fate of RDX.

Here, we evaluate major pathways controlling the fate of RDX in contaminated marine ecosystems by introducing isotopically labelled ^{15}N-[RDX] to large, aquarium-scale, laboratory-simulated coastal marine habitats over 15 days. RDX and its transformation products including reduced nitroso-derivatives and mineralization products in terms of dissolved inorganic nitrogen in dissolved (surface water and porewater) and solid phases (suspended particulate matter, sediment and biota) of the ecosystem were monitored during the experiment. ^{15}N enrichments of bulk sediment ($^{15}N_{sed}$), suspended particulate matter ($^{15}N_{SPM}$) and biota ($^{15}N_{biota}$) were also measured in order to acquire a ^{15}N mass balance of the ecosystem. Mechanistic differences in RDX transformation with respect to redox conditions prevail in the ecosystem and factors controlling the ultimate fate of RDX in coastal habitats were examined in this study.

4.3 Methods

4.3.1 Experimental design

Two 70L glass aquaria (experimental tanks) linked to each other via a glass aquarium reservoir to obtain common circulation and aeration were used as described in [4,13]. Experimental tanks were loaded with an 8cm deep layer of sandy, low organic carbon (OC) containing sediment (0.2 % OC) collected from a subtidal habitat in Long Island Sound (LIS; 41^0 19′ 13″ N , 72^0 2′ 59″ W). The system was maintained under flow through conditions with sea water from LIS (30 PSU) over two weeks to achieve stabilized redox conditions in sediment and then, switched to a closed loop recirculation at 24 hours before the start of the experiment. Two experimental tanks were loaded with macroalgae, epifaunal, bivalve and fish species [4] and water recirculation was continued over the course of the experiment (15 days). Hexahydro-1,3,5-trinitro-1,3,5-triazine (RDX) labeled with ^{15}N in all nitro positions was introduced to the system. The RDX was dissolved in acetone (0.815mL) and was initially introduced as a pulse of concentrated stock into

the aquarium reservoir to achieve initial target RDX concentrations of 0.4mg L^{-1} in the whole system. Subsequent RDX addition was done by continuous metered addition of RDX at a pumping rate of 0.037 mL min^{-1} throughout the experiment in order to maintain a steady state RDX concentration of 0.4 mg L^{-1}.

4.3.2 Sampling plan and techniques

Time series samples (total 10 sampling time points) of overlying water, porewater, suspended particulate matter (SPM) and sediment were taken from the tanks over the course of the experiment including two time points with triplicate samples. Sampling of biota is described in [4]. Overlying water was drawn using a peristaltic pump at a rate of 50 mL min^{-1} and filtered through precombusted 0.7 μm glass fiber filters (GF/F). Suspended particulate matter (SPM) was retained on the filter. Porewater was collected by using a 1/8" stainless steel tube penetrated through the sediment layer, attached to a peristaltic pump at a slow pumping rate of 2.5 mL min^{-1} and filtered through polyethersulfone - 0.2μM (0.2 μM PES) syringe tip filters. Sediment cores with a diameter of 2.6 cm were obtained and subsectioned at 2cm intervals prior to the analysis.

4.3.3 System characterization

Physical parameters of the systems including temperature and salinity were measured using a YSI probe (YSI 556 MPS) over the course of the experiment. Both overlying water and porewaters were analyzed for ammonium, and total nitrate and nitrite using a Smartchem nutrient analyzer (Westco-W12623) following phenol hypochlorite and cadmium azo-dye methods [16], respectively. 40 mL overlying water and porewater samples were analyzed for dissolved organic carbon (DOC) using a total organic carbon (TOC) analyzer (Shimadzu TNM-1). Dissolved ferrous and sulfide were measured on 3 mL of filtered (0.2 μM PES) porewater using ferrozine [17] and methylene blue methods respectively [18]. Samples were reacted with reagents

immediately upon collection to avoid exposure to atmospheric oxygen. The redox potential of sediment was measured using a platinum electrode (Paleo Terra, Amsterdam) relative to an Ag/AgCl reference electrode (Fisher Scientific). Sediment was characterized for TOC, total nitrogen (TN) and total elemental sulfur (S) using a Perkin Elmer elemental analyzer (NA 1500) [19]. Sediment texture was determined using a mechanical sieve analyzer with a set of sieves from 0.063 mm to 2.0 mm.

4.3.4 Dissolved explosive analysis

RDX and its reduced degradation products, including, Hexahyro-1-nitroso-3,5-dinitro-1,3,5-triazine (MNX), Hexahyro-1,3-dinitroso-5-nitro-1,3,5-triazine (DNX), and Hexahyro-1,3,5-trinitroso-1,3,5-nitro-1,3,5-triazine (TNX), were analyzed in both overlying water and porewater samples. A modified salting-out method [20] adapted for smaller sample sizes was used for extraction of munition compounds from aqueous samples following methods described in [8]. An average recovery of 99.1 ± 0.5% was obtained for known amounts of 1, 2-dinitrobenzene (1,2-DNB) in water extractions. Water extracts were analyzed using gas chromatography (GC)/electron-capture detection (ECD) following the methods described by [8,21,22]. 3, 4-dinitrotoluene (3,4-DNT) was added to each extract prior to injection to monitor detection efficiency. Explosive analysis was performed with an Agilent GC/ECD [21] equipped with an HP-DB5 column (30 m x 320 µm, 0.25-µm; Agilent). Quantification was based on an external calibration curve of available standard munitions RDX, MNX, DNX and TNX. (AccuStandard, New Haven, CT). The average reporting limit for all compounds was 1.3 $ngmL^{-1}$.

4.3.5 Sediment, particulate and bio-tissue explosive analysis

Sediment samples were homogenized and 2g of each was extracted with 10mL of ACS-grade acetonitrile (ACN) following the method described by [2,8]. 3,4-dinitrotoluene (3,4-DNT;

Accustandard) was spiked as a recovery standard and extraction efficiencies averaged as 82%. Suspended particulate matter (SPM) in 0.7 μM GF/F filters was spiked with 1, 2-Dinitrobenzene (1, 2-DNB; Accustandard, New Haven, CT) as a recovery standard, and explosives were extracted by 1 h of sonication in 5 mL of acetonitrile. 3,4-Dinitrotoluene (3,4-DNT; Accustandard, New Haven, CT) was added prior to GC-ECD analysis to monitor detection efficiency and extraction efficiencies ranged from 60 to 93%. Sediment and SPM extractions were analyzed for explosives (RDX, MNX, DNX and TNX) using (GC)/electron-capture detection (ECD) as described above. Munition extraction and analysis of bio-tissue samples were described in [4].

4.3.6 Bulk $\delta^{15}N$ analysis

Freeze dried sediment and SPM samples were analyzed using a continuous flow elemental analyzer – isotope ratio mass spectrometry (EA-IRMS: Delta V, Thermofisher) at the University of Connecticut for bulk ^{15}N enrichments. Nitrogen isotope ratios were reported in δ notation as follows:

$$\delta^{15}N = [(R_{sample} - R_{STD})/R_{STD}] \quad (1)$$

where R_{STD} was the $^{15}N/^{14}N$ ratio of atmospheric nitrogen and R_{sample} is the $^{15}N/^{14}N$ ratio of the sample. $\delta^{15}N$ values and N content were calibrated to USGS glutamic acid reference materials USGS 40 and 41 and reported in per mil (‰) notation. Excess ^{15}N mass (mol) above pre tracer levels in the different media: sediment and SPM were calculated from Equations 2 and 3.

$$^{15}N \text{ mols Excess}_{sed} = N \text{ mols}_{sed} * (X^{15}N_{t\ sed} - X^{15}N_{t0\ sed}) \quad (2)$$

$$^{15}N \text{ mols Excess}_{SPM} = N \text{ mols}_{SPM} * (X^{15}N_{t\ SPM} - X^{15}N_{t0\ SPM}) \quad (3)$$

where the total N mass, and mole fractions of ^{15}N at time t ($X^{15}N_{t\ sed}$ and $X^{15}N_{t\ SPM}$) and time zero prior to tracer introduction ($X^{15}N_{t0\ sed}$ and $X^{15}N_{t0\ SPM}$) were obtained from an elemental analyzer – isotope ratio mass spectrometry EA-IRMS (Delta V, Thermofisher). Precision on replicate samples of sediment and SPM samples were 20% and 14% respectively (Percent coefficient of variance, CV. Excess bulk ^{15}N in biota was determined using similar methods as described in Ballantine et al., 2016 [4].

4.3.7 Mineralization products

The mineralization products, $^{15}NH_4^+$, total $^{15}NO_2^-$ and $^{15}NO_3^-$ ($^{15}NO_X$),total $^{15}N_2$ and $^{15}N_2O$ ($^{15}N_{gas}$) in the aqueous phase, were quantified using IRMS techniques. Filtered (0.2 µM PES), $^{15}NH_4^+$ enrichment was determined on NH_4^+ isolated from frozen water via alkaline acid trap diffusion [23,24] and extraction efficiency was between 95-105% based on the recovery of NH_4NO_3 standards and precision on replicate samples is 25%.Moles of $^{15}NH_4^+$ were calculated using NH_4^+ concentrations and mole fractions of ^{15}N in NH_4^+ ($X^{15}N_{t\ NH4+}$ and $X^{15}N_{t0\ NH4+}$) obtained from a Smartchem nutrient analyzer and EA-IRMS respectively (equation 4).

$$^{15}NH_4^+ \text{ mols Excess} = NH_4^+ \text{ mols} * (X^{15}N_{t\ NH4+} - X^{15}N_{t0\ NH4+}) \quad (4)$$

$\delta^{15}NO_X$ values were obtained via the denitrifier method using *Pseudomonas aureofaciens* [25,26] at the US Geological Survey (USGS) in Reston, VA on water samples filtered through a 0.2µM PES filters and frozen. Moles of $^{15}NO_X$ were calculated using NO_X concentration and the mole fractions of ^{15}N in NO_X ($X^{15}N_{t\ NOX}$ and $X^{15}N_{t0\ NOX}$) obtained from a Smartchem nutrient analyzer and GB-IRMS respectively (equation 5).

$$^{15}NO_X \text{ mols Excess} = NO_X \text{ mols} * (X^{15}N_{t\ NOX} - X^{15}N_{t0\ NOX}) \quad (5)$$

$^{15}N_{gas}$ in water samples was determined using continuous flow isotope ratio mass spectrometry on a Thermo Delta V Plus with a Gas Bench interface (GB-IRMS). Gas samples were collected at each time point by pumping unfiltered water into 30 mL serum bottles that had previously been sealed, pre-loaded with 750µl of 2N KOH (for preservation), and flushed with He for 12 minutes [27]. After at least 6 hours of headspace equilibration, the isotopic composition of N_2 ($\delta^{15}N_2$) was measured. Dissolved ambient N_2 concentrations were assumed to be in equilibrium with the atmosphere and were calculated as a function of temperature and salinity [28]. Because dissolved N_2O was converted to N_2 at alkaline conditions (pH 11 and 12) during storage, measured N_2 value ($^{15}N_{gas}$) corresponded to both dissolved N_2 and N_2O those were present in the water at the time of sampling. Measured $^{15}N_2$ production was corrected (Equation S1) for the alkaline hydrolysis of RDX which though minor (<1.7%), may occur during prolonged storage of samples between pH 11 and 12 at 20^0C [7,29,30]. Moreover, since the experiment was conducted as an open system, we calculated $^{15}N_{gas}$ amount that had evaded to the atmosphere using measured dissolved $^{15}N_{gas}$ amounts. Evasion rates (i.e. loss rates of excess $^{15}N_2$ from the tanks) were calculated using the method described in [2].

4.3.8 Data analysis

A mass balancing approach was based on ^{15}N equivalents in masses of each analyzed N-containing parent and derivative pool and illustrated in the equation 6. ^{15}N quantities derived from RDX, MNX, DNX and TNX were calculated by multiplying their concentrations by 3 since each compound has three ^{15}N labelled nitrogen atoms.

$$^{15}N\text{-}RDX_{system} = {}^{15}N\text{-}\sum RDX_{\text{surface water}} + {}^{15}N\text{-}\sum RDX_{\text{porewater}} + {}^{15}N\text{-}\sum RDX_{\text{sediment}} + {}^{15}N\text{-}\sum RDX_{\text{biota}} + {}^{15}N_{SPM} + {}^{15}N\text{-}NH_4^+{}_{\text{dissolved}} + {}^{15}N\text{-}NO_{X\ \text{dissolved}} + {}^{15}N\text{-}N_{gas\ \text{dissolved}} + {}^{15}N\text{-}N_{gas\ \text{evaded}} + \text{unidentified } {}^{15}N\text{-compounds in the system} \quad (6)$$

where, $^{15}N\text{-}RDX_{system}$ represents total mol of ^{15}N-RDX introduced into the system and the remaining terms represent ^{15}N measured in different RDX-derived metabolites in surface water, porewater, sediment, bio-tissues, mineralization products, and SPM. ∑ RDX represents RDX and measurable derivatives including MNX, DNX and TNX.

Principle component analysis (PCA) was carried out to evaluate the covariance of various fates of the ^{15}N-RDX tracer and with geochemical variables. PCA was performed using all measured pools of ^{15}N and geochemical variables as metrics for the system using 'Excelstat'. Metrics used in PCA were mean normalized, and data gaps were filled using the instrument detection limits for a particular analysis.

4.4 Results

4.4.1 RDX

The initial water column RDX concentration in the tanks was 1.9 µM (0.42 mg/L) and RDX was lost from the water column following first order kinetics with a decay constant of 0.025 day^{-1} (R^2 = 0.7). It obtained steady state concentration of 1.1 ± 0 .18 µM (0.25 ± 0.04 mg/L) by day 9 (Figure 1, Table S1-a) although the target concentration of RDX in the tanks was 1.8 µM (0.4 mg/L) by continuous addition of RDX. Over the 21 days, the bulk fraction of the total detectable cumulative RDX in the system remained in the water column in the surface water aqueous phase (79% - 41%) (Figure 2). RDX was not detected in the SPM particulates. RDX was detected at trace amounts in porewater (Table S1-b) and biota but each phase accounted for only 0.2% of the RDX lost [4]. RDX was not found on both shallow (0-2cm) and deep (2-4cm) sediments throughout the experiment.

Figure 1: Time series water column munition concentrations; Error bars are standard deviations (n=3); DNX was not detected.

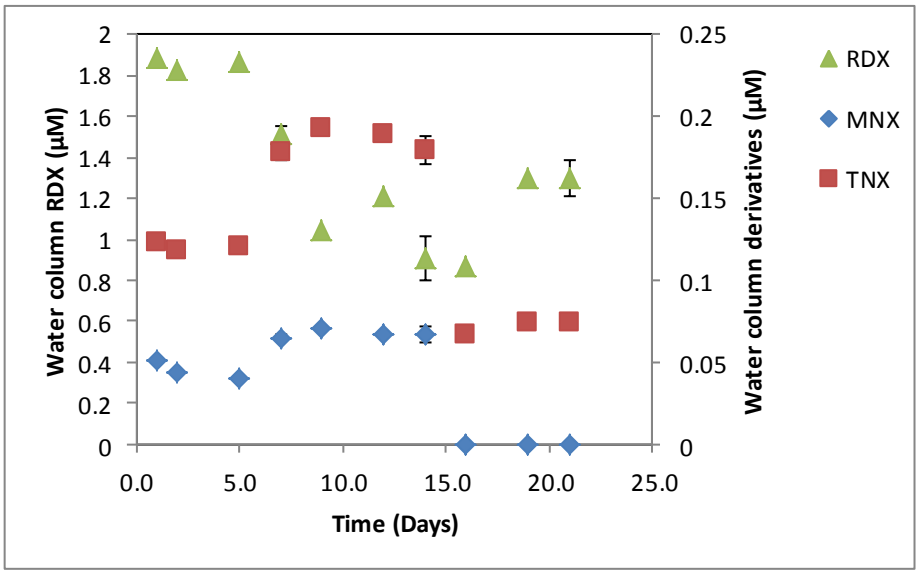

Figure 2: Fraction of cumulative ^{15}N added to the system in each detected pool as a full ^{15}N mass balance. ∑ Derivatives water column = [MNX + TNX]; ∑ RDX porewater = [RDX + MNX + DNX + TNX]; ^{15}N biota, ^{15}N POM, ^{15}N sed = Total ^{15}N from bulk analysis in bio tissue, particulate organic matter and sediment (0-2cm + 2-4cm depths) respectively.

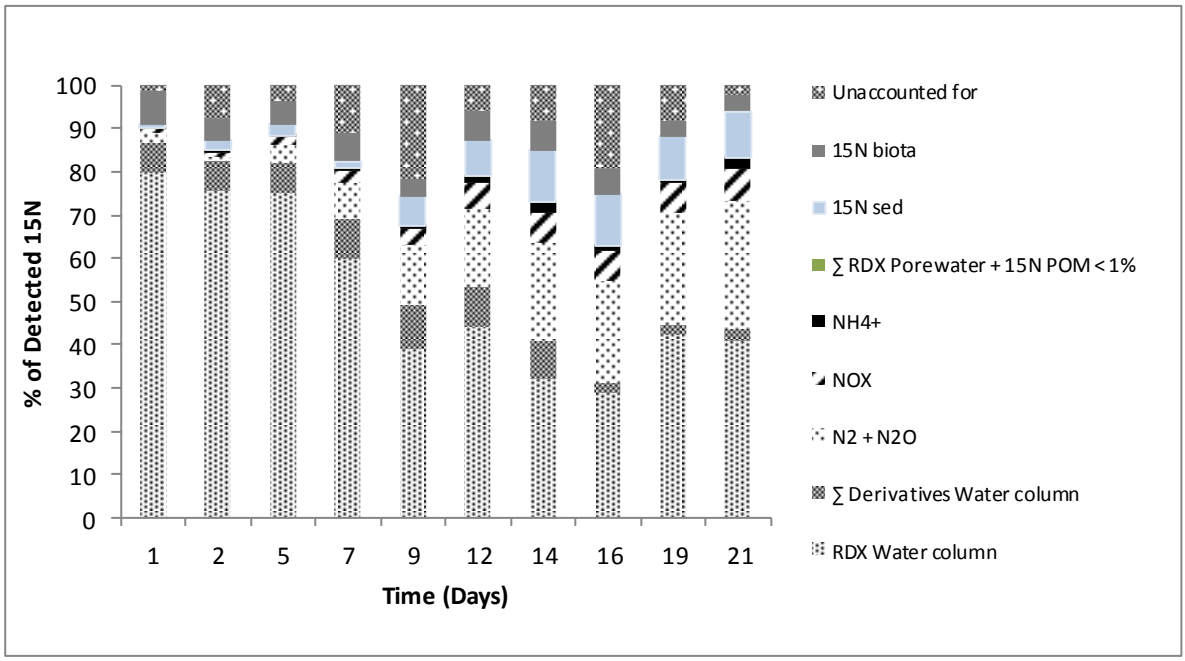

4.4.2 Derivatives

Reduced nitroso-derivatives of RDX including MNX, DNX and TNX were detected in both dissolved and particulate pools in the ecosystem. The ratio of water column TNX (0.12 - 0.19 μM) and MNX (0.04 – 0.07 μM) concentrations varied in the range of 2.4 – 3.0 until day 14 when TNX concentrations decreased to 0.07 μM while MNX was no longer detected in the water column (Table S1-a). DNX was also not identified in the water column and the total detected nitroso-derivatives as a percentage of total cumulative RDX increased from 7 % to 10% until day 9 and then, decreased to 2% and remained constant (Table S1-a, Figure 2). All the three nitroso-derivatives (MNX, DNX and TNX) were identified in porewater in trace concentrations, in the range of 0.001 - 0.022 μM (0.01% – 0.22 %) (Table S1-b, Figure 2). Average ratios of RDX to total derivatives in the water column and porewater were 10 and 0. 6 respectively during the experimental time period. Thus, the fraction of nitroso-derivatives relative to cumulative RDX input, partitioned onto sediment and bio tissue in the ecosystem is fairly low; 0.6% - 4.2% (Table S1-c; [4]). RDX and derivatives extracted from SPM was consistently below detection limits in the system. TNX was the only detected nitroso-derivative in shallow sediment varied in the range of 0.03% and 4.09% (Table S1-c) and none of the nitroso-derivative was identified in deep sediment. The percentage of total nitroso-derivatives found in bio-tissue samples was also small, dropping from 0.6% to 0.1% of total input of RDX during the experiment [4].

4.4.3 Mineralization products

^{15}N isotopic enrichment was observed in all dissolved inorganic nitrogen (DIN) pools, including $^{15}NO_2^- + {}^{15}NO_3^-$ ($^{15}NO_x$), $^{15}NH_4^+$, $^{15}N_2$ (Table 1). Maximum $\delta^{15}N$ values for each were $\delta^{15}NH_4^+$ =1400‰, $\delta^{15}NO_x$ =2200‰ were higher than $\delta^{15}N_2$ (31‰) in the water column while. The $\delta^{15}N_2$ in porewater yielded higher values (22 - 130‰) than those values observed in the water column

towards the end of the experiment (Table 1). Calculated ^{15}N excess (µmol) increased in all mineralization products whereby excess $^{15}NH_4^+ < {}^{15}NO_x < {}^{15}N_{gas}$ (N_2 and N_2O) (Table 1; Table S2). The percent of ^{15}N in mineralization products ($^{15}NH_4^+$, $^{15}NO_x$, $^{15}N_2$ and $^{15}N_2O$) in both the water column and porewater, and gas lost via evasion to atmosphere) relative to cumulative RDX input increased steadily over the duration of the experiment (Table 1). $^{15}NH_4^+$ production in porewater (0.03-5.3%) was higher than in the water column (0.06-0.7%). Evidence of net $^{15}NO_x$ production was not observed in porewater though it was detected in the water column with an increasing trend (0.90 - 7.2%) over the duration of the experiment (Table S2). The majority of $^{15}N_{gas}$ ($^{15}N_2$ and $^{15}N_2O$) production in the ecosystem was evaded to the atmosphere (90% of total $^{15}N_{gas}$ production), based on gas transfer calculations over the course of the experiment (Table S2).

Table 1: Inorganic nitrogen production from RDX as $\delta^{15}N$, µmol ^{15}N excess and % values.

Time, days	$\delta^{15}N$ water column			$\delta^{15}N$ porewater		^{15}N excess water column, µmol			^{15}N excess porewater, µmol		Evaded $^{15}N_2$ excess, µmol	Spiked ^{15}N-[RDX], µmol	% Inorganic nitrogen
	NH_4^+	NO_X	N_2	NH_4^+	N_2	NH_4^+	NO_X	N_2	NH_4^+	N_2			
0	280	140	0	3.1	0	0	0	0	0	0	0	0	0
1	230	2200	26	6.8	26	0.85	5.5	6.8	0.17	1.6	4.2	590	3.2
2	130	1600	2.4	27	2.4	0.69	5.3	0.61	0.43	0.14	6.4	590	2.3
5	480	1760	12	13	12	2.6	11	3.2	0.3	0.75	22	600	6.6
7	400	2000	15	33	100	1.6	17	3.7	1.2	6.2	40	610	11
9	720	2200	31	60	130	1.5	24	7.5	2.4	8.1	70	610	19
12	770	2000	22	760	22	2.3	37	5.1	33	1.3	110	620	30
14	920	1800	27	1100	74	1.8	44	6.3	11	4.5	130	630	31
16	1400	2000	5	79	110	4.5	44	1.1	4.3	6.7	140	640	31
19	990	1600	15	150	110	0.45	44	3.3	3.7	6.9	160	650	34
21	120	1700	30	680	88	0.42	47	6.4	17	5.3	180	650	39

% DIN of spiked (detectable) ^{15}N-[RDX] is calculated using µmols of spiked ^{15}N-[RDX], and sum of ^{15}N excess of $NH_4^+ + NO_x + N_2$ gas in water column, ^{15}N excess of $NH_4^+ + N_2$ gas in porewater and evaded ^{15}N gas excess in µmols.

4.4.4 Particulates and biological tissue

Significant isotopic enrichment was observed in throughout the duration of the experiment (Table S3). $\delta^{15}N_{SPM}$ values increased from 3.5‰, before the initial RDX spike to a range of 360 – 2200 ‰ during the experiment (average = 1100 ± 600 ‰), with no discernible trends in the data. Normalized bulk ^{15}N values in SPM rapidly increased to a value of 140 nmol/g SPM followed by a small decrease and almost remained constant throughout the experiment (average = 82 ± 32) (Table S3) . $\delta^{15}N$ of shallow surface sediments (0-2cm) increased from a pre-spike value of 72 ‰ to a range of 87 – 530 ‰, with the highest value occurring at day 16. $\delta^{15}N$ of deeper sediments (2-4cm) also increased from a pre-spike value of 33 ‰ to a range of 39 – 100 ‰. Normalized bulk ^{15}N values in shallow sediments (0-2cm) were higher (averaged 4 times) than that of in deeper sediments (2-4cm). Total sediment ^{15}N values including shallow and deep sediments increased and stayed constant in the range of 9.0 ±0.61 nmol ^{15}N/g sed for the rest of the experimental duration (Table S3). $\delta^{15}N$ values of bio-tissue samples were highly variable with time and space and ranged in between 14 ‰ and 277 ‰ [4].

4.4.5 Geochemical conditions of the experiment

Porewater NH_4^+ concentrations (130-780 µM) were 6 - 85 times higher than in the water column (4.3-40 µM) while NO_X concentrations were 16-470 times higher in the water column (6.8-110 µM) than in porewater (0.16-0.42 µM) of the ecosystem. Total dissolved nitrogen concentrations ($NH_4^+ + NO_x$ + DON) in porewater (90-1000 µM) were 2-25 higher than water column values (28-140µM) in the ecosystem, although water column concentrations increased with the time (Table S4). The redox potential of surface water was 63 mV and sediment depth profiles were significantly varied between sampling sites in the ecosystem, indicating significant spatial and temporal heterogeneity (Table S5). Porewater pH varied over time among sampling sites,

ranging from 7.5 to 8.2 and spatial heterogeneity (CV of 4%) in the system was comparable to the temporal variation (CV of 2%). Fe^{+2} concentrations in porewater from deeper (2-4cm) sediments were higher than shallow and shallow (0-2cm) sediments. Though the Fe^{2+} concentrations increased over the duration of the experiment, there was no discernable pattern with time. Reduced sulfur (H_2S) was not detected in either shallow or deeper levels of sediment in the ecosystem.

4.5 Discussion

4.5.1 Mass balance

The use of ^{15}N enabled a much more complete assessment of the fate and transport of RDX relative to analysis using isotopically unlabeled RDX. The total ^{15}N added during the entire experiment amounted to 652 μmol. Of this 78% - 99% was accounted for and the distribution of tracer ^{15}N among all measured pools, from largest to smallest, at the end was:

RDX in water column > N gases (surface water + porewater + evasion) > shallow sediment (0-2cm) > NO_x > biota > NH_4^+ > ^{15}N as ∑ derivatives in water column > deep sediment (2-4cm) > ∑ derivatives in porewater > RDX in porewater > water column POM

Here, ∑derivatives is the sum of MNX, DNX and TNX. In this study, we discuss new insights gained into fate of RDX including transformation, mineralization and partitioning processes in the marine environment through the observed distribution of ^{15}N.

4.5.2 Transformation

The RDX half-life in the water column of 28 days was comparatively shorter than previous studies of fresh water and terrestrial systems demonstrating longer half-lives of days [13,31,32]. Mono and tri-nitroso-triazines (MNX and TNX) were observed in oxygenated surface water and probably RDX had degraded at the sediment surface and derivatives had been released into the

surface water because aerobic degradation of RDX is relatively uncommon in the environment [14]. MNX formation is an important part of RDX reduction [33] and MNX can be further reduced to produce nitroso-triazines (DNX and TNX), denitrate or denitrosate forming ring cleavage products under aerobic conditions [34]. TNX can be removed from the well-aerated water column via further degradation to ring cleavage products, but here we identified TNX as a relatively stable product in the aerobic water column probably because other competitive degradation processes outcompeted TNX degradation in the ecosystem. RDX diffused into the surface sediment where hypoxic conditions prevailed and biodegraded forming nitroso- triazines, MNX, DNX and TNX [10] at higher rates than it did in water column [13].

4.5.3 Partitioning

RDX and RDX-derived metabolite partitioning into the particulate pools (sediment, POM and biota) has been measured in marine ecosystems as seen in sediment slurries [8,10], groundwater systems [35] and terrestrial ecosystems [36]. Due to the relatively low hydrophobicity in terms of log K_{ow} and structure of RDX and its derivatives [8], passive partitioning especially, onto the sediment and SPM did not constitute a major pathway in the fate of RDX. And our results were consistent with these results as evidenced by low ^{15}N percent of RDX loss on SPM. Bulk ^{15}N derived from RDX rapidly sorbed onto SPM in the water column and sorption was irreversible under aerobic conditions illustrating constant concentrations in SPM during the experiment. Bulk ^{15}N in SPM was likely due to unmeasured derivatives such as 4-nitro-2,4-diazabutanal (NDAB) that can be formed in oxygenated environments or sorption of liberated $^{15}NH_4^+$ to particles. [34,37]. However, bulk ^{15}N derived from RDX sorbed onto the surface sediment was increasing steadily until day 14 where it reached steady state. Considerably, lower bulk sediment ^{15}N values in deeper sediment confirmed the low vertical diffusion of RDX and its derivatives in sediment.

Marine microbial assemblages (*Shewanella halifaxensis,Clostridium sp.*) provided significant contribution for degradation of RDX under oxygen limited conditions [34] resulting primarily TNX, since TNX was the only identifiable ^{15}N containing compound in sediment. Unidentified ^{15}N in sediment might reside in non-measured derivatives such as Medina [34,37] or as microbially incorporated ^{15}N.

4.5.4 Mineralization

Mineralization of RDX in terms of inorganic nitrogen production ($^{15}NO_X$, $^{15}NH_4^+$, $^{15}N_2$ and $^{15}N_2O$ gases) played an important role in the fate of RDX in marine ecosystems and the movement of the tracer from RDX to the mineralization pools confirms the capability of marine microbial assemblages to decompose RDX [2,34,38]. Among the other inorganic nitrogen products, gaseous mineralization products ($^{15}N_2$ and $^{15}N_2O$) formation was favored by the available microbes and prevailing environmental conditions in the system [2,33]. Mineralization pathways showed significant differences depending on the prevailing redox conditions in sub-environments such as sediment and surface water of the ecosystem. Moreover, production of nitrogen containing mineralization products varied in terms of types of products formed and quantitative production in well aerated surface water and hypoxic sediment (porewater). Di-denitration of RDX followed by hydroxylation, and mono-denitration of MNX followed by denitrosation resulted NDAB yielding $^{15}NO_X$ from both pathways in aerobic conditions [34]. NDAB was more stable in water under ambient conditions and to a lower extent, it could be degraded with marine microbes (eg: Methylobacterium and Chrysosporium) [34] leading to the production of $^{15}N_2O$ and $^{15}NH_4^+$ in the water column. In hypoxic conditions, mono-denitration of RDX followed by hydroxylation forms Methylenedinitramine (Medina) which was very unstable and had the potential to degrade to N_2O [34]. Medina formation has been identified as a common

NH_4^+ releasing process under low oxygen conditions [34], consistent with the elevated $^{15}NH_4^+$ in surface sediment porewaters here. Besides the decomposition of Medina, mono or poly-denitration of RDX and nitroso triazines including MNX, DNX and TNX was also involved in the formation of $^{15}N_2O$ by denitrification of cleaved $^{15}NO_X$ found in the sediment (porewater). Moreover, $^{15}N_2O$ could be further denitrified to form $^{15}N_2$ in sediment [2]. The above processes indicated that gaseous mineralization product formation ($^{15}N_2O$ and $^{15}N_2$) was significant in hypoxic environments and diffused to the overlying water. Finally, they escaped to the atmosphere [2] as an efficient removal mechanism of RDX from coastal marine ecosystems.

4.5.5 Fate of RDX in marine ecosystem

Tracing the fate of RDX with ^{15}N provided a descriptive picture of partitioning, degradation and mineralization of RDX in coastal marine ecosystems. Although RDX was known to be a fairly stable compound in surface water or in low organic carbon groundwater, here, we illustrated the fate of RDX in a multi-compartment marine ecosystem (surface water, porewater, sediment, biota). From a mass balancing perspective, partitioning of RDX and identified RDX-derived compounds onto solid phases of the ecosystem was not a dominant process due to relatively low sorption properties of the compounds. Active and passive partitioning of RDX and RDX derived compounds onto biota was a rapid process (Figure 2) although it contributed less than 10% to the total mass balance [4].

Degradation and mineralization of RDX were favored by lower redox potential (iron reducing condition) and available microbial assemblage in surface sediment of the ecosystem. However, aerobic degradation of RDX forming nitroso-triazines and mineralization forming $^{15}NO_X$ also provided considerable contribution to the ^{15}N mass balance. Though ammonia was produced as one of the mineralization products under both aerobic and hypoxic conditions, it was not

cumulative and the pool was insignificant for the overall mass balance. Continual production of nitrogen containing gaseous mineralization products became the ultimate fate of RDX in coastal marine ecosystems. Surface sediment acted as the main mineralization zone for production of $^{15}N_2$ and $^{15}N_2O$ gases in the presence of marine microbial assemblages [2]. PCA analysis provided the evidence for potential involvement of iron reducing bacteria in sediment on gas production [39] since ^{15}N-(N_2+N_2O) and reduced iron species in porewaters of surface sediment were clustered together in the PCA plot (Figure 3) $^{15}N_2$ and $^{15}N_2O$ gases produced in surface sediment diffused into the surface water column and ultimately escaped to the atmosphere [2]. Moreover, surface water $^{15}NO_X$ was also clustered with Fe^{2+} and ^{15}N-(N_2+N_2O) inferring some contribution of $^{15}NO_X$ liberated from denitriration to the production of ^{15}N gases in the in this anaerobic environment. Further, rates of ^{15}NOx production in surface water and conversion to gases may also be similar since we observed constant concentration of $^{15}NO_x$ towards the end of the experiment. And by day 21, estimates of the net gas flux were sufficient to close the RDX mass balance completely. Although, the mineralization of RDX into nitrogen containing gaseous products, were confirmed in this study, it is worthwhile to track concentrations of $^{15}N_2$ and $^{15}N_2O$ separately in future work to improve degradation rate estimates and pathways. Here, we concluded that over 21 days in an open system, 28% of nitrogen derived from RDX was efficiently removed from contaminated coastal marine habitat via the production of gaseous mineralization products which escaped to the atmosphere. The half-life for ^{15}N retained in the system as both dissolved and partitioned, RDX and derivatives after the evasion was 59 days. Therefore, ^{15}N derived from RDX is retained in the ecosystem longer than RDX by a factor of 2.1; 28 days vs 59 days.

4.6 Acknowledgment

This work was funded by Department of Defense- SERDP under Project ID ER-2122. We would like to thank D. Cady and V. Rollinson for analytical support.

4.7 References

[1] Hawari J, Halasz A, Sheremata T, Beaudet S, Groom C, Paquet L, Rhofir C, Ampleman G, Thiboutot S. 2000. Characterization of metabolites during biodegradation of hexahydro- 1,3,5-trinitro-1,3,5-triazine (RDX) with municipal anaerobic sludge. *Appl Environ Microbiol* 66:2652-2657.

[2] Smith RW, Tobias C, Vlahos P, Cooper C, Ballentine M, Ariyarathna T, Fallis S, Groshens TJ. 2015. Mineralization of RDX-derived nitrogen to N2 via denitrification in coastal marine sediments. *Environ Sci Technol* 49:2180-2187.

[3] Rosen G, Lotufo GR. 2005. Toxicity and fate of two munitions constituents in spiked sediment exposures with the marine amphipod Eohaustorius estuarius. *Environ Toxicol Chem* 24:2887-2897.

[4] Ballentine ML, Ariyarathna T, Smith RW, Cooper C, Vlahos P, Fallis S, Groshens TJ, Tobias C. 2016. Uptake and fate of hexahydro-1,3,5-trinitro-1,3,5-triazine (RDX) in coastal marine biota determined using a stable isotopic tracer, 15N - [RDX]. *Chemosphere* 153:28-38.

[5] Public works technical bulletine 200-1-95. 2011. *Soil Composting for Explosives Remediation: Case Studies and Lessons Learned.*

[6] Kalderis D, Juhasz AL, Boopathy R, Comfort S. 2011. Soils contaminated with explosives: Environmental fate and evaluation of state-of the-art remediation processes (IUPAC technical report). *Pure and Applied Chemistry* 83:1407-1484.

[7] Pichtel J. 2012. Distribution and fate of military explosives and propellants in soil: A review. *Applied and Environmental Soil Science* 2012.

[8] Ariyarathna T, Vlahos P, Tobias C, Smith R. 2015. Sorption kinetics of TNT and RDX in anaerobic freshwater and marine sediments: Batch studies. *Environ Toxicol Chem* 35(1)47-55.

[9] Anke H., Kuhn A., Weber R.W.S. 2003. The role of nitrate reductase in the degradation of the explosive RDX (hexahydro-1,3,5-trinitro-1,3,5-triazine) by Penicillium sp. AK96151. *Mycological Progress 2* 3:219-225.

[10] Sheremata TW, Halasz A, Paquet L, Thiboutot S, Ampleman G, Hawari J. 2001. The fate of the cyclic nitramine explosive RDX in natural soil. *Environmental Science and Technology* 35:1037-1040.

[11] Best EPH, Sprecher SL, Larson SL, Fredrickson HL, Bader DF. 1999. Environmental behavior of explosives in groundwater from the Milan Army Ammunition Plant in aquatic and

wetland plant treatments. Removal, mass balances and fate in groundwater of TNT and RDX. *Chemosphere* 38:3383-3396.

[12] Kwon MJ, O'Loughlin EJ, Antonopoulos DA, Finneran KT. 2011. Geochemical and microbiological processes contributing to the transformation of hexahydro-1,3,5-trinitro-1,3,5-triazine (RDX) in contaminated aquifer material. *Chemosphere* 84:1223-1230.

[13] Smith RW, Vlahos P, Tobias C, Ballentine M, Ariyarathna T, Cooper C. 2013. Removal rates of dissolved munitions compounds in seawater. *Chemosphere* 92:898-904.

[14] Felt D.R., Bednar A., Arnett C., Kirgan R. 2009. Bio-Geochemical Factors That Affect RDX Degradation. *Proceedings of the Annual International Conference on Soils, Sediments, Water and Energy* 14:Article 17.

[15] Montgomery MT, Coffin RB, Boyd TJ, Osburn CL. 2013. Incorporation and mineralization of TNT and other anthropogenic organics by natural microbial assemblages from a small, tropical estuary. *Environ Pollut* 174:257-264.

[16] Smith P, Bogren K. 2001. Determination of nitrate and/or nitrite in brackish or seawater by flow injection analysis colorimeter: QuickChem Method. *Methods manual Lachat Instruments*.

[17] Stookey LL. 1970. Ferrozine - A new spectrophotometric reagent for iron. *Anal Chem* 42:779-781.

[18] Cline JD. 1969. Spectrophotometric determination of hydrogen sulfide in natural waters. Limnol. Oceanogr., 14, 454-458. *Limnol Oceanogr* 14:454-455,456,457,458.

[19] Hedges JI, Stern JH. 1984. Carbon and nitrogen determinations of carbonate-containing solids. *Limnology & Oceanography* 29:657-663.

[20] Townsend DM MT. 1996. *Recent Developments in Formulating Model Descriptors for Subsurface Transformation and Sorption of TNT, RDX and HMX*. Technical report IRRP-96-1. US Army Engineer Waterways Experiment Station, Vicksburg,MS,USA.

[21] Pan X, Zhang B, Cobb GP. 2005. Extraction and analysis of trace amounts of cyclonite (RDX) and its nitroso-metabolites in animal liver tissue using gas chromatography with electron capture detection (GC-ECD). 67:816-816-823.

[22] Zhang B, Pan X, Smith JN, Anderson TA, Cobb GP. 2007. Extraction and determination of trace amounts of energetic compounds in blood by gas chromatography with electron capture detection (GC/ECD). *Talanta* 72:612-619.

[23] Holmes R, McClelland J, Sigman D, Fry B, Peterson B. 1998. Measuring 15N-NH4+ in marine, estuarine and fresh waters: An adaptation of the ammonia diffusion method for samples with low ammonium concentrations. **1998**, *60*, 235-243. *Mar Chem* 60:235-243.

[24] Holmes RM, McClelland JW, Sigman DM, Fry B, Peterson BJ. 1998. Measuring $^{15}N\text{-}NH_4^+$ in marine, estuarine and fresh waters: An adaptation of the ammonia diffusion method for samples with low ammonium concentrations. *Mar Chem* 60:235-243.

[25] Sigman DM, Casciotti KL, Andreani M, Barford C, Galanter M, Böhlke JK. 2001. A bacterial method for the nitrogen isotopic analysis of nitrate in seawater and freshwater. *Anal Chem* 73:4145-4153.

[26] Casciotti KL, Sigman DM, Hastings MG, Böhlke JK, Hilkert A. 2002. Measurement of the oxygen isotopic composition of nitrate in seawater and freshwater using the denitrifier method. *Anal Chem* 74:4905-4912.

[27] Smith LK, Voytek MA, Bo¨hlke JK, Harvey JW. 2006. Denitrification in nitrate-rich streams: application of N_2:Ar and ^{15}N-tracer methods in intact cores. *Ecological applications* 16(6):2191–2207.

[28] Weiss RF. 1970. The solubility of nitrogen, oxygen and argon in water and seawater. *Deep-Sea Research and Oceanographic Abstracts* 17:721-735.

[29] Heilmann HM, Wiesmann U, Stenstrom MK. 1996. Kinetics of the alkaline hydrolysis of high explosives RDX and HMX in aqueous solution and adsorbed to activated carbon. *Environ Sci Technol* 30:1485-1492.

[30] Karakaya P, Sidhoum M, Christodoulatos C, Nicolich S, Balas W. 2005. Aqueous solubility and alkaline hydrolysis of the novel high explosive hexanitrohexaazaisowurtzitane (CL-20). *J Hazard Mater* 120:183-191.

[31] Bernstein A, Adar E, Ronen Z, Lowag H, Stichler W, Meckenstock RU. 2010. Quantifying RDX biodegradation in groundwater using d15N isotope analysis. *J Contam Hydrol* 111:25-35.

[32] Jenkins T.F, Bartolini C., Ranney T.A. 2003. Stability of CL-20, TNAZ, HMX, RDX,NG, and PETN in Moist, Unsaturated Soil. *Cold Regions Research and Engineering Laboratory* US Army Corps of Engineers,Hanover, New Hampshire.

[33] Sheremata TW, Hawari J. 2000. Mineralization of RDX by the white rot fungus Phanerochaete chrysosporium to carbon dioxide and nitrous oxide. *Environ Sci Technol* 34:3384-3388.

[34] Halasz A, Hawari J. 2011. Degradation routes of RDX in various redox systems. *ACS Symp Ser* 1071:441-462.

[35] Zheng W, Lichwa J, D'Alessio M, Ray C. 2009. Fate and transport of TNT, RDX, and HMX in streambed sediments: Implications for riverbank filtration. *Chemosphere* 76:1167-1177.

[36] Brannon JM, Price CB, Yost SL, Hayes C, Porter B. 2005. Comparison of environmental fate and transport process descriptors of explosives in saline and freshwater systems. *Mar Pollut Bull* 50:247-251.

[37] Fuller ME, Heraty L, Condee CW, Vainberg S, Sturchio NC, Böhlke JK, Hatzinger PB. 2016. Relating carbon and nitrogen isotope effects to reaction mechanisms during aerobic or anaerobic degradation of RDX (hexahydro-1,3,5- trinitro-1,3,5-triazine) by pure bacterial cultures. *Appl Environ Microbiol* 82:3297-3309.

[38] Bhatt M, Zhao J-, Monteil-Rivera F, Hawari J. 2005. Biodegradation of cyclic nitramines by tropical marine sediment bacteria. *J Ind Microbiol Biotechnol* 32:261-267.

[39] Gregory KB, Larese-Casanova P, Parkin GF, Scherer MM. 2004. Abiotic Transformation of Hexahydro-1,3,5-trinito-1,3,5-triazine by Fe II Bound to Magnetite. *Environmental Science and Technology* 38:1408-1414.

4.8 Supplemental data

$$\text{Corrected mols}_{gas} = \text{Measured mols}_{gas} - \text{Calculated mols}_{A.H.-RDX} \quad (1)$$

where mols_{gas} and $\text{mols}_{A.H.-RDX}$ represent mols of N_2 and N_2O gases and mols of RDX hydrolyzed under alkaline condition respectively.

Alkaline hydrolysis of RDX is consistent with a second-order rate law (Karakaya et al., 2005), thus, the amount of dissolved RDX hydrolyzed ($\text{mols}_{A.H.-RDX}$) is quantified using equation 6.

$$1/[RDX]_t = 1/[RDX]_{t0} + k_2 t \quad (2)$$

where $[RDX]_t$ and $[RDX]_{t0}$ represent RDX concentrations at time t and initial RDX concentration. k_2 is second order rate constant (obtained from Karakaya et al., 2005 as 0.15 $M^{-1}min^{-1}$) and t represents time.

The percent of alkaline hydrolysis of RDX was between 0.5% -1.7% during the experiment. But, RDX- derivatives including MNX, DNX and TNX may undergo alkaline hydrolysis insignificantly (< %) but, no published literature is found for correction purposes.

Table S1: Variation of RDX and nitroso-derivatives in terms of concentration and percentage of cumulatively added RDX into the system; bd = below detection

a) Water column

Time, days	RDX		MNX	TNX	Total derivatives	
	µM	%	µM	µM	µM	%
1	1.9	79	0.051	0.12	0.17	7.3
2	1.8	76	0.044	0.12	0.16	6.7
5	1.9	75	0.041	0.12	0.16	6.5
7	1.5	60	0.065	0.18	0.24	9.6
9	1.0	39	0.071	0.19	0.26	9.9
12	1.2	44	0.067	0.19	0.26	9.3
14	0.91	32	0.067	0.18	0.25	8.7
16	0.86	29	bd	0.067	0.067	2.2
19	1.3	42	bd	0.075	0.075	2.4
21	1.3	41	bd	0.075	0.075	2.4

b) Porewater

Time, days	RDX		MNX	DNX	TNX	Total derivatives	
	µM	%	µM	µM	µM	µM	%
1	0.0030	0.03	0.0014	bd	bd	0.0014	0.014
2	0.0042	0.04	0.0052	0.011	0.0059	0.023	0.220
5	bd	bd	bd	bd	bd	bd	bd
7	bd	bd	bd	bd	bd	bd	bd
9	0.0028	0.03	0.0023	0.0072	0.0042	0.014	0.130
12	bd	bd	0.0038	0.0097	bd	0.014	0.13
14	bd	bd	0.0053	0.012	bd	0.018	0.16
16	0.0020	0.02	bd	0.0051	bd	0.0051	0.046
19	0.0046	0.04	0.0032	0.0096	bd	0.013	0.11
21	0.0026	0.02	0.0009	0.0048	bd	0.0057	0.050

c) Sediment: 0-2cm depth

Time, days	TNX	
	(n mol/g sed)	%
1	0.0064	0.03
2	0.037	0.16
5	0.067	0.28
7	0.17	0.73
9	0.51	2.1
12	0.85	3.5
14	0.73	2.9
16	0.90	3.6
19	1.0	4.1
21	0.98	3.8

Table S2: Subdivision of inorganic nitrogen production as percentages of spiked (detectable) μmols ^{15}N-[RDX].

Time, days	^{15}N excess in water column, %			^{15}N excess in porewater, %		Evaded $^{15}N_{gas}$ excess, %
	NH_4^+	NO_X	N_{gas}	NH_4^+	N_{gas}	
1	0.14	0.93	1.2	0.03	0.27	0.71
2	0.12	0.9	0.1	0.07	0.024	1.1
5	0.43	1.8	0.53	0.05	0.13	3.7
7	0.27	2.8	0.61	0.2	1	6.7
9	0.24	3.9	1.2	0.39	1.3	11
12	0.38	6	0.82	5.3	0.21	18
14	0.29	6.9	1	1.7	0.71	21
16	0.7	7	0.17	0.67	1	22
19	0.07	6.8	0.51	0.57	1.1	25
21	0.06	7.2	0.99	2.6	0.82	28

Table S3: Measured isotopic enrichments (δ^{15}N) and normalized ^{15}N values (^{15}N, nmol/g) of sediment $_{0\text{-}2cm}$, sediment $_{2\text{-}4cm}$ and SPM.

Time	Sediment, 0-2cm		Sediment, 2-4cm		SPM	
Days	δ^{15}N, ‰	^{15}N, nmol/g sed	δ^{15}N, ‰	^{15}N, nmol/g sed	δ^{15}N, ‰	^{15}N, nmol/g SPM
0	72	0	33	0	3.5	0
1	87	0.41	39	0.16	2200	140
2	95	1.1	43	0.48	1200	93
5	430	0.99	60	0.82	390	18
7	99	0.85	45	0.33	360	61
9	33	2.9	96	1.8	530	100
12	240	5.0	99	1.3	590	67
14	240	7.9	86	1.1	1100	68
16	530	7.4	96	1.4	1400	100
19	410	6.9	39	0.81	1600	99
21	300	8.0	46	0.067	1200	69

Table S4: Variation of geochemical parameters in the system.

Time, days	Water Column				Porewater						
	NH_4^+	NO_X	DOC	TN	NH_4^+	NO_x	DOC	TN	pH	$Fe^{+2}{}_{0\text{-}2cm}$	$Fe^{+2}{}_{2\text{-}4cm}$
0	10	6.8	260	43	130	0.43	280	200	7.7	3.5	6.4
1	25	8.9	260	28	410	0.16	580	700	7.8	1.3	3.1
2	40	15	270	56	240	ND	460	330	7.8	37	25
5	24	23	220	47	380	ND	240	90	7.8	51	57
7	21	30	300	59	520	0.28	640	1000	7.7	2.1	51
9	12	40	560	92	570	ND	590	820	7.5	1.5	42
12	15	69	420	95	630	0.32	620	280	7.6	30	65
14	11	75	490	120	140	0.32	480	890	8.2	80	80
16	15	84	560	130	780	0.42	490	930	7.6	39	82
19	5.2	110	540	130	370	0.24	410	790	7.6	71	86
21	4.3	100	590	140	370	ND	480	220	7.5	60	53

All the values are in the unit of μM except for pH; TN = Total Nitrogen (Inorganic and Organic Nitrogen); TN is corrected for spiked N as RDX.

Table S5: Redox potentials in different sampling sites in the ecosystem; * indicates depth from sediment surface

	Redox potential, mV				
Depth profile	**Site 1**	**Site 2**	**Site 3**	**Site 4**	**Site 5**
Surface water	63	63	63	63	63
1 cm*	51	50	59	52	44
2 cm*	42	18	34	53	40
3 cm*	2.1	3.7	8.6	45	22
4 cm*	-7.0	-0.9	-2.9	19	8.3
5 cm*	-8.9	-5.4	-11	6.3	0.7
6 cm*	-8.7	-9.8	-16	-2.0	-2.8
7 cm*	-8.5	-12	-21	-6.6	-5.0

5.0 Comparative study of the biodegradation and metabolism of hexahydro-1,3,5-trinitro-1,3,5-triazine in three coastal habitats using a stable isotopic tracer, ^{15}N-RDX

5.1 Abstract

It has been estimated that there are hundreds of explosive-contaminated marine sites all over the world and managing these contaminated sites is an international challenge. The demand for data on the sorption, biodegradation and mineralization of trinitrotriazine (RDX) in coastal ecosystems is the impetus for this study. Stable nitrogen (^{15}N) isotope labeled RDX was used to track its processing in three coastal ecosystem types. Mesocosm experiments representing subtidal vegetated, subtidal non-vegetated and intertidal marsh ecosystems were conducted and a steady state supply of RDX was maintained in the systems throughout 17-day experiments. Sediment, pore-water and overlying water samples were analyzed for RDX and transformation products including nitroso-triazines and dissolved inorganic nitrogen (DIN) pools including ammonium, nitrate, nitrite, nitrous oxide and nitrogen gases that contained the ^{15}N tracer. 50%, 44% and 25% of supplied RDX were transformed in intertidal marsh, subtidal vegetated and subtidal non-vegetated mesocosms respectively. RDX was biodegraded to nitroso-derivatives (MNX, DNX and TNX) via reduction (2% - 3% of system sequestrated RDX) and further breakdown formed inorganic nitrogen as mineralization products (50% - 72% of system sequestrated RDX) in coastal marine ecosystems. RDX was mineralized to N_2O (primarily) and N_2 (secondarily) through a series of intermediates (47% - 70% of system sequestrated RDX) and escaped to the atmosphere. Degradation and mineralization of RDX were favored by lowered redox potential and available microbial assemblage in surface sediment of the ecosystem. Subtidal vegetated and intertidal marsh ecosystems containing fine grained, organic carbon rich sediment where significant anaerobic respiration prevailed (presence of H_2S) showed notably

higher mineralization of RDX. Subtidal non-vegetated ecosystem with organic carbon poor sediment where moderate anaerobic respiration prevailed (presence of Fe^{+2}) conditions showed the least mineralization and highest persistence of RDX in the system compared to the subtidal vegetated and intertidal marsh mesocosms. Partioning of RDX and degradation products onto particulates was a negligible process in the overall mass balance of the systems (2% - 4%) and sorption onto the sediment decreased from intertidal marsh, subtidal vegetated to subtidal non-vegetated systems based on the available organic carbon content and grain size of the sediment. The fate of RDX quantitatively differed in different coastal marine habitats based on prevailing sediment redox condition in the ecosystem.

5.2 Introduction

The explosive compound, Hexahydo-1,3,5-trinitro-1,3,5-triazine (RDX) is utilized globally, mainly as a military munition since the second world war. Contamination of soil, surface water, groundwater, wetlands and coastal ecosystems with RDX has become a global environmental issue [1]. RDX has been found to be toxic to aquatic [2] and terrestrial species [3], and a carcinogen to humans [1]. The US coast has been significantly exposed to munitions via disposal of unexploded ordnances [4,5] while military training and weapon testing add an additional source.

Based on the physico-chemical properties of RDX, it has been found that RDX is less soluble in water [5] and persistent in surface water bodies where aerobic conditions prevail [6]. Different removal strategies have been proposed for RDX [7] based on the characteristic properties of RDX [5,8] and geochemical variables in the system [9,10]. Sorption has not been identified as an effective removal mechanism of RDX from water due to its relatively low K_{OW} value [8].

RDX tends to degrade biotically [11,12] and abiotically [8] forming various transformation products in aquatic systems. Abiotic degradation is comparatively less favorable than microbial degradation of RDX [13] and the role sediments play in enhancing biotic degradation of RDX depends on sediment properties including organic carbon content, texture, microbial population and redox conditions [8,10].

The degradation of RDX occurs via a chain of nitroso compounds, Hexahyro-1-nitroso-3,5-dinitro-1,3,5-triazine (MNX), Hexahyro-1,3-dinitroso-5-nitro-1,3,5-triazine (DNX), and Hexahyro-1,3,5-trinitroso-1,3,5-nitro-1,3,5-triazine (TNX) and has been widely documented in the literature, under both hypoxic and/or anoxic conditions [8,9,14]. Ring cleavage and complete mineralization are also reported for RDX [9,12,14]. For instance, it has been identified that the cleavage of either N- NO_2 or C-H bonds in RDX produces unstable intermediates (with ring C-N bonds of 2 kcal/mol) leading to rapid ring cleavage. Therefore, any successful initial enzymatic attack on RDX can initiate degradation resulting in ring cleavage [15]. Nitrites, nitrates and ammonium resulting via denitration [9,13,14] can be used as nitrogen sources by microorganisms [16,17], and N_2O and N_2 are formed as the ultimate mineralization products, mainly in low oxygen conditions [12,14,15,18,19]. Therefore, hypoxic/anoxic degradation and mineralization of RDX has been commonly observed in the literature coupled with microbial populations from soil, sediment and sewage sludge [12,17,20], under nitrate-reducing [21] iron-reducing [10] and sulfate reducing conditions [15,22]. Although, biodegradation pathways of RDX have been studied to a certain extent, most studies have been conducted using specific microbial cultures in controlled laboratory conditions [12,16,20,23]. However, research in natural environmental conditions with different geochemical parameters and complex bacterial assemblages may yield considerable differences in the transformation of RDX in terms of

breakdown products (quality and quantity), compound removal rates, biodegradation and mineralization efficiencies etc.

Vegetated marine ecosystems generally contain organic carbon rich, fine grain textured sediments while non-vegetated ecosystems contain organic carbon poor, coarse grain textured sediments [24]. Microbial populations habituated in vegetated and non-vegetated marine ecosystems vary in terms of types of microbes and microbial population size, depending on the available resources in systems [24]. Prevailing sediment redox potentials in these systems are quite different and all these factors affect sorption, degradation and mineralization of RDX in coastal marine ecosystems. Furthermore, intertidal marsh ecosystems experience tidal variation which alters the geochemistry of water and sediment, redox conditions and microbial populations in the system during high tide and low tide cycles [25].

The objective of this research is to reveal the differences and compare the fate and metabolism of RDX in different nitrogen limited coastal marine habitats by tracking the transformation of RDX in different pools of the ecosystem including well aerated surface water and hypoxic/anoxic sediment using ^{15}N isotope labelled RDX as a tracer. Such a comparison has not been performed to date. This utilizes an integrated mass balancing approach with a stable ^{15}N isotope tracer which facilitates tracking a number of the RDX pathways that remove bioavailable, dissolved RDX from the ecosystem. Resulting outcomes from above mentioned comprehensive analysis of fate and metabolism of RDX helps to determine the most suitable remediation techniques for different coastal marine systems. This study also benefits future efforts related to the investigations and characterization of munition contaminated coastal sites since it identifies variations in removal rates and pathways.

5.3 Methods

Three experimental set-ups representing different coastal marine ecosystems, non-vegetated, subtidal vegetated and intertidal marsh were constructed in Rankin Seawater facility, University of Connecticut, Avery Point in order to compare fate and metabolism of RDX in different coastal marine habitats.

5.3.1 Experimental design, sampling plan and techniques

5.3.1.1 Non-vegetated mesocosm

1000 L fiber glass experimental tank was connected to a reservoir tank filled with raw seawater from Long Island Sound (30 PSU) and loaded with an 8cm deep layer of sandy, low organic carbon (OC) containing sediment (0.2 % OC) collected from a subtidal habitat in Long Island Sound (LIS) (latitude: 41^0 19′ 13″ N and longitude: 72^0 2′ 59″ W) (Figure 1). Raw sea water was pumped to the experimental tank continuously from the reservoir tank under flow through conditions over two weeks to achieve stabilized redox conditions in sediment and then, experimental tank was loaded with macroalgae, epifaunal, bivalve and fish species typical of that habitat. The tank was aerated using air stones and overlying water was well mixed using pumps, and total water volume was 686 L. The system was reconfigured to recirculation mode, and the seawater inflow rate was adjusted to 3.29 mL s^{-1} over the course of the experiment (17 days). ^{15}N labelled RDX (99 At% ^{15}N with respect to nitro groups) dissolved in methanol was introduced into the experimental tank as a pulse of concentrated stock (20.4 mL) to achieve initial target RDX concentrations of 1 mgL^{-1}, followed by continuous addition at a rate of 0.07 mL min^{-1} - 0.08 mL min^{-1} to target a conservatively mixed steady state RDX concentration of 0.5 mgL^{-1} throughout the experiment. The water residence time in the tank was 2.5 days.

Figure 1: Schematic diagram of non-vegetated mesocosm (1: reservoir tank; 2: overlying water in experimental tank; 3: sediment layer)

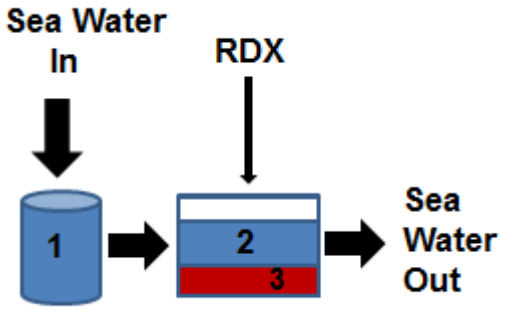

Time series samples (total 9 sampling time points) of overlying water, porewater, suspended particulate matter (SPM) sediment and biota were taken from the tanks over the course of the experiment including two time points with triplicate samples. Overlying water was drawn using a peristaltic pump at a rate of 50 mL min^{-1} and filtered through Whatman 25 mm, 0.7 µm glass fiber filters (GF/F). Suspended particulate matter (SPM) was sampled by filtering 250−300 mL of overlying water through pre-weighed combusted (450 °C) GF/F filters, and split for analysis of bulk ^{15}N enrichment ($\delta^{15}N$ SPM) and extractable explosives concentrations. Porewater was using a $1/16^{th}$ in inch stainless steel tube inserted into the sediment layer, attached to a peristaltic pump. Porewater was collected at a slow pumping rate of 2.5 mL min^{-1} and filtered through polyethersulfone - 0.2 µM (0.2 µM PES) syringe tip filters. Sediment cores with a diameter of 2.6 cm were obtained and sliced at 2cm intervals prior to the analysis.

5.3.1.2 Subtidal vegetated (eel grass) mesocosm

The experimental setup was constructed similarly to the non-vegetated mesocosm except it contained fine grained, organic carbon rich sediment collected from Mumford Cove, LIS (latitude: 41^0 19′ 15″ and longitude: 72^0 0′ 24″) and sods of eel grass (Zostera marina) collected from LIS were transplanted in the sediment (Figure 2). In terms of sea water pumping, compound introduction, maintaining specific concentrations in the system, and sampling were performed identically to the non-vegetated system over an 18 day-experimental time duration.

Porewater sampling techniques was adjusted due to the clogging issues of fine sediment particles in sampling tube. At each time point, porewater was extracted by centrifuging sediment slices obtained from above and below the oxic-anoxic interface of the sediment.

Figure 2: Schematic diagram of subtidal vegetated mesocosm (1: reservoir tank; 2: overlying water in experimental tank; 3: sediment layer; 4: vegetation layer of eel grass)

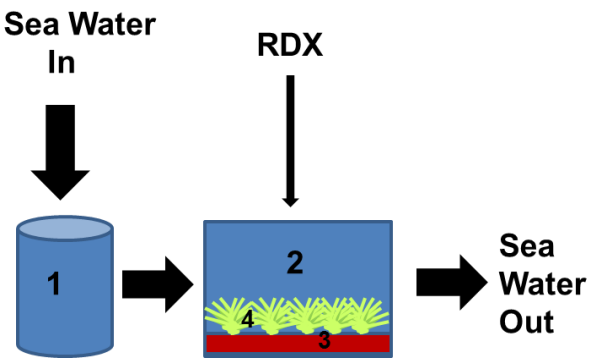

5.3.1.3 Intertidal marsh mesocosm

The intertidal marsh mesocosm was constructed using two connected 1000 L tanks (reservoir and mesocosm) and the mesocosm tank was filled with fine grained, high organic carbon containing, compacted peaty sediment (15cm thickness) collected from Stonington, LIS (latitude: 41^0 20′ 5″ and longitude: 71^0 54′ 10″) (Figure 3). Intact sods of marsh grasses (Spartina alterniflora) were transplanted in the sediments of the mesocosm tanks and stocked with biota (macroalgae, epifaunal, bivalve and fish species). Raw sea water was pumped into the reservoir tank with a rate of 5.22 mL sec^{-1}. Pumps, timers, and float switches were used to exchange water back and forth between the reservoir and mesocosm tanks every 6 hours to simulate a flooding/draining tidal cycle with a 1 foot tidal range. Water in the reservoir tank was mixed with a pump while the reservoir tank and mesocosm were sufficiently well mixed by the exchange of water between both tanks using a pump. Both tanks were aerated using air stones and the system was maintained at

steady state conditions. ^{15}N labelled RDX (99 At% ^{15}N respect to nitro groups) was introduced into the reservoir tank using an initial slug dissolved in acetone to achieve an RDX concentration of 1 mgL^{-1} followed by continuous addition of RDX at a rate of 0.064 mL min^{-1} to achieve a 0.5 mgL^{-1} steady state concentration of RDX in the system.

Figure 3: Schematic diagram of intertidal marsh mesocosm (1: reservoir tank; 2: Mixing tank; 3: surface water in experimental tank; 4: sediment layer; 5: vegetation layer of marsh grass)

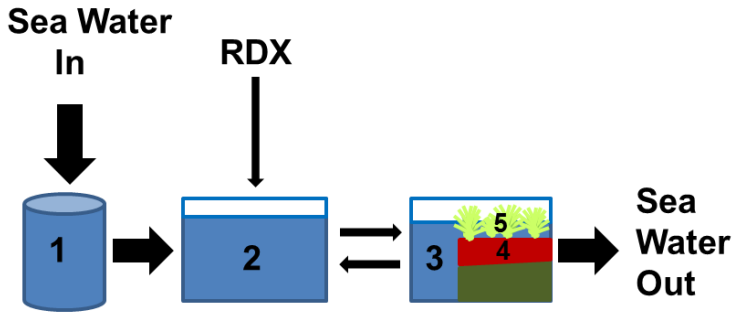

Time series of overlying water, porewater and sediment samples were taken using similar techniques used in the non-vegetated mesocosm over an experimental duration of 17 days including 5 time points with triplicates (total of 10 sampling times). Overlying water and sediment samples were taken when the water level has reached its maximum height (High tide) in the mesocosm. Sediment cores of 8cm were sliced into 2cm intervals for the analysis. Porewater samples were taken when the water level had saturated the sediment surface (flood tide) and when it reached its maximum height (High tide). Flood tide samples were taken only from shallow depths of sediment (2cm from sediment surface) while high tide samples were obtained as a profile of two depths (2cm and 4cm from sediment surface).

pH, dissolved oxygen, hydrogen sulfide profiles of sediment were obtained using the microsensors during both flood tide and high tide at each sampling point from three static wells

permanently constructed in the sediment in order to avoid breakage of the microsensors.

5.3.2 Analytical techniques

5.3.2.1 System characterization

Physical parameters of the systems including temperature and salinity were measured using a YSI probe (YSI 556 MPS) over the course of the experiments. Both overlying water and porewaters were analyzed for nutrients (ammonium, total nitrate and nitrite (NO_x)) using a Smartchem nutrient analyzer (Westco-W12623) following cadmium azo-dye and phenol hypochlorite methods [26], respectively. 3 mL of filtered (0.2 µM PES) porewater were directly introduced to the reagents to minimize exposure to atmospheric oxygen and analyzed using the ferrozine method [27] and methylene blue method [28] for dissolved ferrous and hydrogen sulfide respectively by UV/Vis spectrophotometry (Hitachi-U-30110). The redox potential of sediment was measured using a platinum electrode (Paleo Terra, Amsterdam) relative to an Ag/AgCl reference electrode (Fisher Scientific). In-situ profiles of dissolved oxygen, hydrogen sulfide and pH profiles in sediment were obtained using a Unisense DO, H_2S and pH microsensors (OX-50, H_2S-50, pH-50 micron). Sediment was characterized for TOC, total nitrogen (TN) and total elemental sulfur (S) using a Perkin Elmer elemental analyzer (NA 1500) [29]. Sediment texture was determined using a mechanical sieve analyzer with a set of sieves from 0.063 mm to 2.0 mm.

5.3.2.2 Explosive analysis

RDX and its reduced degradation products, including, MNX, DNX and TNX, were analyzed in both overlying water and porewater samples. A modified salting-out method [30] adapted for smaller sample sizes was used for extraction of munition compounds from aqueous samples following methods described in [8]. An average recovery of 99.1 ± 0.5% was obtained for known

amounts of 1, 2-dinitrobenzene (1,2-DNB) in water extractions. Water extracts were analyzed using gas chromatography (GC)/electron-capture detection (ECD) following the methods described by [8] 3, 4-dinitrotoluene (3,4-DNT) was added to each extract prior to injection to monitor detection efficiency. Explosive analysis was performed with an Agilent GC/ECD equipped with an HP-DB5 column (30 m x 320 µm, 0.25-µm; Agilent). Quantification was based on an external calibration curve of available standard munitions RDX, MNX, DNX and TNX. (AccuStandard, New Haven, CT). The average reporting limit for all compounds was 7.8 ng mL^{-1}. Sediment samples were homogenized and 2g of each was extracted with 10mL of ACS-grade acetonitrile (ACN) following the method described by [8,31]. 3,4-dinitrotoluene (3,4-DNT; Accustandard) was spiked as a recovery standard and extraction efficiencies averaged as 82%. Sediment extractions were analyzed for explosives (RDX, MNX, DNX and TNX) using gas chromatography (GC)/electron-capture detection (ECD) as mentioned above.

5.3.2.3 Bulk δ^{15}N analysis

Freeze dried sediment and SPM samples were analyzed using a continuous flow elemental analyzer – isotope ratio mass spectrometry (EA-IRMS: Delta V, Thermofisher) at the University of Connecticut for bulk ^{15}N enrichments. Nitrogen isotope ratios are reported in δ notation as follows:

$$\delta^{15}N = [(R_{sample} - R_{STD})/R_{STD}] \quad (1)$$

where R_{STD} is the $^{15}N/^{14}N$ ratio of atmospheric nitrogen and R_{sample} is the $^{15}N/^{14}N$ ratio of the sample. δ^{15} N values are reported in parts per mil (‰) and external calibration was done using glutamic acid standards USGS 40 and USGS 41. The delta values were converted to mole fractions ($X^{15}N$) and excess ^{15}N tracer derived from the RDX was calculated from mole fractions and total N mass according to (Equation 2).

^{15}N mols Excess = N mols * ($X^{15}N_t - X^{15}N_{t0}$) (2)

For eq 2, the total N mass, and mole fractions of ^{15}N at time t ($X^{15}N_t$) and time 0 ($X^{15}N_{t0}$) were obtained from an elemental analyzer – isotope ratio mass spectrometry EA-IRMS (Delta V, Thermofisher). Analytical precision for sediment and SPM samples was 10% and 14% respectively (Percent coefficient of variance, CV).

5.3.2.4 Mineralization product analysis The mineralization products, $^{15}NH_4^+$, total $^{15}NO_2^-$ and $^{15}NO_3^-$ ($^{15}NO_X$), $^{15}N_2$ and $^{15}N_2O$ in the aqueous phase (surface water and porewater), were quantified using IRMS techniques. Filtered (0.2 µM PES), frozen water samples (from subtidal non-vegetated and intertidal marsh mesocosms) and sediment (from subtidal vegetated) were extracted for NH_4^+ following the methods from [32,33] respectively. Ammonium extraction from sediment was done using a 2M KCl solution. $\delta^{15}N$ isotopic enrichment of ammonium extractions were obtained using a continuous flow EA-IRMS. Extraction efficiency was between 95-105% based on the recovery of NH_4NO_3 standards and analytical precision is 25% (percent coefficient of variance, CV). Moles of $^{15}NH_4^+$ were calculated using NH_4^+ concentrations and mole fractions of ^{15}N ($X^{15}N_t$ and $X^{15}N_{t0}$) obtained from EA-IRMS (equation 3).

$^{15}NH_4^+$ mols Excess = NH_4^+ mols * ($X^{15}N_t - X^{15}N_{t0}$) (3)

$\delta^{15}NO_X$ values of overlying and porewater were obtained via the denitrifier method using *Pseudomonas aureofaciens* [31] at the US Geological Survey (USGS) in Reston, VA on water samples filtered through a 0.2µM PES filters and frozen. Moles of $^{15}NO_X$ were calculated using NO_X concentration and the mole fractions of ^{15}N ($X^{15}N_t$ and $X^{15}N_{t0}$) obtained from isothermal GC-IRMS (equation 4).

$^{15}NO_X$ mols Excess = NO_X mols * ($X^{15}N_t$ - $X^{15}N_{t0}$) (4)

Gas samples were collected at each time point by pumping unfiltered water into 30 mL and 60 mL serum bottles for N_2 and N_2O respectively that had previously been sealed, pre-loaded with 3N $NaHSO_4$ (for preservation), and flushed with He for 12 minutes [14]. Following sample collection, At least after 6 hours of headspace equilibration, the isotopic composition of N_2 and N_2O ($\delta^{15}N$-N_2 and $\delta^{15}N$-N_2O) was measured. $^{15}N_2$ in water samples was determined using continuous flow isotope ratio mass spectrometry (IRMS) on a Thermo Delta V Plus with a Gas Bench interface (GB-IRMS). Dissolved ambient N_2 concentrations were assumed to be in equilibrium with the atmosphere and were calculated as a function of temperature and salinity [34]. $^{15}N_2O$ in water samples was measured via continuous flow IRMS interfaced to a modified Gas Bench. Dissolved gases in samples were He sparged and passed through a chemical soda lime trap to remove CO_2. N_2O was quantitatively cryo-trapped using liquid N. The trapped N_2O was then released and separated from any remaining trace CO_2 using a poraplot Q column, and then analyzed for $^{15}N_2O$ via IRMS. Dissolved N_2O concentrations were obtained from GC-ECD and analytical precision of the analysis is 30% (Percent coefficient of variance, CV). Evasion rates for $^{15}N_2$ and $^{15}N_2O$ were calculated from excess ^{15}N masses of each gas and gas transfer coefficients measured following known gas tracer additions (SF6) using the method described in [14].

Table 4 shows the time series concentrations of bulk ^{15}N in sediment, $^{15}NH_4^+$, $^{15}N_2$ and $^{15}N_2O$ at depth 1 (0-2cm) and depth 2 (2-4cm) of peaty sediment in intertidal marsh mesocosm. All the measured ^{15}N-RDX pools (bulk ^{15}N in sediment, $^{15}NH_4^+$, $^{15}N_2$ and $^{15}N_2O$) in deeper (2-4cm) level sediment show quantitatively lower values compared to those values in shallow (0-2cm) level sediment, although, the time series trends follow the same patterns as they appear in

shallow sediment (Table 4). The ratio of bulk ^{15}N values in shallow sediment to deeper sediment varies within the range of 1.4 to 6.4 during the experiment of 16 days. Measured dissolved inorganic nitrogen (DIN) containing mineralization products, $^{15}NH_4^+$, $^{15}N_2$ and $^{15}N_2O$ show average ratios of shallow to deeper level concentrations in porewater during the experiment as 1.6, 1.8 and 6.3 respectively.

5.3.2.5 Data analysis

A mass balancing approach was based on ^{15}N equivalents in masses of each analyzed N-containing parent and derivative pools and illustrated in following equations (Equation 5).

$$^{15}N\text{-}RDX_{system} = {}^{15}N\text{-}\sum RDX_{\text{surface water}} + {}^{15}N\text{-}\sum RDX_{\text{porewater}} + {}^{15}N\text{-}\sum RDX_{\text{sediment}} + {}^{15}N\text{-}\sum RDX_{\text{biota}} + {}^{15}N_{SPM} + {}^{15}N\text{-}NH_4^+{}_{\text{dissolved}} + {}^{15}N\text{-}NO_{X\ \text{dissolved}} + {}^{15}N\text{-}N_2 + {}^{15}N\text{-}N_2O + \text{unidentified } {}^{15}N\text{-compounds in the system} \quad (5)$$

where, $^{15}N\text{-}RDX_{system}$ represents system sequestrated ^{15}N-RDX based on rates (cumulative influx of ^{15}N-RDX into the system – cumulative outflux from the system) and the remaining terms represent ^{15}N measured in different RDX-derived metabolites in overlying water, porewater, sediment, bio-tissues and SPM. The aqueous terms are adjusted for outflow, and the gas terms are adjusted (included) outflow and evasion to the atmosphere. $\sum$ RDX represents RDX and measurable derivatives including MNX, DNX and TNX.

Removal kinetics of munitions were analyzed determining removal rate constants (Equation 6) and half-lives (Equation 7) using the following equations.

$$\ln [C_i] = -kt + \ln [C_i]_{t=0} \quad (6)$$

$$t_{1/2} = \ln 2 / k \quad (7)$$

where t is time (hr) and k is the first order removal rate constant in hr^{-1}

5.6 Results

5.6.1 Characterization and mass balance of the ecosystem

Measured physical and chemical parameters those describe the variations among mesocosms are shown in Table 1. System sequestrated ^{15}N-RDX (cumulative input of RDX into the system - cumulative output of RDX from the system) (Figure 4) was found in different compartments of the mesocosm including dissolved fractions in surface water and porewater, sorbed fractions in sediment, particulate organic matter and biota, and gaseous fractions that escaped to the atmosphere. Loss of RDX (cumulative input of RDX into the system - cumulative output of RDX from the system - total RDX stored in surface water, porewater and sediment) at the end of the experiment in subtidal non-vegetated, subtidal vegetated and intertidal marsh mesocosms were 25%, 44% and 50% respectively (Table 2). First order removal rate constants of RDX from overlying waters were 0.029 hr^{-1}, 0.066 hr^{-1}, and 0.095 hr^{-1} in non-vegetated, vegetated and marsh, respectively. Half-lives of RDX decreased in the order of non-vegetated (24 days), vegetated (11 days) and marsh mesocosms (7 days) (Table 2).

Table 1: Physical and chemical properties in subtidal non-vegetated, subtidal vegetated and intertidal marsh mesocosms.

Medium	**Parameter**	**Mesocosm Type**		
		Subtidal non-vegetated	**Subtidal vegetated**	**Intertidal marsh**
Porewater: 0-2cm	Redox (mV)	(-265) – (-306)	(-440) – (-450)	(-317) - (-325)
	Fe^{+2} (µM)	1.0 - 17	BD	6.8 - 430
	H_2S (µM)	BD	222 - 686	58 - 412
	Ammonium (µM)	12 - 44	47.7 - 128	11.5 – 73.9
Sediment: 0-2cm	Sand (%)	97	40	-
	Silt and Clay (%)	3	60	-
	Density (g cm^{-3})	2.01	1.42	0.51
	TOC (mg/g sed)	1.23	27.5	34.4
	TN (mg/g sed)	0.15	2.84	13.7
	S (mg/g sed)	0.22	5.2	10.2

BD = below detection

Table 2: Removal rate constants, half-lives and loss percentage (%) of RDX in mesocosms.

Treatment	RDX		
	Removal rate constant (day^{-1})	Half-life (days)	Loss (%)
Subtidal non-vegetated	0.029	24	76
Subtidal vegetated	0.066	11	90
Intertidal Marsh	0.095	7	94

Loss percentage of RDX corresponds to the end of the experiment.

Amount of RDX stayed in water is higher in subtidal non-vegetated mesocosm (25%), compared to the subtidal vegetated (10%) and intertidal marsh (6%) mesocosms. ^{15}N-RDX was partitioned onto particulates in the ecosystem (sediment and SPM) and higher in intertidal marsh mesocosm (4%) than vegetated (3%) and non-vegetated (2%) mesocosms. Nitroso-derivatives did not show significant variation in between mesocosms: non-vegetated (3%), vegetated (2%) and marsh (2%). The distribution of tracer ^{15}N mass into various pools in mesocosms in terms of the amount of RDX stays in water, amount of derivatives and mineralization products in water, and the amount of RDX derived ^{15}N partitioned onto solids at end of the experiment is shown as a cumulative mass balance in figure 5. Subtidal vegetated (68%) and intertidal marsh (72%) ecosystems showed notably higher mineralization of RDX forming dissolved inorganic nitrogen (ammonia, nitrates, nitrous oxide and nitrogen gases). Subtidal non-vegetated ecosystem showed the least mineralization (50%). Nitrous oxide was the prominent mineralization product of RDX for all the treatments (95-96% of total mineralization) that escaped to the atmosphere (Figure 6). Highest amount of ^{15}N gas production (N_2O and N_2) was found in marsh mesocosm, followed by vegetated silt, and finally the low organic non-vegetated sandy mesocosm.

Figure 4: Time series system sequestration (cumulative influx – cumulative outflux) of ^{15}N-RDX in a) subtidal non-vegetated b) subtidal vegetated c) intertidal marsh.

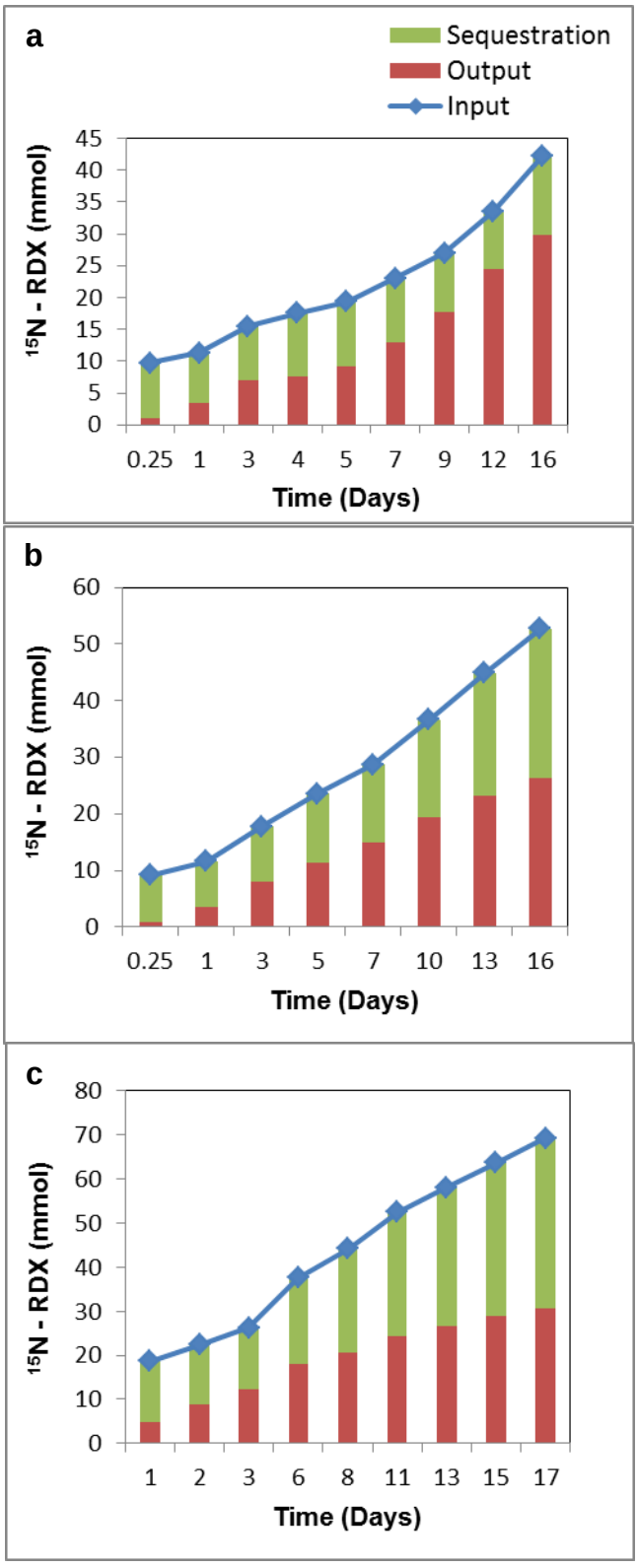

Figure 5: ^{15}N cumulative mass balance of system sequestrated ^{15}N-RDX on the last day of the experiment in a) subtidal non-vegetated b) subtidal vegetated c) intertidal marsh.

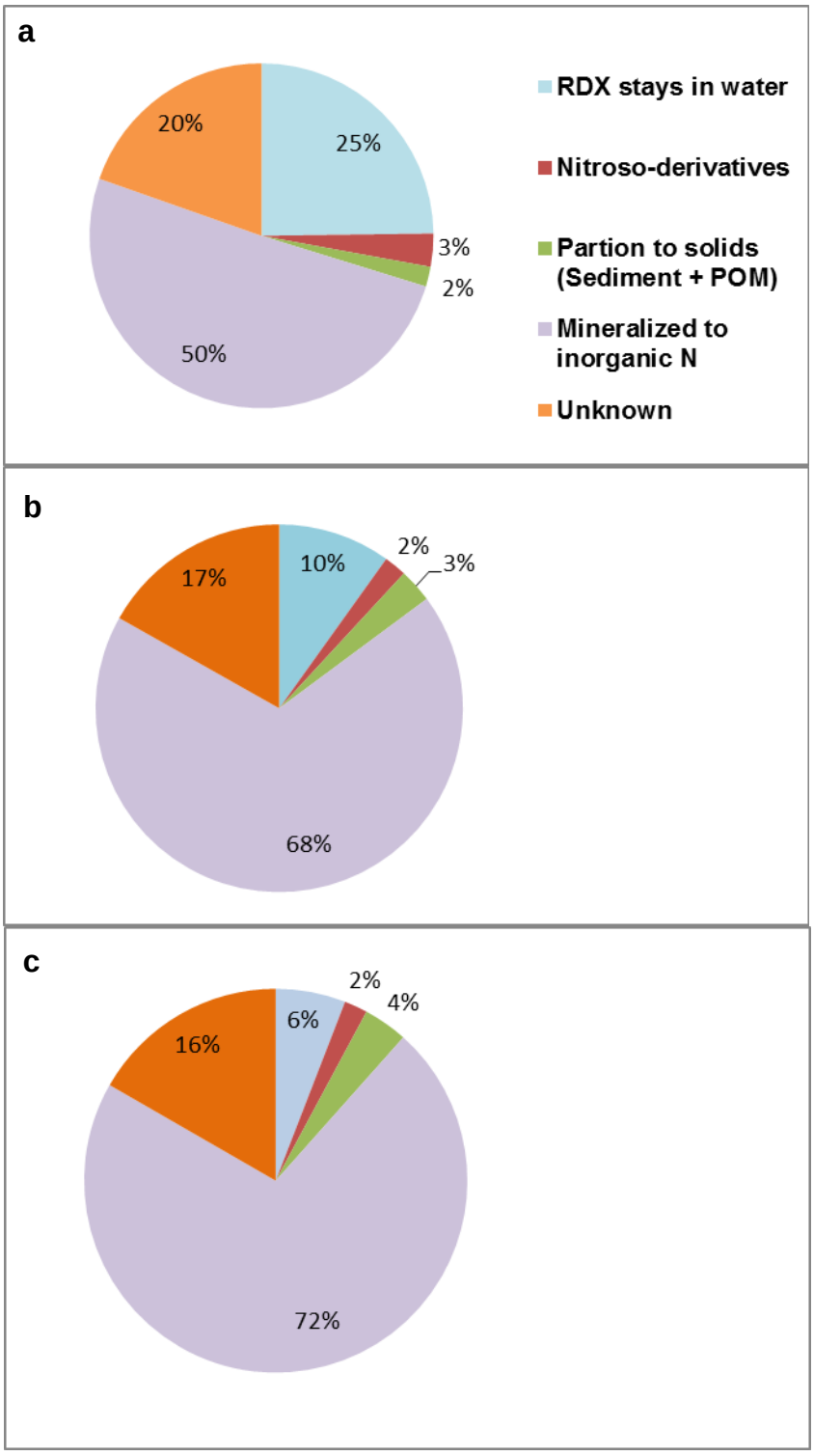

Figure 6: Time series distribution of inorganic nitrogen (dissolved and evaded) of total mineralization in a) subtidal non-vegetated b) subtidal vegetated c) intertidal marsh.

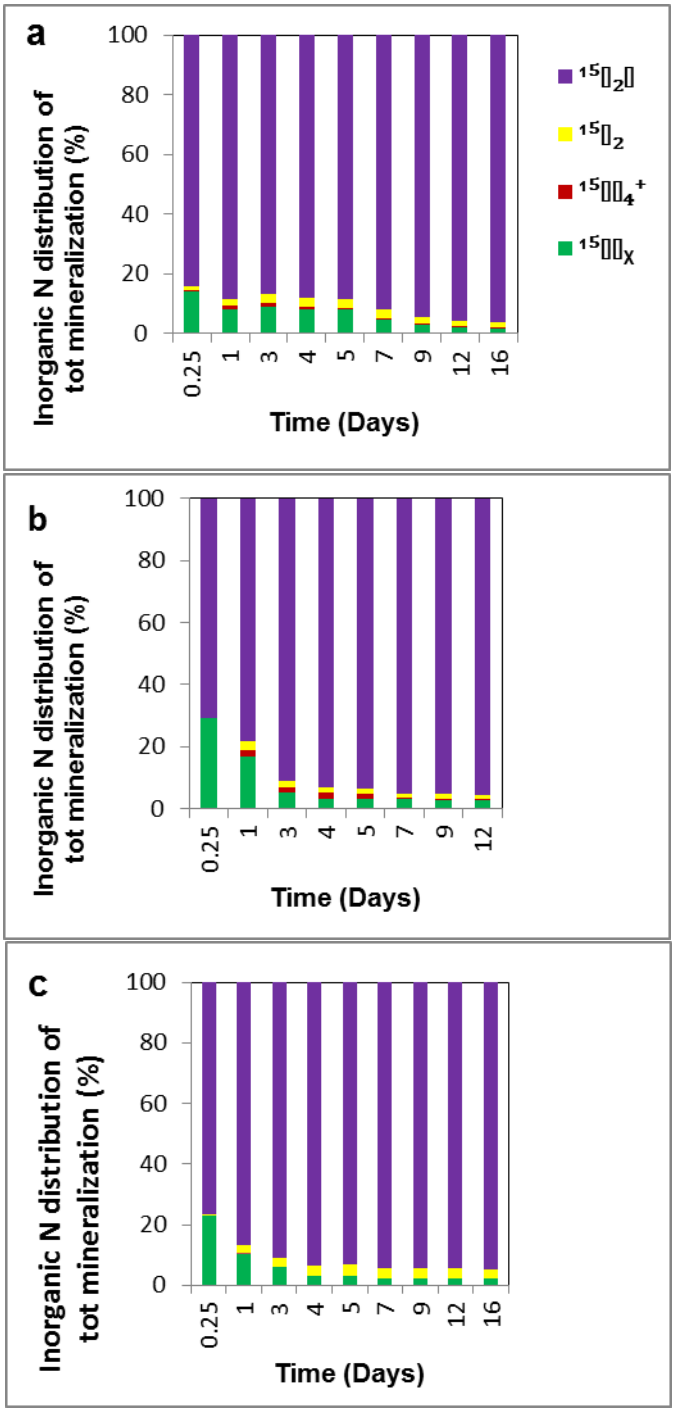

5.6.2 Transformation

Figure 7: Time series total aqueous derivative concentrations (sum of MNX, DNX and TNX) in a) subtidal non-vegetated b) subtidal vegetated c) intertidal marsh.

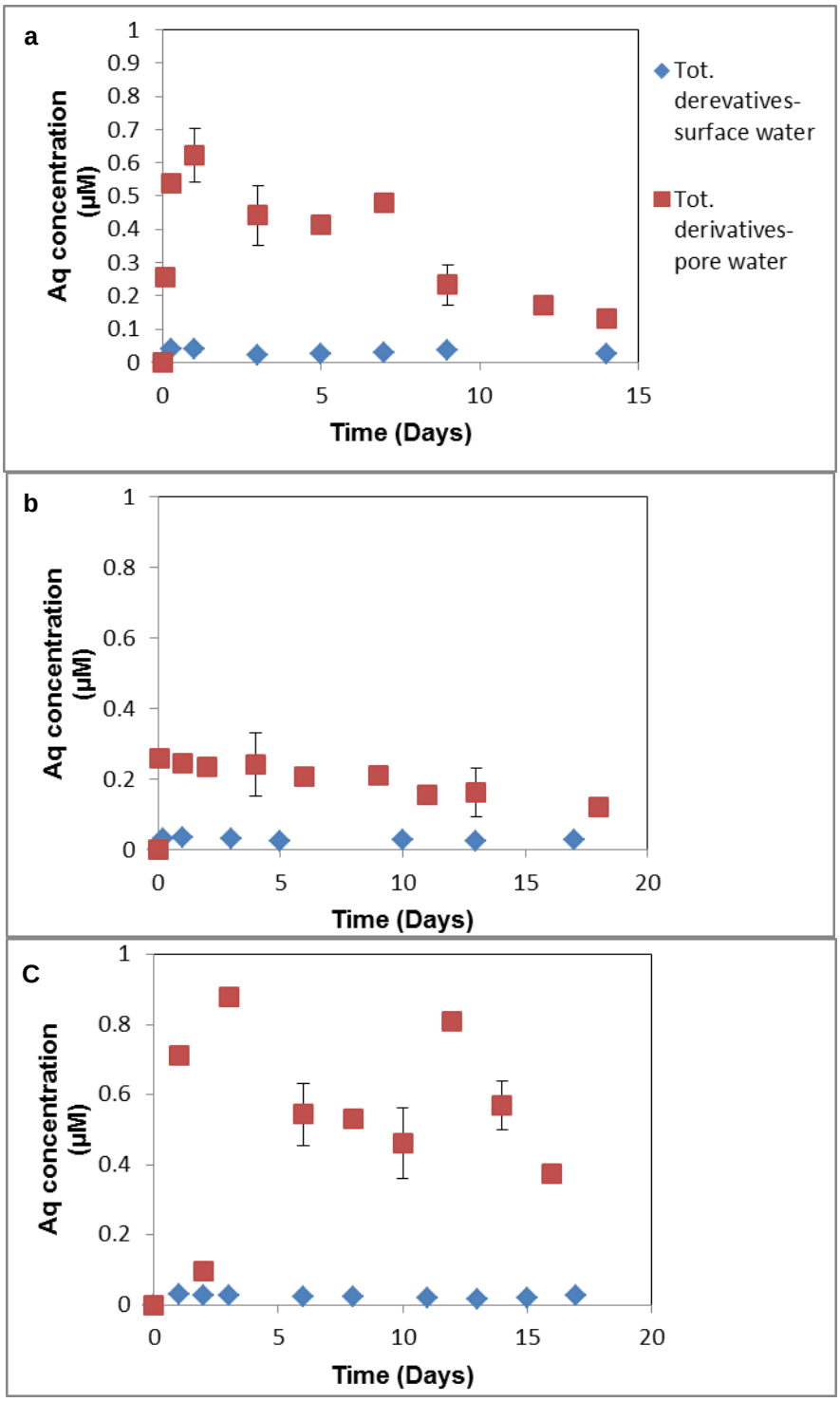

RDX transformation products, nitroso-triazines (MNX, DNX and TNX) were present in both surface water and porewater throughout the experimental duration in all three mesocosms (Table S1). The amount of total detected nitroso-triazines in surface water stayed relatively constant during the experiment and concentration ranges did not show significant variations among ecosystems (Figure 7). Total detected nitroso-triazines in porewater decreased with the time in all three treatments and highest porewater concentrations were found in the intertidal marsh mesocosm (Figure 7). The ratio of total detected nitroso-triazines in porewater to surface water on day 17 in non-vegetated, vegetated and marsh mesocosms were 14, 7 and 24 respectively. Rapid transformation of RDX was observed in coastal marine mesocosms showing the highest total detected nitroso-triazines in surface water after 6 hr of spiking and at 24 hr for porewater.

5.6.3 Partitioning

Partitioning of ^{15}N-RDX onto particulates (sediment and SPM) followed similar trends in all the studied coastal mesocosms showing rapid increase in sorbed ^{15}N-RDX onto particulates followed by a drop and then, remaining constant during the remainder of the experiment (Figure 8). Sorption of ^{15}N-∑RDX (^{15}N from RDX and derivatives) onto SPM (1.31 - 344 nmol/g SPM) showed higher values than those values sorbed onto surface sediment (1.18 – 96.3 nmol/g sed) in coastal marine mesocosms (Figure 8). But, sediment became a better sink for ^{15}N-∑RDX than SPM because depth integrated total sediment mass in the mesocosms was huge compared to SPM. Sorption of ^{15}N-∑RDX onto SPM was highest in the non-vegetated mesocosm (8.22 – 344 nmol/g SPM) while it was lowest in the subtidal vegetated mesocosm (1.31 – 89.2 nmol/g SPM). ^{15}N-∑RDX values found in SPM of intertidal marsh mesocosm ranged from 53.9 nmol/g SPM to 244 nmol/g SPM during the experiment (Figure 8-a). Bulk ^{15}N-∑RDX found in surface sediment decreased in the order of intertidal marsh, subtidal vegetated and subtidal non-vegetated showing

value ranges of 14.8 - 96.3 nmol/g sed, 1.30 – 31.7 nmol/g sed and 0.32 – 25.5 nmol/g sed respectively (Figure 8-b). The highest RDX amount in sediment (6 - 40% of bulk ^{15}N in sediment) was found at the beginning of the experiment in all the three mesocosms and decreased with time, disappearing by the end of the experiment in subtidal vegetated and intertidal marsh mesocosms (Figure S1). Nitroso-triazines were identifiable in surface sediment of coastal marine mesocosms with ratios of RDX to total nitroso-triazines were 4.5, 0.5 and 3.1 in non-vegetated, vegetated and marsh mesocosms respectively. The highest DNX amount in sediment (10% of bulk ^{15}N in sediment) was found in the non-vegetated system after 6 hours of spiking while TNX appeared at a slower rate with time. TNX was formed as the main nitroso-derivative in both subtidal vegetated and intertidal marsh mesocosms (Figure S1).

Figure 8: Time series bulk ^{15}N in a) SPM b) sediment in coastal marine mesocosms: subtidal non-vegetated, subtidal vegetated and intertidal marsh; Error bars represent standard deviations and are included only to the time points when sampling was done in triplicates.

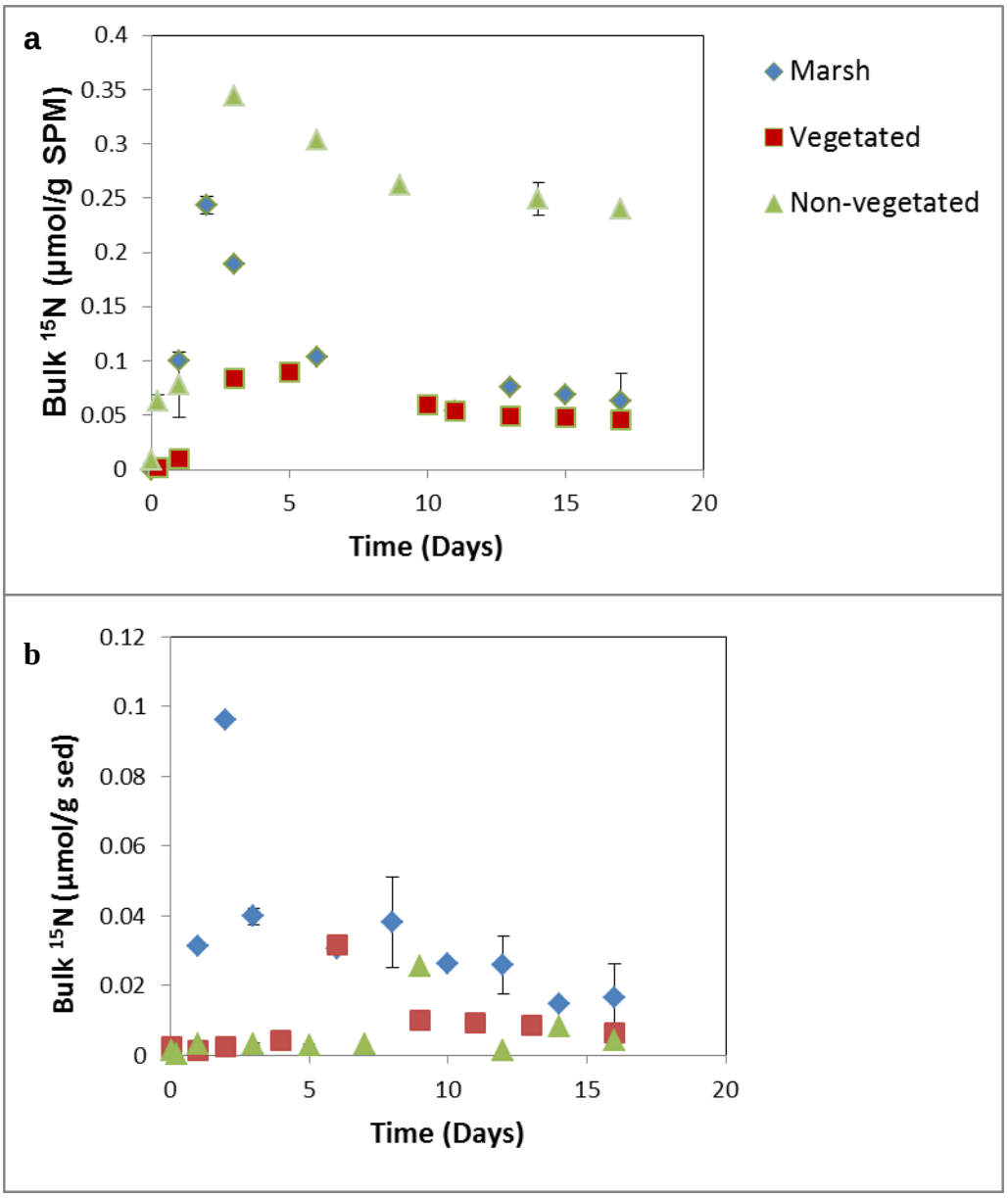

5.6.4 Mineralization

Mineralization in terms of detected inorganic nitrogen was identified as the main fate of RDX in all the three coastal marine ecosystems: subtidal non-vegetated, subtidal vegetated and intertidal marsh mesocosms. Figure 5 shows the contribution of different mineralization products ($^{15}NH_4^+$, $^{15}NO_x$, $^{15}N_2$ and $^{15}N_2O$) to the total mineralization. N_2O was produced as the prominent mineralization product of RDX, but $^{15}N_2O$ contribution to the total mineralization did not significantly vary among non-vegetated (84% - 96%), vegetated (71% - 96%) and marsh (76% - 95%) mesocosms. $^{15}NO_x$ peaked at the very first sampling time point (6 hr after spiking) and gradually decreased approaching steady state concentrations in all three mesocosms. The ranges of percentages of $^{15}NO_X$ out of total mineralization were found as 14% - 2%, 29% - 3% and 23% - 2% in non-vegetated, vegetated and marsh mesocosms respectively. Although $^{15}NH_4^+$ (1%) and $^{15}N_2$ (2%) were detected in the mesocosms, they did not significantly contribute to the total mineralization in coastal mesocosms. Ammonium production from RDX in porewater was higher than in surface water and ratios of standing stock $^{15}NH_4^+$ in sediment porewater to surface water were 5, 50 and 10 in non-vegetated, vegetated and marsh mesocosms respectively. Porewater $^{15}NH_4^+$ production was highest in subtidal vegetated mesocosm among three studied coastal mesocosms (Table 3). $^{15}N_2O$ production was significantly higher (30 times) than $^{15}N_2$ production (Figure 5). Time series N_2O production and the mole fraction of $^{15}N_2O$ are shown in figure 9. Mole factions of $^{15}N_2O$ in non-vegetated and marsh mesocosms varied within the range of 0.4 to 0.5 while they are 0.3 to 0.4 in vegetated mesocosm.

Figure 9: Time series a) concentration of surface water N_2O b) mole fraction of surface water $^{15}N_2O$ in coastal marine mesocosms: subtidal non-vegetated, subtidal vegetated and intertidal marsh.

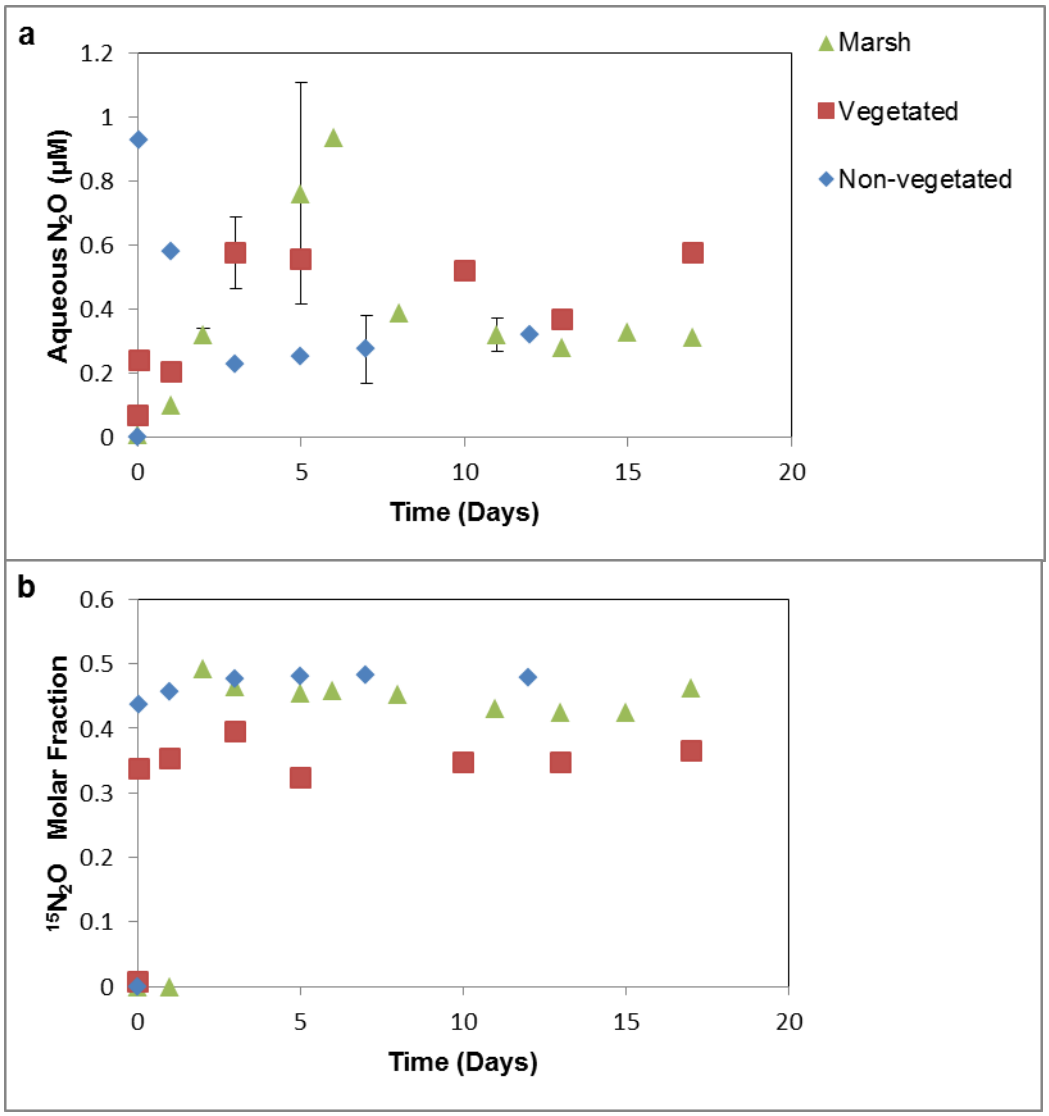

5.6.5 Depth influence on fate of RDX in intertidal marsh mesocosm

Table 3 shows the time series concentrations of bulk ^{15}N in sediment, $^{15}NH_4^+$, $^{15}N_2$ and $^{15}N_2O$ at depth 1 (0-2cm) and depth 2 (2-4cm) of peaty sediment in intertidal marsh mesocosm. All the

measured ^{15}N-RDX pools (bulk ^{15}N in sediment, $^{15}NH_4^+$, $^{15}N_2$ and $^{15}N_2O$) in deeper (2-4cm) level sediment showed quantitatively lower values compared to those values in shallow (0-2cm) level sediment, although, the time series trends followed the same patterns as they appeared in shallow sediment (Table 3). The ratio of bulk ^{15}N values in shallow sediment to deeper sediment varied within the range of 1.4 to 6.4 during the experiment of 16 days. Measured dissolved inorganic nitrogen (DIN) containing mineralization products, $^{15}NH_4^+$, $^{15}N_2$ and $^{15}N_2O$ showed average ratios of shallow to deeper level concentrations in porewater during the experiment as 1.6, 1.8 and 6.3 respectively.

Table 3: Time series concentrations of different ^{15}N-RDX pools at depth 1 (0-2 cm) and depth 2 (2-4 cm) in intertidal marsh mesocosm.

Time (days)	Bulk ^{15}N (μmol/g sed)		$^{15}NH_4^+$ (nM)		$^{15}N_2$ (nM)		$^{15}N_2O$ (nM)	
	D1	D2	D1	D 2	D1	D 2	D1	D 2
1	31.4	4.90	54.7	54.5	56.7	18.5	733	322
2	96.2	40.0	112	91.9	491	301	1800	1071
3	29.6	5.69	70.6	70.7	198	160	787	210
6	30.7	16.8	51.9	51.7	271	207	316	317
8	38.2	27.9	9.74	9.47	31	30.8	433	108
10	26.1	17.6	37.3	25.2	67.1	47.4	202	123
12	25.9	7.24	24.3	23.7	96.8	49.2	318	50.1
14	14.8	7.26	82.8	16.7	157	43.6	552	105
16	16.6	7.29	44.7	28.6	82.4	60.7	416	13.7

D1 = Depth 1 (0-2cm); D 2 = Depth 2 (2-4cm)

5.7 Discussion

5.7.1 Behavior of RDX in mesocosms

Depending on the differences in redox potential and available resources, different microbial populations including nitrate-reducers, iron-reducers and sulfate-reducers were involved in RDX transformation in coastal marine mesocosms [9]. The least loss of RDX was seen in subtidal non-vegetated mesocosm containing sandy sediment with low organic carbon content that only

permitted nitrate and iron reduction in the sediment. But, subtidal vegetated and intertidal marsh mesocosms with higher organic carbon containing sediment those could have accessed nitrate, iron and even sulfate reduction resulted higher loss of RDX than non-vegetated system [35]. Further, marsh had the highest RDX loss because the system was not diffusion limited like subtidal vegetated system. The shortest half-life of RDX in surface water was found in intertidal marsh since it was a more dynamic system experiencing tidal variation. The non-vegetated mesocosm had the longest half-life and the highest persistence of RDX in surface water in the system. RDX loss is mainly resulted due to degradation and mineralization of RDX in sediment while sorption onto particulates was not a significant process.

The use of ^{15}N enabled a much more complete assessment of the fate and transport of RDX in coastal marine ecosystems. A mass balancing approach based on sequestrated ^{15}N-RDX into the systems illustrated that 80% - 84% of the ^{15}N contained in RDX that processed in the mesocosm was recovered in the measured pools. Subtidal vegetated and intertidal marsh ecosystems showed a notably higher mineralization of RDX to inorganic nitrogen, since prevailing reduced redox condition forming H_2S from SO_4^{2-} in organic carbon rich sediment donated a surplus of electrons for reductive anaerobic mineralization of RDX [14]. The subtidal non-vegetated ecosystem showed the least mineralization and highest persistence of RDX in compared to the subtidal vegetated and intertidal marsh mesocosms, since it had low organic carbon containing sediment which only permitted iron reduction in the sediment. [22]. Partitioning onto particulates, sediment and suspended organic matter and degradation of RDX into nitroso-triazines did not contribute significantly to the ecosystem-wide ultimate fate of RDX in coastal marine mesocosms. Here, we discuss new insights gained into fate of RDX including transformation, mineralization and partitioning processes in different coastal marine

environments through the observed distribution of ^{15}N. RDX biodegraded to nitroso-derivatives (MNX, DNX and TNX) via reduction in surface waters of marine mesocosms. Some of RDX diffused into the surface sediment where hypoxic conditions prevailed followed by degradation via reduction forming nitroso- triazines in the presence of coastal marine microbial assemblages [14]. RDX biodegraded in aerated surface water by aerobic microorganisms (eg: *Rhodococcus* sp., *Acremonium, Phanerochaete chrysoporium*) less effectively which was consistent with previous studies of fresh water and terrestrial systems demonstrating longer half-lives of RDX by days [36,37].

5.7.2 Transformation

Total detected nitroso-triazines remained constant in surface water without a significant quantitative variation in the production of nitroso derivatives among three marine ecosystems, since further breakdown to dissolved inorganic nitrogen was less favorable in aerated conditions [38]. The total detected nitroso-triazine amount was higher in porewater than in surface water of all the three mesocosms, so that sediment played an important role in the transformation of RDX [39]. Enhanced mineralization of nitroso derivatives in hypoxic surface sediments [14] resulted in a decreasing pattern of total detected nitroso-triazines in porewaters of all the three mesocosms with time. The lowest total nitroso-triazine production was found in subtidal vegetated ecosystems where the lowest redox potential persisted among three mesocosms, confirming further breakdown of nitroso products under low oxygen conditions by anaerobic microorganisms (eg: *Clostridium* sp., *Shewanella halifaxensis*) to use as a nitrogen and energy source [9].

5.7.3 Partitioning

Due to the relatively low hydrophobicity in terms of log Kow, the structure of RDX and its derivatives, passive partitioning onto sediment and SPM did not constitute a major pathway in the fate of RDX [8]. However, RDX and RDX-derived metabolite partitioning into the particulate pools (sediment, SPM) in subtidal non-vegetated, vegetated and intertidal marsh mesocosms showed significant differences among treatments based on sediment characteristics [8]. Generally, RDX and derivatives rapidly sorbed onto the particulates. Both SPM and sediment [8], attained steady state conditions of bulk ^{15}N from RDX and derivatives (^{15}N-$\sum$RDX) in particulates towards the end of the experiment and it might be a result of similar sorption and desorption rates. The least ^{15}N-$\sum$ RDX in SPM was found in the subtidal vegetated system where partitioned RDX might be degraded to nitroso-derivatives under lower redox potentials and transferred to the dissolved fraction in surface water. Well aerated surface water in non-vegetated mesocosms did not provide favorable conditions for biodegradation [15] allowing higher partitioned ^{15}N-$\sum$ RDX amount to stay in SPM as a sorbed fraction. However, partitioning of RDX and derivatives was significantly enhanced by the elevated organic carbon content and finer grain size of peaty sediments in the intertidal marsh system while considerably lower bulk ^{15}N-$\sum$ RDX values in deeper sediment confirmed the low vertical diffusion of RDX and its derivatives in peaty sediment of the intertidal marsh mesocosm. Lower organic carbon and clay fraction containing sandy sediment in the subtidal non-vegetated mesocosm is not a favorable zone for partitioning of RDX and derivatives [8]. Marine microbial assemblages (*Shewanella halifaxensis, Clostridium sp*.) provided significant contribution for degradation of RDX under oxygen limited conditions [40], especially, in the subtidal vegetated ecosystem, with the lowest RDX amount detected in sediment at all stages of the experiment. Since sandy sediment which only permitted iron reduction in the non-vegetated mesocosm was not a

favorable zone for biodegradation, RDX persisted in the sediment to a certain extent even after the two-week time duration. Anaerobic biodegradation under lower redox potential which permitted sulfate reduction [22,41] in subtidal vegetated and intertidal marsh mesocosms resulted TNX as the main identifiable ^{15}N containing compound in sediment. Unidentified ^{15}N in sediment might reside as non-measured derivatives such as Medina [40] or as microbially incorporated ^{15}N.

5.7.4 Mineralization

Mineralization of RDX in terms of inorganic nitrogen production ($^{15}NO_X$, $^{15}NH_4^+$, $^{15}N_2$ and $^{15}N_2O$ gases) played an important role in the fate of RDX in marine mesocosms and among the other inorganic nitrogen products, gaseous mineralization product, $^{15}N_2O$ formation was favored by the available microbes and prevailing environmental conditions in all the three marine ecosystems [14]. $^{15}N_2O$ was produced under lower redox potential which permitted nitrate, iron and sulfate reduction in surface sediment [9] via breakdown of Methylenedinitramine (Medina), an anaerobic ring cleavage product formed via denitration of RDX followed by hydroxylation [9]. Mole fraction of $^{15}N_2O$ (~ 0.5) produced in this study also revealed that Triazine ring in RDX opened up to form $^{15}N_2O$ which was consisted of one isotopically labelled ^{15}N atom coming from nitro group and another unlabelled ^{14}N atom coming from the ring of RDX. It might be the primary pathway of formation of $^{15}N_2O$ which was then readily diffused through the water column and escaped to the atmosphere [14]. Besides the decomposition of Medina, mono or poly-denitration of RDX and nitroso-triazines including MNX, DNX and TNX were also secondarily involved in the formation of $^{15}N_2O$ by denitrification of cleaved $^{15}NO_X$ from nitroso-triazines that acted as an intermediate mineralization product. Mineralization of RDX producing $^{15}N_2O$ significantly elevated in organic carbon rich subtidal vegetated and intertidal marsh

mesocosms those showed anaerobic respiration forming H_2S via sulfate reduction [6]. Although, there was a possibility of formation of $^{15}N_2$ from denitrification of $^{15}N_2O$ under anaerobic conditions [14], it was a negligible mineralization pathway of RDX quantitatively in all the studied marine coastal mesocosms. $^{15}NO_X$ is identified as the second highest mineralization product of RDX and it was rapidly formed in surface water via denitration and denitrosation [9] in all the three marine ecosystems.

Figure 10: proposed transformation pathways of RDX in hypoxic surface sediment in coastal marine habitats.

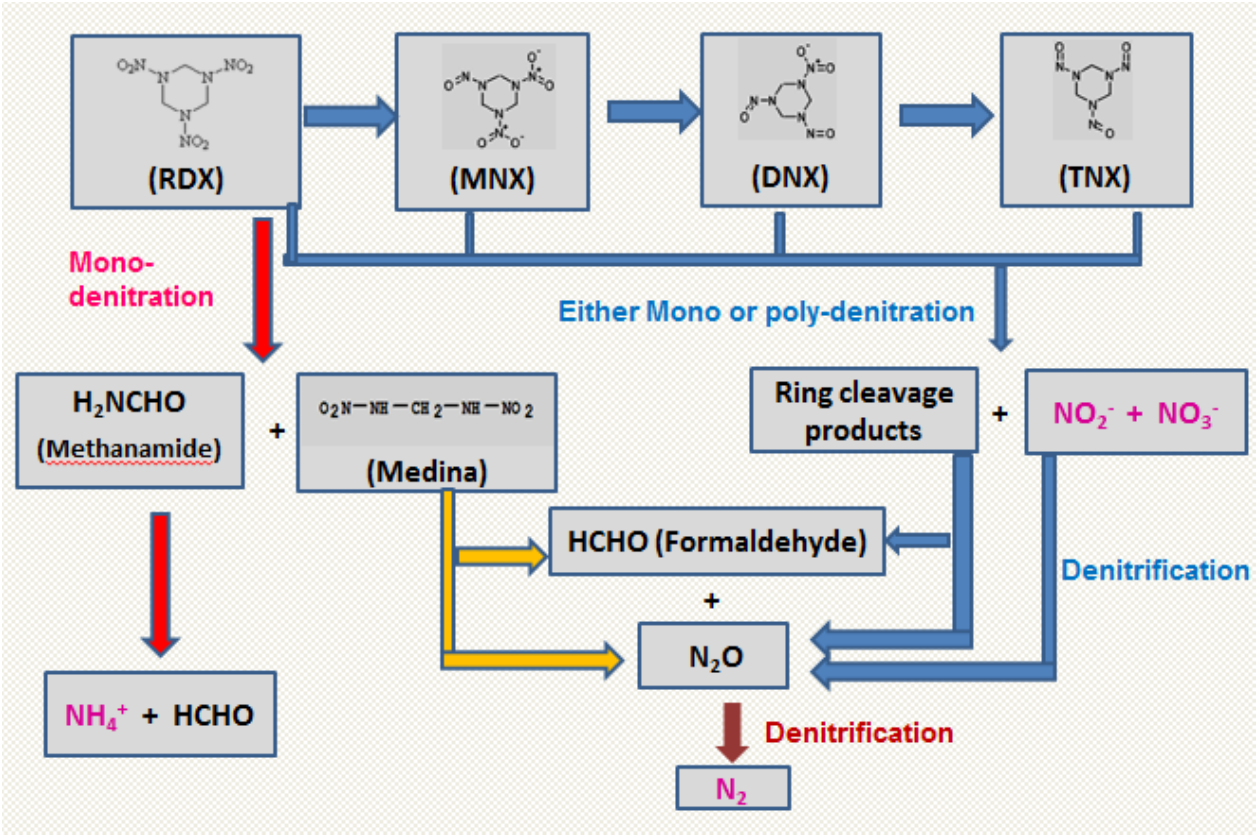

Denitration of RDX was augmented by reduced redox conditions [14] resulting in the highest and lowest $^{15}NO_X$ productions found in subtidal vegetated and non-vegetated mesocosms

respectively. $^{15}NO_X$ was not a stable mineralization product of RDX though it might be rapidly consumed via biological uptake [2] or acted as an intermediate during the process of forming $^{15}N_2O$ via denitrification in the systems [14]. Formation of Medina has been identified as a common $^{15}NH_4^+$ releasing process from RDX under low oxygen conditions [9], consistent with the elevated $^{15}NH_4^+$ in sediment porewaters versus surface water in subtidal non-vegetated, vegetated and intertidal marsh mesocosms here. Although nitrate reducing conditions prevailed in all the studied mesocosm sediments enabling ammonium formation [21], the subtidal non-vegetated mesocosm had the highest ammonium production among all the treatments and it was consisted with previous studies [13] those reported NH_4^+ as the main mineralization product in anaerobic sediments. The above processes indicated that gaseous mineralization products, specially, $^{15}N_2O$ formation from RDX, was significant in hypoxic environments and escaped to the atmosphere [14] as an efficient removal mechanism of RDX from coastal marine ecosystems.

5.8 Conclusions

Tracing the fate of RDX with ^{15}N provided a descriptive picture of partitioning, degradation and mineralization of RDX in coastal marine ecosystems. The fate of RDX in marine coastal ecosystems including subtidal non-vegetated, subtidal vegetated, intertidal marsh varied depending on different sediment characteristics and prevailing redox conditions. Persistence of RDX in the system decreased in the order of subtidal non-vegetated, subtidal vegetated and intertidal marsh mesocosms based on half-lives of RDX in the systems. Degradation and mineralization of RDX were favored by lowered redox potential (presence of Fe^{+2} and H_2S) and available microbial assemblages in surface sediments of the ecosystem. RDX degradation products, nitroso-triazines were stable in aerated surface water while they further broke down to form inorganic nitrogen products in surface sediments. Subtidal vegetated and intertidal marsh

ecosystems containing fine, organic carbon rich sediment which permitted sulfate reduction showed notably higher mineralization of RDX in terms of inorganic nitrogen products (nitrates, nitrites, ammonium, nitrogen and nitrogen dioxide gas). The subtidal non-vegetated system with sandy, organic carbon poor sediment which only permitted anaerobic respiration forming ferrous from iron reduction showed the least mineralization among treatments. Both $^{15}N_2$ and $^{15}N_2O$ gases produced in surface sediment diffused into the surface water and ultimately escaped to the atmosphere. $^{15}N_2O$ is the major mineralization product of RDX in all the three mesocosms showing production decreasing from intertidal marsh, subtidal vegetated to subtidal non-vegetated system while $^{15}N_2$ production is insignificant in the overall mass balance. The second highest mineralization product was $^{15}NO_X$ which formed at early stages of the experiment and latter disappeared from surface water. Medina formation from RDX released $^{15}NH_4^+$ into the surface sediment and a significant increase in the production was seen in subtidal vegetated system. Although $^{15}NO_X$ and $^{15}NH_4^+$ were detected in coastal marine ecosystems as mineralization products of RDX, their contribution to the fate of RDX was negligible. From a mass balancing perspective, partitioning of RDX and RDX-derived compounds onto particulates, SPM and sediment of the ecosystem was also not a dominant process on fate of RDX. However, sorption onto the sediment decreased in the order of intertidal marsh, subtidal vegetated and non-vegetated ecosystems due to the decrease in organic carbon and fine particle content in sediment of these systems in the same order.

Here, we conclude that 50%, 44% and 25% losses of RDX were reported in contaminated intertidal marsh, subtidal vegetated and subtidal non-vegetated coastal marine habitats respectively. Processed RDX in mesocosms were mainly ended up in atmosphere as gaseous mineralization product, $^{15}N_2O$ and production increased from non-vegetated, vegetated to marsh

mesocosms. Therefore, prevailing redox condition based on organic carbon content of sediment in the ecosystem became the key factor for natural attenuation of RDX in contaminated coastal marine habitats.

5.9 Acknowledgement

This work was funded by Department of Defense- SERDP under Project ID ER-2122. We would like to thank D. Cady and V. Rollinson for analytical support.

5.10 References

[1] Pichtel J. 2012. Distribution and fate of military explosives and propellants in soil: A review. *Applied and Environmental Soil Science* 2012.

[2] Ballentine ML, Ariyarathna T, Smith RW, Cooper C, Vlahos P, Fallis S, Groshens TJ, Tobias C. 2016. Uptake and fate of hexahydro-1,3,5-trinitro-1,3,5-triazine (RDX) in coastal marine biota determined using a stable isotopic tracer, 15N - [RDX]. *Chemosphere* 153:28-38.

[3] Hawari J, Beaudet S, Halasz A, Thiboutot S, Ampleman G. 2000. Microbial degradation of explosives: Biotransformation versus mineralization. *Appl Microbiol Biotechnol* 54:605-618.

[4] MacDonald JA, Small MJ, Morgan MG. 2009. Quantifying the risks of unexploded ordnance at closed military bases. *Environmental Science and Technology* 43:259-265.

[5] Kalderis D, Juhasz AL, Boopathy R, Comfort S. 2011. Soils contaminated with explosives: Environmental fate and evaluation of state-of the-art remediation processes (IUPAC technical report). *Pure and Applied Chemistry* 83:1407-1484.

[6] Felt D.R., Bednar A., Arnett C., Kirgan R. 2009. Bio-Geochemical Factors That Affect RDX Degradation. *Proceedings of the Annual International Conference on Soils, Sediments, Water and Energy* 14:Article 17.

[7] An C, Shi Y, He Y, Huang G, Liang J, Liu Z. 2014. Effect of different carbon substrates on the removal of hexahydro-1,3,5-trinitro-1,3,5-triazine (RDX) and octahydro-1,3,5,7-tetranitro-1,3,5,7-tetrazocine (HMX) by anaerobic mesophilic granular sludge. *Water Air Soil Pollut* 225.

[8] Ariyarathna T, Vlahos P, Tobias C, Smith R. 2015. Sorption kinetics of TNT and RDX in anaerobic freshwater and marine sediments: Batch studies. *Environ Toxicol Chem* 35(1):47-55.

[9] Halasz A, Hawari J. 2011. Degradation routes of RDX in various redox systems. *ACS Symp Ser* 1071:441-462.

[10] Gregory KB, Larese-Casanova P, Parkin GF, Scherer MM. 2004. Abiotic Transformation of Hexahydro-1,3,5-trinito-1,3,5-triazine by Fe II Bound to Magnetite. *Environmental Science and Technology* 38:1408-1414.

[11] Juhasz, A. L. and Naidu, R. 2007. Explosives: Fate, dynamics, and ecological impact in terrestrial and marine environments. *Environ Contam Toxicol* 191:163-163-215.

[12] Sheremata TW, Hawari J. 2000. Mineralization of RDX by the white rot fungus Phanerochaete chrysosporium to carbon dioxide and nitrous oxide. *Environ Sci Technol* 34:3384-3388.

[13] Ariyaratha T, Vlahos P, Smith R W, Fallis S, Groshens T, Tobias C. 2016. Biodegradation and mineralization of isotopically labelled TNT and RDX in anaerobic marine sediments. *Environ Toxicol Chem (Accepted)*.

[14] Smith RW, Tobias C, Vlahos P, Cooper C, Ballentine M, Ariyarathna T, Fallis S, Groshens TJ. 2015. Mineralization of RDX-derived nitrogen to N2 via denitrification in coastal marine sediments. *Environ Sci Technol* 49:2180-2187.

[15] Hawari J, Halasz A, Sheremata T, Beaudet S, Groom C, Paquet L, Rhofir C, Ampleman G, Thiboutot S. 2000. Characterization of metabolites during biodegradation of hexahydro- 1,3,5-trinitro-1,3,5-triazine (RDX) with municipal anaerobic sludge. *Appl Environ Microbiol* 66:2652-2657.

[16] Beller HR. 2002. Anaerobic biotransformation of RDX (hexahydro-1,3,5-trinitro-1,3,5-triazine) by aquifer bacteria using hydrogen as the sole electron donor. *Water Res* 36:2533-2540.

[17] Montgomery MT, Coffin RB, Boyd TJ, Osburn CL. 2013. Incorporation and mineralization of TNT and other anthropogenic organics by natural microbial assemblages from a small, tropical estuary. *Environ Pollut* 174:257-264.

[18] Best EPH, Sprecher SL, Larson SL, Fredrickson HL, Bader DF. 1999. Environmental behavior of explosives in groundwater from the Milan Army Ammunition Plant in aquatic and wetland plant treatments. Removal, mass balances and fate in groundwater of TNT and RDX. *Chemosphere* 38:3383-3396.

[19] Kwon MJ, O'Loughlin EJ, Antonopoulos DA, Finneran KT. 2011. Geochemical and microbiological processes contributing to the transformation of hexahydro-1,3,5-trinitro-1,3,5-triazine (RDX) in contaminated aquifer material. *Chemosphere* 84:1223-1230.

[20] Ronen Z, Yanovich Y, Goldin R, Adar E. 2008. Metabolism of the explosive hexahydro-1,3,5-trinitro-1,3,5-triazine (RDX) in a contaminated vadose zone. *Chemosphere* 73:1492-1498.

[21] Freedman DL and Sutherland KW 1998. Biodegradation of hexahydro-1,3,5-trinitro-1,3,5-triazine (RDX) under nitrate-reducing conditions. *Water Science and Technology* 38:33-40.

[22] Boopathy R, Kulpa CF, Manning J. 1998. Anaerobic biodegradation of explosives and related compounds by sulfate-reducing and methanogenic bacteria: A review. *Bioresour Technol* 63:81-89.

[23] Sheremata TW, Halasz A, Paquet L, Thiboutot S, Ampleman G, Hawari J. 2001. The fate of the cyclic nitramine explosive RDX in natural soil. *Environmental Science and Technology* 35:1037-1040.

[24] Cammen LM. 1982. Effect of particle size on organic content and microbial abundance within four marine sediments. *Mar Ecol Prog Ser* 9:273-280.

[25] Zheng Y, Hou L, Liu M, Liu Z, Li X, Lin X, Yin G, Gao J, Yu C, Wang R, Jiang X. 2016. Tidal pumping facilitates dissimilatory nitrate reduction in intertidal marshes.*Sci Rep* 6.

[26] Smith P, Bogren K. 2001. Determination of nitrate and/or nitrite in brackish or seawater by flow injection analysis colorimeter: QuickChem Method. *Methods manual Lachat Instruments*.

[27] Stookey LL. 1970. Ferrozine - A new spectrophotometric reagent for iron. *Anal Chem* 42:779-781.

[28] Cline JD. 1969. Spectrophotometric determination of hydrogen sulfide in natural waters. Limnol. Oceanogr., 14, 454-458. *Limnol Oceanogr* 14:454-455,456,457,458.

[29] Hedges JI, Stern JH. 1984. Carbon and nitrogen determinations of carbonate-containing solids. *Limnology & Oceanography* 29:657-663.

[30] Miyares PH Jenkins TF. 1990. *Salting-Out Solvent Extraction for Determining Low Levels of Nitroaromatics and Nitramines in Water.* Special Report 90-30. US Army Corps of Engineers, Cold Regions Research and Engineering Laboratory, Hanover, NH.

[31] Smith RW, Vlahos P, Böhlke JK, Ariyarathna T, Ballentine M, Cooper C, Fallis S, Groshens TJ, Tobias C. 2015. Tracing the Cycling and Fate of the Explosive 2,4,6-Trinitrotoluene in Coastal Marine Systems with a Stable Isotopic Tracer, 15N-[TNT]. *Environ Sci Technol* 49:12223-12231.

[32] Holmes R, McClelland J, Sigman D, Fry B, Peterson B. 1998. Measuring 15N-NH4+ in marine, estuarine and fresh waters: An adaptation of the ammonia diffusion method for samples with low ammonium concentrations. *Mar Chem* 60:235-243.

[33] Holmboe N and Kristensen E. 2002. Ammonium adsorption in sediments of a tropical mangrove forest (Thailand) and a temperate Wadden sea area (Denmark). *Wetlands ecology and management* 10:453 - 460.

[34] Weiss RF. 1970. The solubility of nitrogen, oxygen and argon in water and seawater. *Deep-Sea Research and Oceanographic Abstracts* 17:721-735.

[35] Delaune RD Reddy KR. 2005. Redox potential. In Hillel D (ed), *Encyclopedia of Soils in the Environment*, Academic Press, pp 366-371.

[36] Zheng W, Lichwa J, D'Alessio M, Ray C. 2009. Fate and transport of TNT, RDX, and HMX in streambed sediments: Implications for riverbank filtration. *Chemosphere* 76:1167-1177.

[37] Fuller ME, Heraty L, Condee CW, Vainberg S, Sturchio NC, Böhlke JK, Hatzinger PB. 2016. Relating carbon and nitrogen isotope effects to reaction mechanisms during aerobic or anaerobic degradation of RDX (hexahydro-1,3,5- trinitro-1,3,5-triazine) by pure bacterial cultures. *Appl Environ Microbiol* 82:3297-3309.

[38] Khan MI, Lee J, Park J. 2012. Microbial degradation and toxicity of hexahydro-1,3,5-trinitro-1,3,5-triazine. *J Microbiol Biotechnol* 22:1311-1323.

[39] Smith RW, Vlahos P, Tobias C, Ballentine M, Ariyarathna T, Cooper C. 2013. Removal rates of dissolved munitions compounds in seawater. *Chemosphere* 92:898-904.

[40] Anke H, Kuhn A, Weber RWS. 2003. The role of nitrate reductase in the degradation of the explosive RDX (hexahydro-1,3,5-trinitro-1,3,5-triazine) by Penicillium sp. AK96151. *Mycological Progress 2*3:219-225.

[41] Boopathy R, Widrig DL, Manning JF. 1997. In situ bioremediation of explosives-contaminated soil: A soil column study. *Bioresour Technol* 59:169-176.

5.11 Supplemental data

Table S1: Subdivision of time series aqueous concentrations of munitions in a) surface water b) porewater in subtidal non-vegetated, vegetated and intertidal marsh mesocosms.

a)

Mesocosm type	Time (Days)	Surface water (µM)			
		RDX	MNX	DNX	TNX
Subtidal non-vegetated	0.25	4.95	0.027	BD	0.012
	1	4.45	0.026	BD	0.012
	3	1.49	0.008	BD	0.013
	5	1.43	0.009	BD	0.015
	7	2.60	0.017	BD	0.013
	9	3.00	0.019	BD	0.016
	14	1.81	0.010	BD	0.015
Subtidal vegetated	0.21	4.26	0.017	BD	0.014
	1	4.03	0.021	BD	0.014
	3	2.59	0.015	BD	0.016
	5	2.40	0.013	BD	0.011
	10	1.83	0.011	BD	0.015
	13	1.64	0.009	BD	0.015
	17	1.45	0.009	BD	0.017
Intertidal marsh	1	3.56	0.016	0.003	0.011
	2	2.89	0.013	0.003	0.010
	3	2.47	0.012	0.003	0.010
	6	0.96	0.006	0.006	0.010
	8	1.00	0.007	0.005	0.013
	11	0.82	0.004	BD	0.012
	13	0.89	0.005	BD	0.013
	15	0.81	0.006	BD	0.015
	17	0.72	0.006	BD	0.020

BD = below detection

b)

Mesocosm type	Time (Days)	Porewater (µM)			
		RDX	MNX	DNX	TNX
Subtidal non-vegetated	0.063	0.138	0.135	0.070	0.051
	0.25	2.89	0.356	0.114	0.069
	1	3.59	0.351	0.177	0.094
	3	1.04	0.153	0.183	0.105
	5	1.22	0.121	0.195	0.097
	7	1.56	0.155	0.215	0.109
	9	0.86	0.070	0.100	0.063
	12	1.77	0.044	0.073	0.054
	14	0.10	0.032	0.060	0.038
Subtidal vegetated	0.0623	0.127	0.045	0.010	0.112
	1	0.130	0.044	0.097	0.102
	2	0.110	0.042	0.093	0.097
	4	0.100	0.041	0.095	0.103
	6	0.239	0.036	0.084	0.084
	9	0.085	0.044	0.095	0.071
	11	0.169	0.044	0.076	0.036
	13	0.100	0.043	0.087	0.032
	18	BD	0.042	0.052	0.026
Intertidal marsh	1	1.75	0.216	0.237	0.257
	2	1.68	BD	0.040	0.058
	3	0.364	0.271	0.295	0.314
	6	0.294	0.259	0.284	BD
	8	0.206	0.298	0.228	0.312
	10	0.241	0.221	0.242	BD
	12	0.301	0.284	0.309	0.324
	14	0.301	0.272	0.297	BD
	16	0.208	0.033	0.231	0.338

BD = below detection

Figure S1: Time series of munition contribution to total ^{15}N in sediment in coastal marine mesocosms: subtidal non-vegetated, subtidal vegetated and intertidal marsh

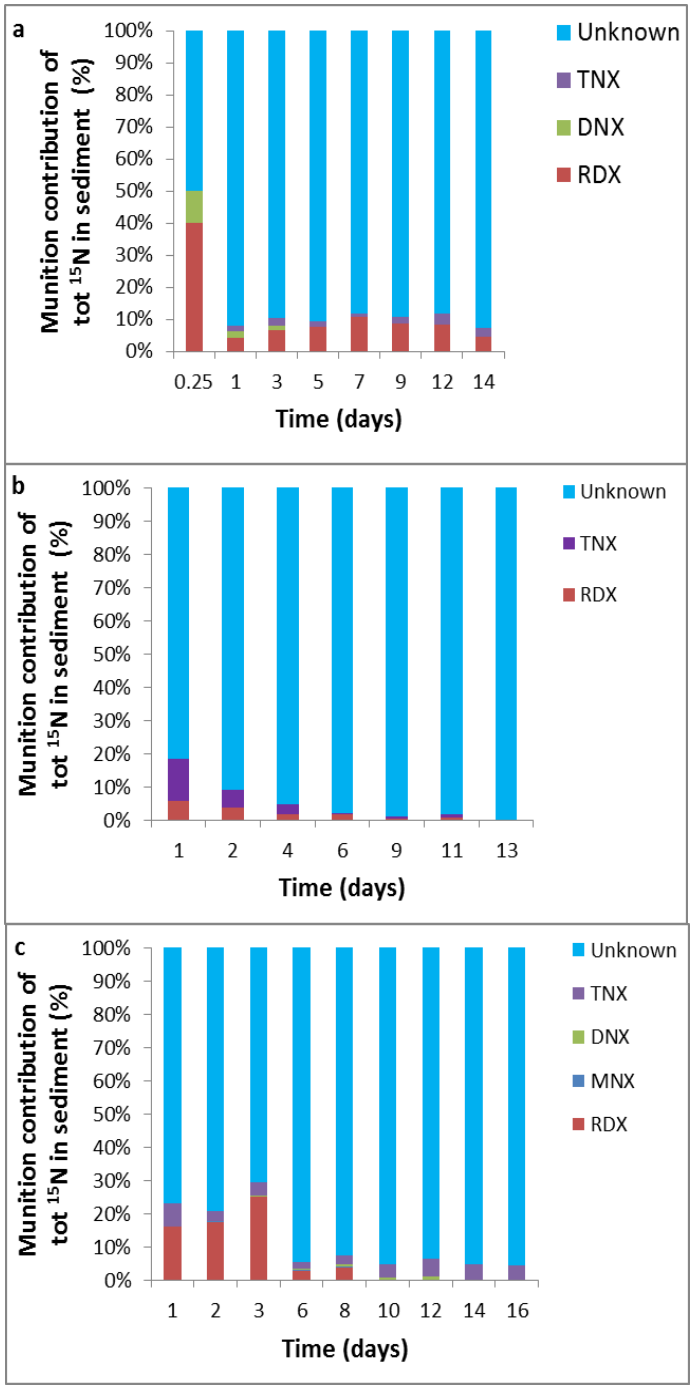

6.0 Conclusions

6.1 Overview

Abiotic sorption studies indicated that TNT and RDX were rapidly removed from aqueous phase of the anaerobic sediment slurries under abiotic conditions following first order kinetics and attained equilibrium with sediment. Marine sediments showed significantly higher compound uptake rates (0.30 - 0.64 hr^{-1}) than freshwater silt (0.0046 – 0.0065 hr^{-1}) for both TNT and RDX likely because of lower compound solubilities and a higher pH in marine systems. Equilibrium partition constants were on the same order of magnitude for marine silt (1.1 – 2.0 Lkg^{-1}sed) and freshwater silt (1.4 – 3.1 Lkg^{-1}sed) but lower for marine sand (0.72 - 0.92 Lkg^{-1}sed). Total organic carbon content in marine sediments varied linearly with equilibrium partition constants of TNT and RDX suggesting the role of total organic carbon as the key determinant of sorption of compounds onto the sediment. Uptake rates and equilibrium constants of explosives were inversely correlated to temperature regardless of sediment type because of kinetic barriers associated with low temperatures.

Anaerobic biotransformation of TNT and RDX was observed in anaerobic sediment slurries in the presence of microorganisms. TNT was removed from the aqueous phase at a faster rate (0.75 hr^{-1}) than RDX (0.37 hr^{-1}) and both rates were also higher than the abiotic rates (0.53 hr^{-1} for TNT and 0.31 hr^{-1} for RDX). Sediment accumulation of ^{15}N derived from parent compound was higher in the TNT microcosms (13%) than RDX (2%). Mono-amino-dinitrotoluenes were identified as intermediate biodegradation products of TNT. TNT-N (2% of the total spiked) was mineralized to NO_X (nitrates and nitrites) and NH_4^+ through two different pathways: denitration, and deamination and formation of NH_4^+, possibly facilitated by iron and sulfate reducing bacteria in the sediments. RDX (10%) biodegraded to nitroso-derivatives, while 13% of RDX-N in nitro

groups was mineralized to NO_X, NH_4^+ and N_2 gas anaerobically by day 16. A reasonable production of N_2 (13%) was seen in the RDX system, but not in the TNT system. N_2 was possibly formed from RDX via N_2O, a product of RDX which was not quantified in this study. NH_4^+ was the primary identified mineralization end-product of RDX (40%) in present study which was exclusively anaerobic, and generated through mono-denitration followed by ring breakdown. Majority of TNT (85%) still resided as unidentified metabolites while it was lower for RDX (68%). Marine sediment played an important role in mineralization providing favorable anaerobic conditions, iron bearing minerals and natural microbial assemblages including iron and sulfate reducers those enhanced transformation of TNT and RDX.

Ecocosm studies which permitted both aerobic and anaerobic pathways to co-exist revealed that the extent and pathways of partitioning and transformation of RDX differed in different sub-compartments in the ecosystem including surface water and sediment (porewater), and also among different coastal marine ecosystems. Transformation of RDX was enhanced by microbial assemblages and lower redox potentials. RDX was biodegraded to nitroso-derivatives (MNX, DNX and TNX) via reduction and were further broken down, specially, in sediment, forming inorganic nitrogen in coastal marine ecosystems. RDX was mineralized to N_2 and N_2O through a series of intermediates and escaped to the atmosphere. Subtidal vegetated and intertidal marsh ecosystems containing fine grained, organic carbon rich sediment where significant anaerobic respiration prevailed (presence of H_2S) showed notably higher mineralization of RDX. Subtidal non-vegetated ecosystem with organic carbon poor sediment where moderate anaerobic respiration prevailed (presence of Fe^{+2}) yielded the least mineralization and principle component analysis showed the possible direct involvement of iron reducing bacteria on gaseous mineralization product formation from RDX. Highest persistence of RDX in the system was

found in subtidal non-vegetated system compared to the subtidal vegetated and intertidal marsh mesocosms based on half-lives of RDX. Partitioning of RDX and degradation products onto solids was a negligible sink for the fate of RDX in the system. The amount of sorption onto sediments decreased from intertidal marsh > subtidal vegetated >subtidal non-vegetated and was correlated to the available organic carbon content (positively) and grain size (negatively) of the sediment.

Finally, we conclude that sediment becomes the most favorable zone for partitioning and transformation regardless of the compound. The greatest predictor of RDX fate is prevailing redox condition based on total organic carbon content of sediment in the ecosystem. The percent RDX loss decreases from marsh (50%) > subtidal vegetated (44%) >subtidal non-vegetated (25%) mesocosms indicating RDX (~ > 50%) still resides in the coastal environment without transformation. The processed RDX in the mesocosm mainly ends up forming gaseous products as the best removal technique from the marine ecosystem, while TNT stays in the system forming different derivatives. Overall results of this study including kinetics and pathways, of partitioning and transformation, of compounds and final mass balances illustrating the fate of the compounds in the system will be a provision that is essential for evaluating efficacy of natural attenuation of explosives in coastal marine habitats.

6.2 Future directions

Data from the large mesocosm approach has led to both insights and questions about how environmental parameters influence the partitioning and transformation of RDX in sediments. Result from the subtidal non-vegetated, subtidal vegetated and intertidal marsh ecosystems remain be evaluated comprehensively by performing multi variant analysis (principle component analysis and advanced modelling techniques). Environmental variables to be correlated with

RDX metabolism include dissolved oxygen, redox, pH, reduced iron and sulfur species in sediment profiles and analysis can be done under three categories: time series data, depth profile data, tidal variation data.

Though transformation and partitioning behavior of RDX was quantified in all the experiments, it still shows a pool of unknowns which need further investigation. Therefore, it is recommended that additional bench-top experiments can be carried out to reveal more degradation pathways of RDX using isotopically ^{15}N ring, nitro-groups and to reveal ring cleavage products and pathways. Mineralization of RDX to form the prominent product, N_2O via hydrazine and methyl hydrazine should specially be addressed. Measuring dissolved and sorbed hydrazine in slurry water and marine sediments respectively will help to identify the role of hydrazine as an intermediate of RDX transformation. Experimental studies involving anaerobic sediment slurries and the approaches of Chapter 2 could focus on the hydrazine intermediate using methods in An et al., (2015) such that rates of degradation of RDX via hydrazine and the significance of that pathway to the fate of RDX could be better assessed. Finally, the extent of bacterial assimilation of ^{15}N derived from RDX can be obtained by analyzing ^{15}N-RDX in bacterial specific amino acids (eg: Diamino pimelic acid, D-Alanine etc.) those generally found in the bacteria habituated in intertidal marsh mesocosms. It can help to confirm the involvement of bacteria on transformation of RDX showing whether ^{15}N-RDX is assimilated to bacterial body mass or used for the metabolic activities.

Regarding TNT, coastal marine ecosystems (subtidal non-vegetated, subtidal vegetated and intertidal marsh) should be evaluated as a comparison study to evaluate partitioning and transformation of TNT similar to RDX experiment described in chapter 4. Based on the literature and our previous bench-top and aquaria scale experiments, it is known that the ultimate fate of

TNT remains difficult to identify leaving significant portion as unknown pools in the aqueous phase of the experimental systems. Therefore, further characterization of unidentified intermediates and products (eg. Triaminotoluene) should be done. Similar to the analysis done for RDX in mesocosms, influence of environmental variables on partitioning and transformation of TNT should be evaluated using time series data, depth profile data, tidal variation data. Incorporation of ^{15}N of TNT into the bacterial specific amino acids can also be analyzed as suggested above for RDX.

6.3 References

An Z., Li P., Zhang X., Liu L. (2014) Simultaneous determination of hydrazine, methylhydrazine, and 1,1-dimethylhydrazine in rat plasma by LC–MS/MS *Journal of Liquid Chromatography & Related Technologies*, 37:1212–1225.

Pelz O., Cifuentes L. A., Hammer B. T., Kelley C. A., Coffin R. B. (1998) Tracing the assimilation of organic compounds using $\delta^{13}C$ analysis of unique amino acids in the bacterial peptidoglycan cell wall, *FEMS Microbiology Ecology*, 25:229-240.

Appendix

Copyrighted material permission details:

1. Khan MI, Lee J, Park J. 2013. A toxicological review on potential microbial degradation intermediates of 2,4,6-trinitrotoluene, and its implications in bioremediation. *KSCE J Civ Eng* 17:1223-1231.
   License number: 4006771473968
   License date: Dec 12, 2016
   License content publisher: Springer
   Reused material: 1 figure
2. Hawari J, Beaudet S, Halasz A, Thiboutot S, Ampleman G. 2000. Microbial degradation of explosives: Biotransformation versus mineralization. *Appl Microbiol Biotechnol* 54:605-618.
   License number: 4006780356936
   License date: Dec 12, 2016
   License content publisher: Springer
   Reused material: 1 figure

3. Reprinted (adapted) with permission from (HALASZ A, HAWARI J. 2011. DEGRADATION ROUTES OF RDX IN VARIOUS REDOX SYSTEMS. *ACS SYMP SER* 1071:441-462) Copyright (2016) American Chemical Society.
4. Ariyarathna T, Vlahos P, Tobias C, Smith R. 2015. Sorption kinetics of TNT and RDX in anaerobic freshwater and marine sediments: Batch studies. *Environ Toxicol Chem* 35(1):47-55.
   License number: 4002770020302
   License date: Dec 05, 2016
   License content publisher: John Wiley & Sons
   Reused material: Full article